Naval Research Laboratory

Washington, DC 20375-5320

NRL/MR/7160--17-9702

Low-Frequency Surface Backscattering Strengths Measured in the Critical Sea Test Experiments

Roger C. Gauss
Joseph M. Fialkowski

Acoustic Signal Processing and Systems Branch
Acoustics Division

January 19, 2017

REPORT DOCUMENTATION PAGE

Form Approved
OMB No. 0704-0188

1. REPORT DATE *(DD-MM-YYYY)*	**2. REPORT TYPE**	**3. DATES COVERED** *(From - To)*
19-01-2017	Memorandum Report	April 1988 – September 2016

4. TITLE AND SUBTITLE

Low-Frequency Surface Backscattering Strengths Measured in the Critical Sea Test Experiments

5a. CONTRACT NUMBER

5b. GRANT NUMBER

5c. PROGRAM ELEMENT NUMBER
0602747N

6. AUTHOR(S)

Roger C. Gauss[1] and Joseph M. Fialkowski

5d. PROJECT NUMBER

5e. TASK NUMBER

5f. WORK UNIT NUMBER
71-6817-06

7. PERFORMING ORGANIZATION NAME(S) AND ADDRESS(ES)

Naval Research Laboratory, Code 7164
4555 Overlook Avenue, SW
Washington, DC 20375-5320

8. PERFORMING ORGANIZATION REPORT NUMBER

NRL/MR/7160--17-9702

9. SPONSORING / MONITORING AGENCY NAME(S) AND ADDRESS(ES)

Naval Research Laboratory, Code 7160
4555 Overlook Avenue, SW
Washington, DC 20375-5350

10. SPONSOR / MONITOR'S ACRONYM(S)

11. SPONSOR / MONITOR'S REPORT NUMBER(S)

12. DISTRIBUTION / AVAILABILITY STATEMENT

Approved for public release; distribution is unlimited.

13. SUPPLEMENTARY NOTES

[1]Retired from NRL.

14. ABSTRACT

Surface scattering strength (SSS) is one of key acoustic inputs to reverberation and active sonar models. This report presents significantly-updated results from 55 broadband SUS SSS measurements in 6 Critical Sea Test (CST) experiments. Since the time of the previously-published results of Ogden and Erskine (and Nicholas et al.), there has been a : 1) major reprocessing effort that extended the grazing-angle coverage of many data sets; 2) recalibration that particularly impacts the lowest frequency band results; 3) significant revision of all the CST wind-speed values; and 4) systematic removal of fish-scattering contributions. This reports documents the updated results, and archives the bistatic SSS data.

15. SUBJECT TERMS

Surface scattering
Surface scattering strength
Reverberation
Underwater acoustics
Active sonar

16. SECURITY CLASSIFICATION OF:			**17. LIMITATION OF ABSTRACT**	**18. NUMBER OF PAGES**	**19a. NAME OF RESPONSIBLE PERSON**
a. REPORT	**b. ABSTRACT**	**c. THIS PAGE**			Joseph M. Fialkowski
Unclassified Unlimited	Unclassified Unlimited	Unclassified Unlimited	Unclassified Unlimited	68	**19b. TELEPHONE NUMBER** *(include area code)* (202) 404-4803

Standard Form 298 (Rev. 8-98)
Prescribed by ANSI Std. Z39.18

TABLE OF CONTENTS

LOW-FREQUENCY SURFACE BACKSCATTERING STRENGTHS MEASURED IN THE CRITICAL SEA TEST EXPERIMENTS

1. INTRODUCTION

The Critical Sea Test (CST) program was an at-sea testing program sponsored by the Space and Naval Warfare Systems Command (SPAWAR PMW-182) that explored issues related to the development and testing of low-frequency undersea active systems (Zittel *et al*., 1996). One objective of the CST program was the measurement of environmental acoustic scattering parameters as reverberation can be a major source of interference for active sonar systems. One of the key acoustic inputs to reverberation models is surface scattering strength (SSS). The results shown in this report demonstrate that SSS has a strong dependence on sea state, grazing angle, and frequency.

The CST surface-scattering data are particularly valuable as these acoustic measurements were complemented by high-quality environmental measurements (such as of wind speed, directional surface-wave spectrum, and subsurface bubble density—e.g., see Hanson 1993) and, in view of the potential contributions that fish could make to the backscatter, dedicated broadband measurements of volume scattering strength (VSS) were also conducted by NRL (see, e.g., Love (1993), and Nero and Huster (1996)).

One of the measurement techniques used throughout the CST tests by Ogden and Erskine (1994a, b) involved the use of omnidirectional SUS (Signals, Underwater Sound) explosive charges as sources and a horizontal line array (HLA) as a receiver. (For an overview of direct-path CST surface-scattering results using coded pulses, see Fialkowski *et al*. (2004).) As noted in their papers, the advantage of impulsive sources is giving results at many frequencies simultaneously (via harmonics of the bubble pulse) (Urick, 1983).

The CST SUS SSS experiments, processing, and results are documented in Ogden and Erskine (1994a, b) and Nicholas *et al*. (1998). **However, there has since been a:**

- **Major reprocessing of many of the data sets to extend the CST SUS results to higher grazing angles** (doubling the coverage in many instances)
- **Recalibration** process that revealed the reported CST SUS scattering strength values needed adjusting. **Particularly impacted were the lowest frequency band results**, generally as in Fig. 1-1. (For run-specific #s, contact the authors.)
- **Significant revision of all the CST wind-speed values** led by J. Hanson and L. White (JHU/APL)—the biggest effect was on the CST-4 values. (Tables 3-1 and 3-2 of this report include the revised values.) As noted in Gauss *et al*. (2005), **these revised wind speeds have resolved the apparent discrepancies between CST-4 and CST-7 SSS values reported in Nicholas *et al*. (1998).**
- **Systematic removal of fish-scattering contributions** via the aforementioned *in-situ* broadband fish measurements and subsequent VSS modeling.

Manuscript approved December 16, 2016.

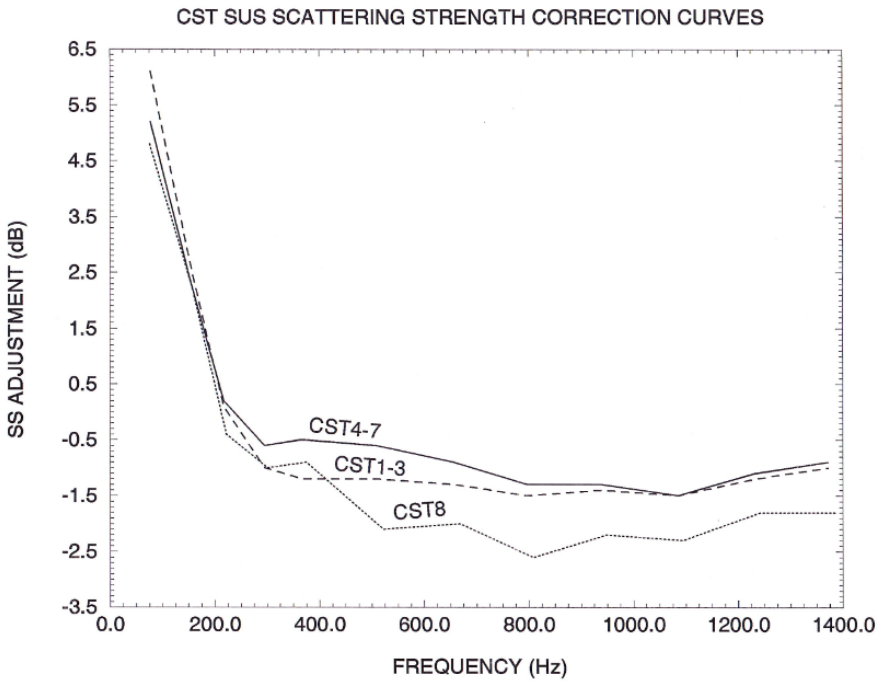

Fig. 1-1 – CST SUS scattering strength (SS) recalibration-adjustment values.
(The adjustment values are to be *added* to previously-reported CST SS values.)

The updated and extended CST data results shown in this report were obtained from 55 SUS SSS measurements in 6 of the 7 CST experiments:

- CST-2 (north Atlantic, Icelandic Basin near Hatton Bank; April 1989)
- CST-3 (western Atlantic, Bermuda Rise and Hatteras Abyssal Plain; Aug. 1989)
- CST-4 (north Pacific, Gulf of Alaska, Aleutian Abyssal Plain; April, 1990)
- CST-5 (Mediterranean Sea, Messina Rise on the Ionian Abyssal Plain; June, 1991)
- CST-7 Phase 2 (north Pacific, Gulf of Alaska, Sila Fracture Zone; February, 1992);
- CST-8 (Mediterranean Sea, Herodotus Abyssal Plain to the Nile Cone; May, 1993).

See Ogden and Erskine (1994a, b; 1997) for more details on all the CST SUS measurements (such as geographic location, water depth, source and receiver depths, and source-receiver separations).

Surface reverberation is driven by the interaction of acoustic energy with environmental features at or very near the ocean surface (McDaniel, 1993; Gilbert, 1993). With sufficient winds, air becomes entrained by breaking waves in the form of subsurface bubbles whose properties are governed by advective transport, gas dissolution, and buoyancy. Under these conditions, both the rough air-sea interface and bubble clouds can be acoustic scattering strength source mechanisms. In the absence of fish, the driving environmental factors behind those air-sea-zone features are the wind speed and significant wave height (SWH) distributions (Gauss *et al*., 2006a. b)—see Fig. 1-2; these values are summarized for each run in Tables 3-1 and 3-2. (The local bubble-free sound speed value at the air-sea interface has relatively minor effects on SSS.)

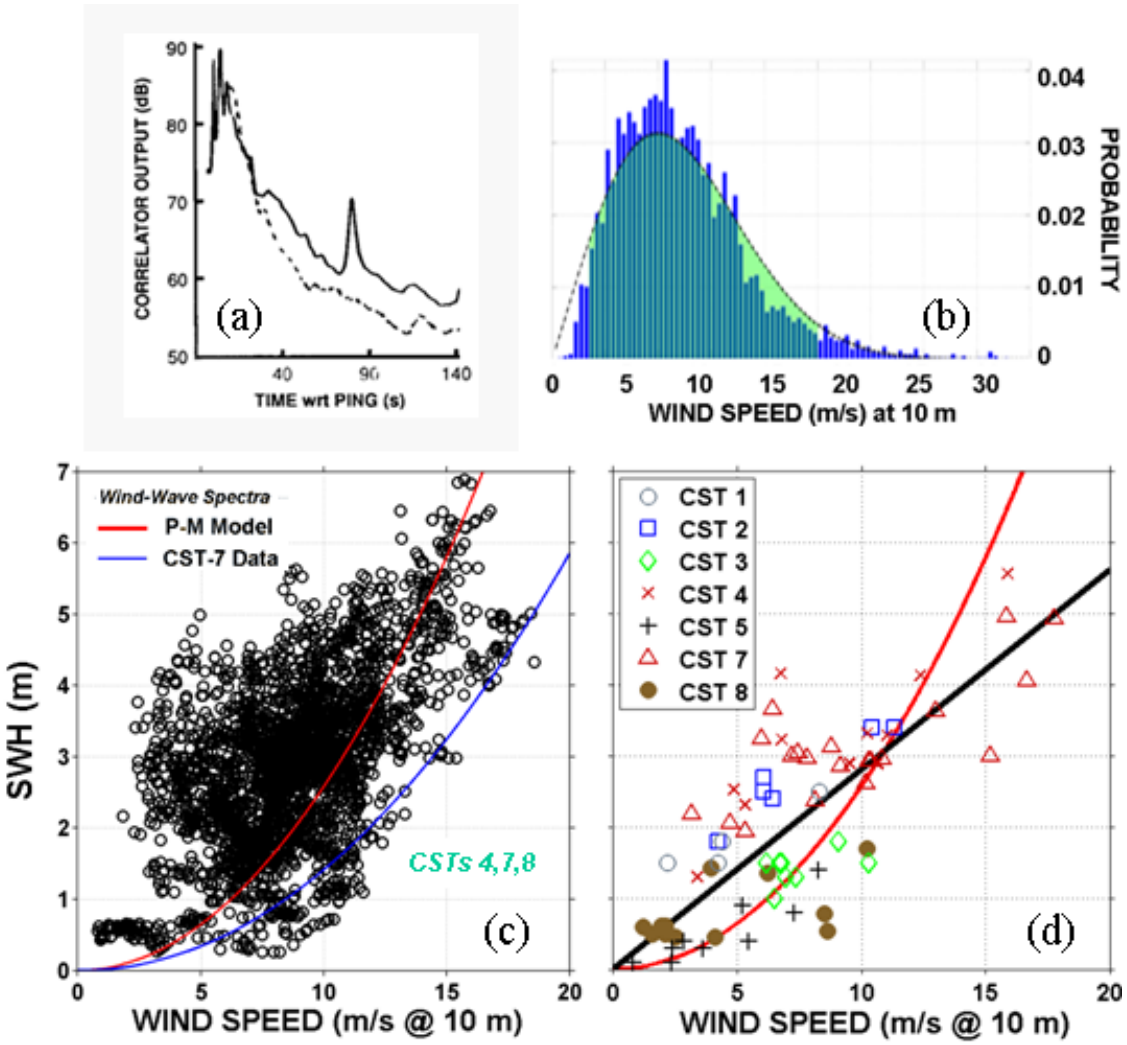

Figure 1-2 – (a) Comparison of NRL-measured 245-Hz reverberation vs. time at 2 wind speeds: 24 m/s (solid curve) and 8 m/s (dashed curve) in a deep-water, surface convergence zone (CZ) environment, showing the higher levels and a strong CZ return in the higher-wind-speed case. (b)-(d) Oceanic wind-speed and SWH distributions: (b) wind speeds (scaled to 10 m) from 7 years of QuikSCAT measurements (Capps and Zender, 2009, 2010), and (c)-(d) CST SWH vs. wind speed measurements (symbols)—the red curve is the empirical Pierson-Moskowitz (P-M) relationship for fully-developed wind seas (no swell); the black curve in (d) is a fit to just those values corresponding to the CST SUS SSS data sets**.** (See Hanson (1996) for more details on isolating wind-wave and swell components using the extensive CST-7 Phase-2 environmental data (overviewed in Hanson, 1993).) **Note the generally lower SWH values for the two non-open-ocean CST experiments: CST 5 and CST 8 (both of which were conducted in the more-swell-limited Mediterranean Sea).**

As noted previously, because of the potential contributions that fish could make to the backscatter, dedicated broadband measurements and modeling of fish scattering were made. (As the SUS are omnidirectional, it was important to model not only those fish in the air-sea interaction zone, but those in the water column as well, such as the deep-layered, common worldwide, grenadier (Nero *et al*., 1997) .) Because acoustic signatures that identify fish scattering have been developed (Gauss *et al*. 2002), these data and models have made it possible to isolate and remove their contributions from the CST data (e.g., Fig. 1-3). The updated CST SUS SSS results **of this report reflect this volume-scattering-contribution removal process.** This has been crucial to determining the relative contributions of the air-water interface and sub-surface bubbles, especially at low-to-moderate wind speeds, and at low grazing angles and frequencies, and so improving our SSS modeling capability. (e.g., Gauss *et al*., 2006b).

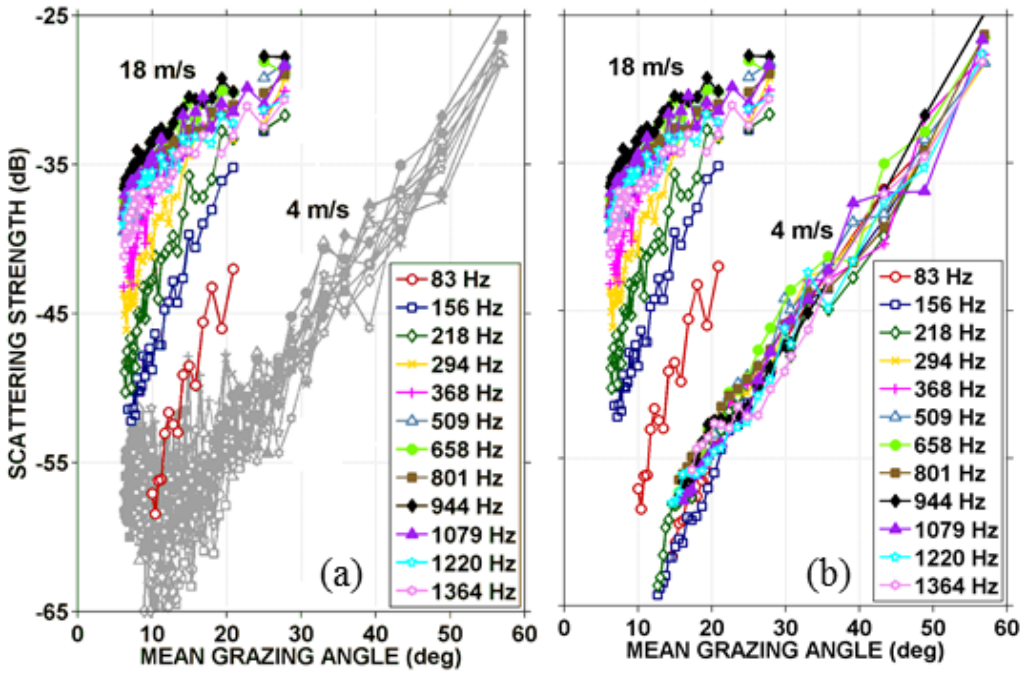

Fig. 1-3 – CST SSS vs. grazing angle example, where (a) and (b) respectively include and exclude fish-scattering contributions based on modeling of *in-situ* fish information.

For a variety of the sites at which a SUS was conducted, SSS-vs.-mean-grazing angle results are shown for a range of frequencies. It should be noted the mean grazing angle is the average of the incident and scattering grazing angles, which can vary considerably from one another, especially at high angles—see Fig. 4 of Ogden and Erskine (1994a). Hence, **for SSS model development and validation it is important to model these CST SUS SSS data taking account of their vertically bistatic geometry,** and not just monostatically (i.e., not just using the mean grazing angle). For this purpose, **the SSS data values as a function of frequency, incident grazing angle, scattered grazing angle, and horizontal bistatic angle are also archived on the report's CD.**

2. DATA PROCESSING AND ANALYSIS

A complete description of the experimental technique and analysis process may be found in Ogden and Erskine (1994a, b), as well as summarized in Ogden and Erskine (1997).

The sonar geometry was vertically bistatic (basically only a vertical source-receiver separation, with only a small horizontal separation). The HLA was towed from the M/V *Cory Chouest* (typically at ~1.5 m/s), with 10 to 20 SUS charges periodically launched from the same vessel over a 0.5- to 1-h period, where they exploded at depth, resulting in a bistatic source-receiver geometry. Spatially-Hammed beams with cosine-spaced main response axes were formed, with the most useful returns coming from the aft-looking beams.

After beamforming, reverberation time-series curves were obtained for individual shots and temporally aligned with respect to the shot-detonation time, and then linearly averaged to produce a single reverberation curve for each beam. In each case, data calibrations were applied to produce an estimate of the received reverberation level in μPa.

A raytrace program was then used to calculate the geometric effects unique to each measurement (using the *in-situ* sound-speed profile): 1) transmission-loss terms to and from the scattering patch were obtained by separately calculating the geometric spreading loss along each ray path; and 2) scattering-patch areas were obtained using computed beam patterns and raytraces. The plane-wave calculation assumes the source of the scattering is the air-sea interface; hence, **all the measured SSS values shown in this report represent effective-surface scattering strengths**.

Finally, the average reverberation curves were combined with these geometric parameters and source level to solve the sonar equation for backscattering strength as a function of frequency, beam, and grazing angles:

$$SSS = RL - SL + TL_s + TL_r - 10 \log A$$

where *SSS* is the surface scattering strength in dB, *RL* is the measured reverberation level in dB *re* $(1\mu Pa)^2$ at 1 m, *SL* is the source level in dB *re* $(1\mu Pa)^2$ at 1 m, TL_s is the transmission loss from the source to the ensonified patch on the bottom in dB, TL_r is the transmission loss from the ensonified patch on the bottom to the receiver in dB, and *A* is the area of the ensonified patch in m^2. The standard deviations due to shot-to-shot variability within a data set were typically ± 2 to 3 dB.

3. DATA SET AND ENVIRONMENTAL INFORMATION

Tables 3-1 and 3-2 catalog environmental conditions for each run: wind speed normalized to the standard 10-m elevation above the surface (U_{10}), SWH, sea-surface temperature (SST), and air-sea temperature difference (TD). Besides the mean U over the data run (typically 0.5 to 1 h in duration), 0.5- & 1-h back-averaged (wind history) values are listed.

ENVIRONMENTAL DATA CSTs 2, 3, 4 & 5

DATA SET		WIND SPEED AT 10-m (m/s)			SWH (m)	TEMPERATURE (°C)	
CST	Run	U_{10}	U_{10}_0.5-h back ave.	U_{10}_1-h back ave.		SST	TD
2	29	**11.32**	11.35	11.39	**3.40**	8.30	3.63
2	33	**10.44**	NA	NA	**3.40**	8.40	−0.99
2	43(M3)	**4.22**	4.13	3.97	**1.80**	8.20	0.14
3	2B	**7.35**	5.99	5.32	**1.30**	27.71	−0.11
3	3B	**6.78**	6.90	6.94	**1.50**	28.54	0.13
3	5D	**6.95**	6.45	6.06	**1.30**	28.16	0.81
3	5H	**10.29**	9.43	9.03	**1.50**	28.17	2.14
3	5J	**6.70**	7.05	7.56	**1.50**	28.20	1.41
3	33A	**9.09**	9.32	9.42	**1.80**	28.36	0.44
3	37A	**6.20**	6.48	6.67	**1.50**	28.30	0.10
3	51B	**6.50**	NA	NA	**1.00**	28.54	0.67
4	7	**6.74**	6.98	7.04	**4.15**	3.21	−1.23
4	28B	**10.23**	10.32	10.23	**3.31**	3.31	−1.39
4	32	**11.04**	10.98	10.63	**3.28**	3.36	−1.45
4	43B	**3.38**	3.29	4.60	**1.30**	3.42	−0.75
4	50E	**10.64**	10.70	10.68	**2.89**	3.71	−0.44
4	51E	**15.88**	15.55	14.84	**5.56**	3.71	0.57
4	52B	**12.37**	12.62	12.75	**4.12**	3.52	−0.63
4	59	**9.52**	9.45	9.69	**2.89**	3.55	−0.95
5	2	**5.20**	4.98	4.91	**0.90**	21.51	−0.03
5	14A	**2.85**	2.91	2.97	**0.40**	22.58	−0.54
5	33	**8.26**	8.21	8.19	**1.40**	23.25	−0.22
5	T1-3	**7.30**	7.36	6.95	**0.80**	23.13	0.16
5	T2-6	**2.37**	2.33	2.50	**0.30**	23.83	0.12
5	46	**5.43**	5.29	5.17	**0.40**	24.57	0.07
5	48	**3.63**	3.68	3.70	**0.30**	23.80	−0.54

Fig. 3-1 – Environmental conditions for CSTs 2–5.

ENVIRONMENTAL DATA CST-7 Phase-2 & CST-8

DATA SET		WIND SPEED AT 10-m (m/s)			SWH (m)	TEMPERATURE (°C)	
CST	Run	U_{10}	U_{10}_0.5-h back ave.	U_{10}_1-h back ave.		SST	TD
7	1A	**7.20**	7.13	7.05	**3.00**	5.74	1.17
7	3C	**15.19**	15.04	14.85	**3.00**	5.46	0.91
7	5B	**8.81**	9.21	9.11	**3.12**	5.50	–1.58
7	11C	**13.02**	12.88	12.60	**3.62**	5.57	1.36
7	12D	**16.66**	16.35	15.95	**4.05**	5.64	1.40
7	13C	**6.44**	5.52	6.20	**3.65**	5.55	–1.48
7	16B	**17.76**	17.39	17.32	**4.92**	5.38	2.79
7	16G	**15.86**	16.05	16.54	**4.95**	5.27	3.15
7	18B	**5.97**	6.17	5.92	**3.23**	5.76	2.45
7	19C	**7.43**	7.22	6.89	**3.04**	5.64	2.69
7	20B	**10.17**	10.11	9.88	**2.61**	5.64	2.77
7	21C	**10.82**	11.05	11.12	**2.95**	5.54	3.00
7	23C	**7.83**	7.82	7.79	**2.97**	5.40	2.65
7	24B	**4.71**	4.64	4.57	**2.05**	5.56	2.92
7	25D	**3.15**	3.64	3.83	**2.18**	5.28	2.00
7	26B	**5.34**	4.92	4.47	**1.93**	5.51	2.24
7	29E	**8.15**	7.98	7.73	**2.36**	5.32	–0.21
7	34A1	**9.18**	8.97	8.79	**2.85**	5.52	2.58
7	34A2	**10.40**	10.28	10.02	**2.92**	5.66	3.13
7	34A3	**10.29**	10.27	10.29	**2.92**	5.72	3.27
8	B3A	**3.94**	4.35	4.59	**1.42**	17.29	0.10
8	B7	**1.93**	2.17	2.50	**0.61**	17.61	0.46
8	B9	**2.10**	2.26	2.16	**0.61**	17.54	0.42
8	B11	**2.10**	2.06	2.02	**0.49**	17.40	0.25
8	B13	**1.58**	1.79	1.99	**0.49**	18.27	0.64
8	B14	**1.20**	1.24	1.37	**0.60**	18.88	0.50
8	B16	**4.09**	3.75	3.58	**0.45**	18.53	0.38
8	B17	**8.64**	8.13	7.67	**0.53**	18.26	–0.12
8	B18	**8.49**	8.94	9.37	**0.78**	18.03	–0.30

Fig. 3-2 – Environmental conditions for CST-7 Phase 2 and CST 8.

4. MEASURED SURFACE BACKSCATTERING STRENGTHS

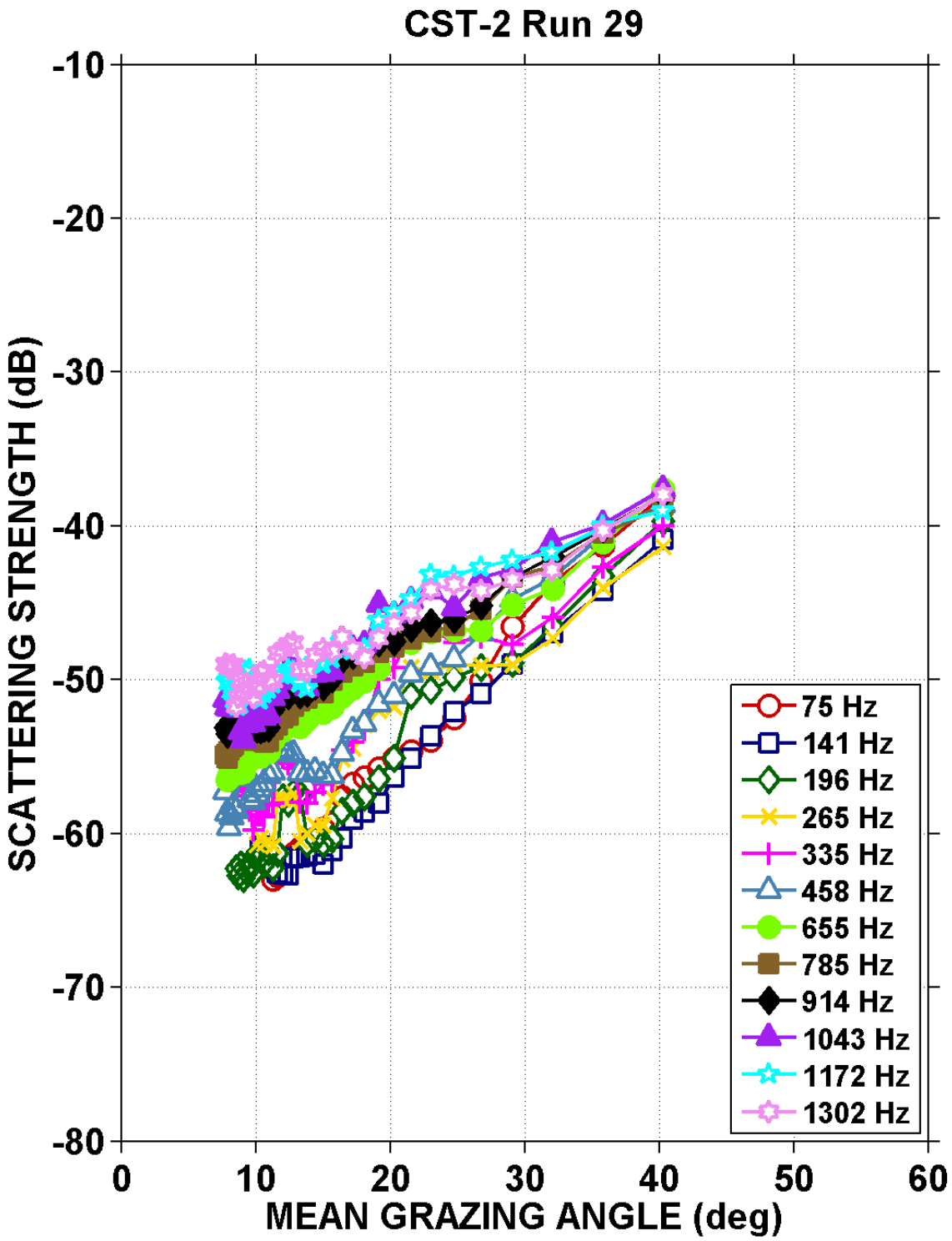

Fig. 4-1 – Surface backscattering strengths vs. mean grazing angle for CST-2 Run 29.

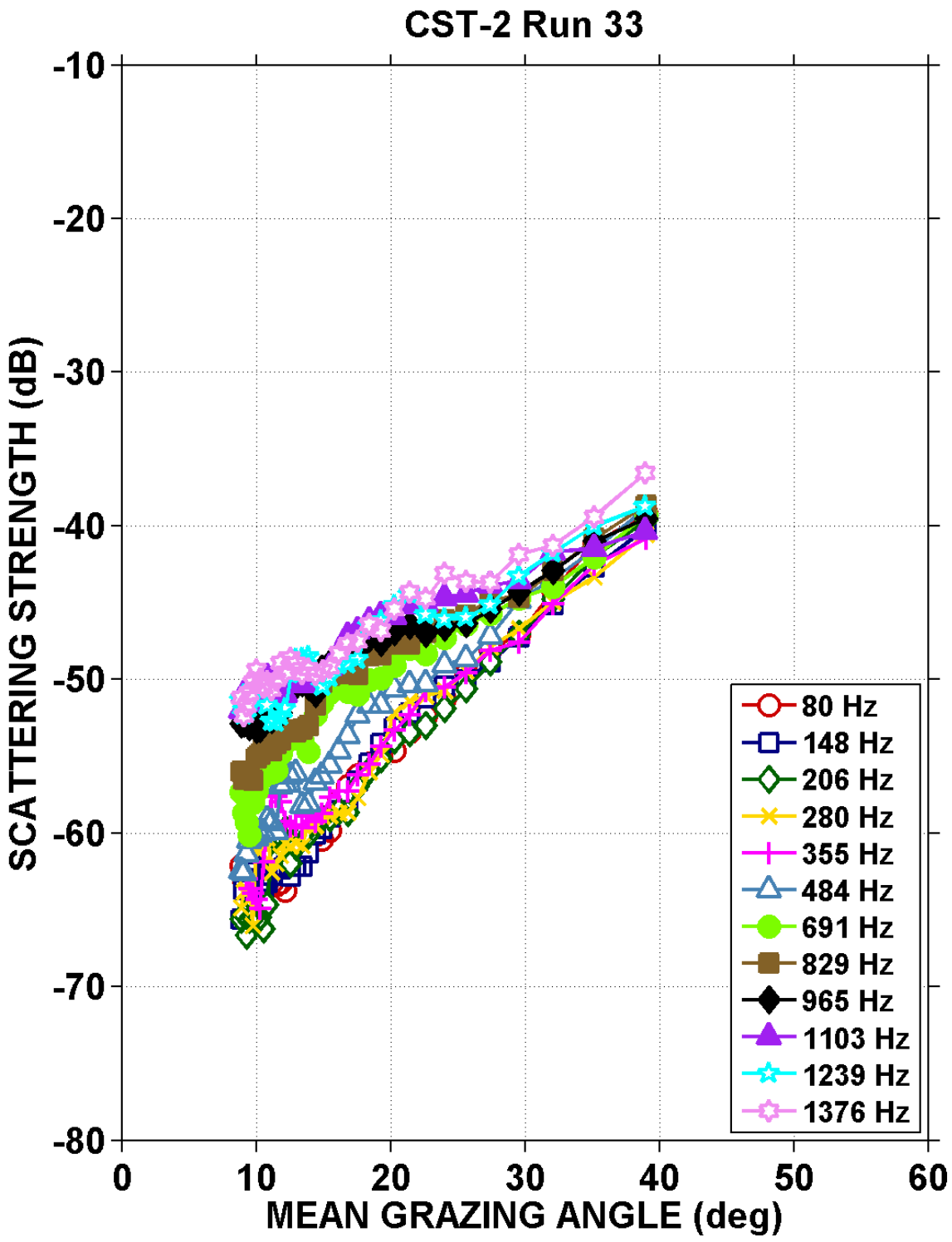

Fig. 4-2 – Surface backscattering strengths vs. mean grazing angle for CST-2 Run 33.

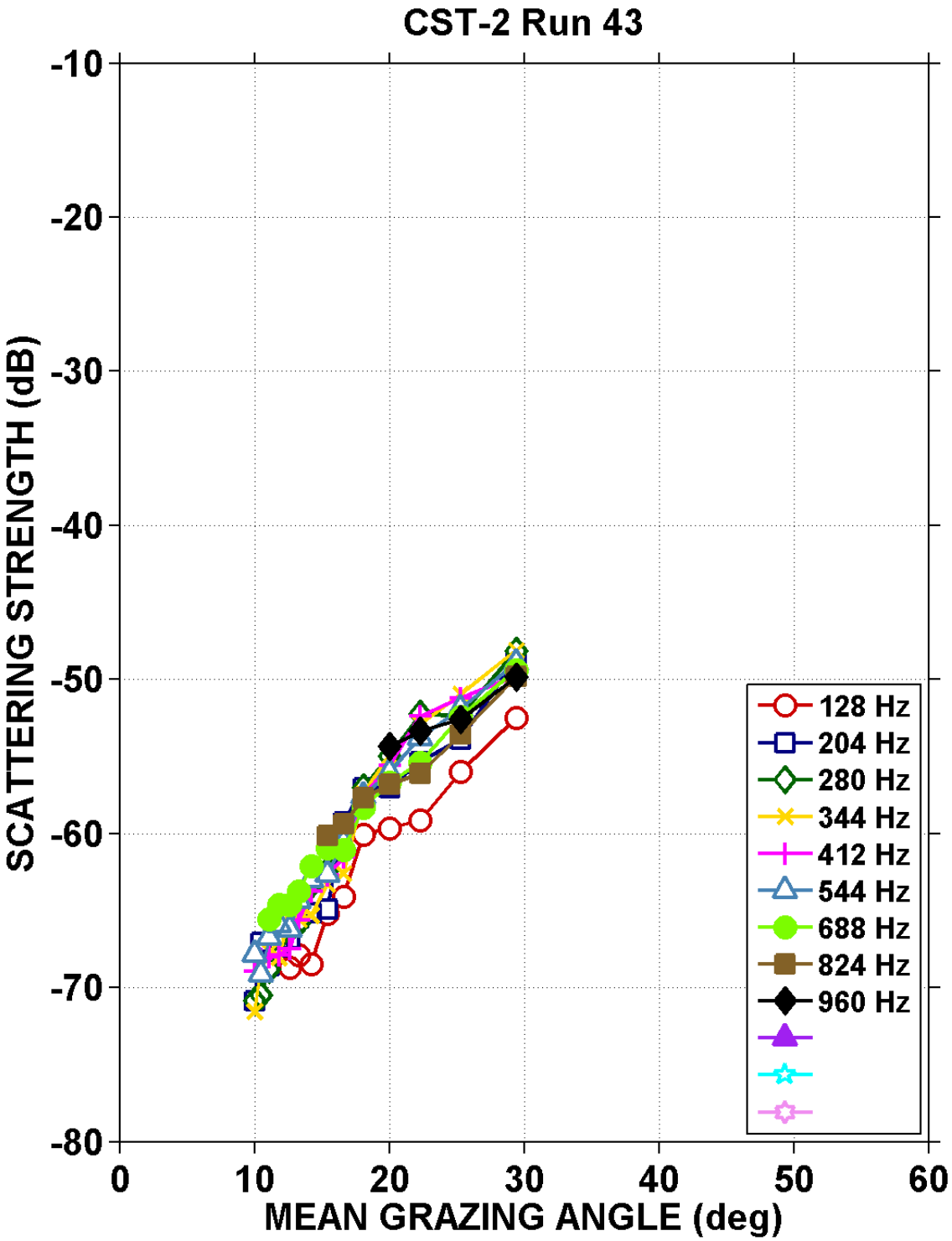

Fig. 4-3 – Surface backscattering strengths vs. mean grazing angle for CST-2 Run 43.

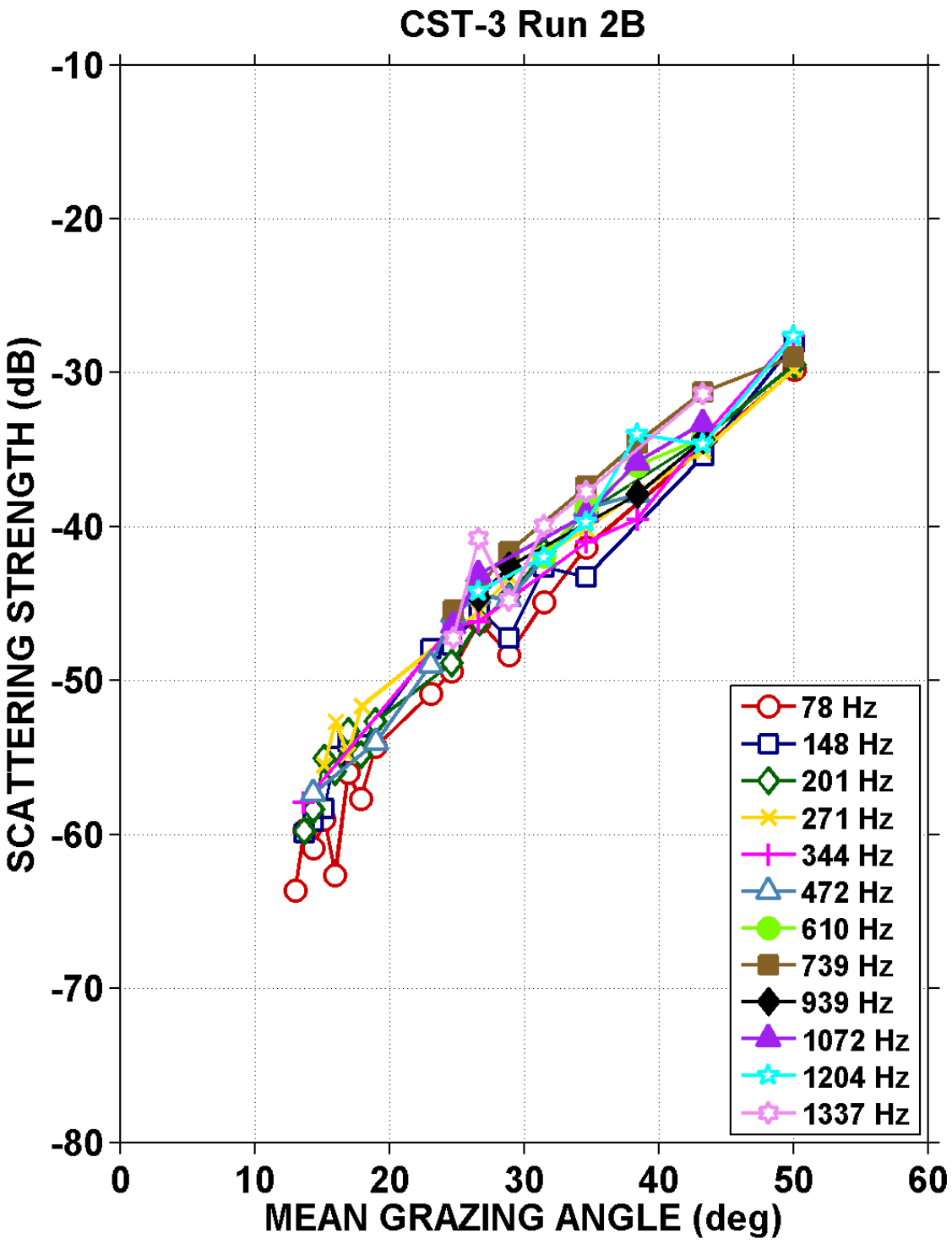

Fig. 4-4 – Surface backscattering strengths vs. mean grazing angle for CST-3 Run 2B.

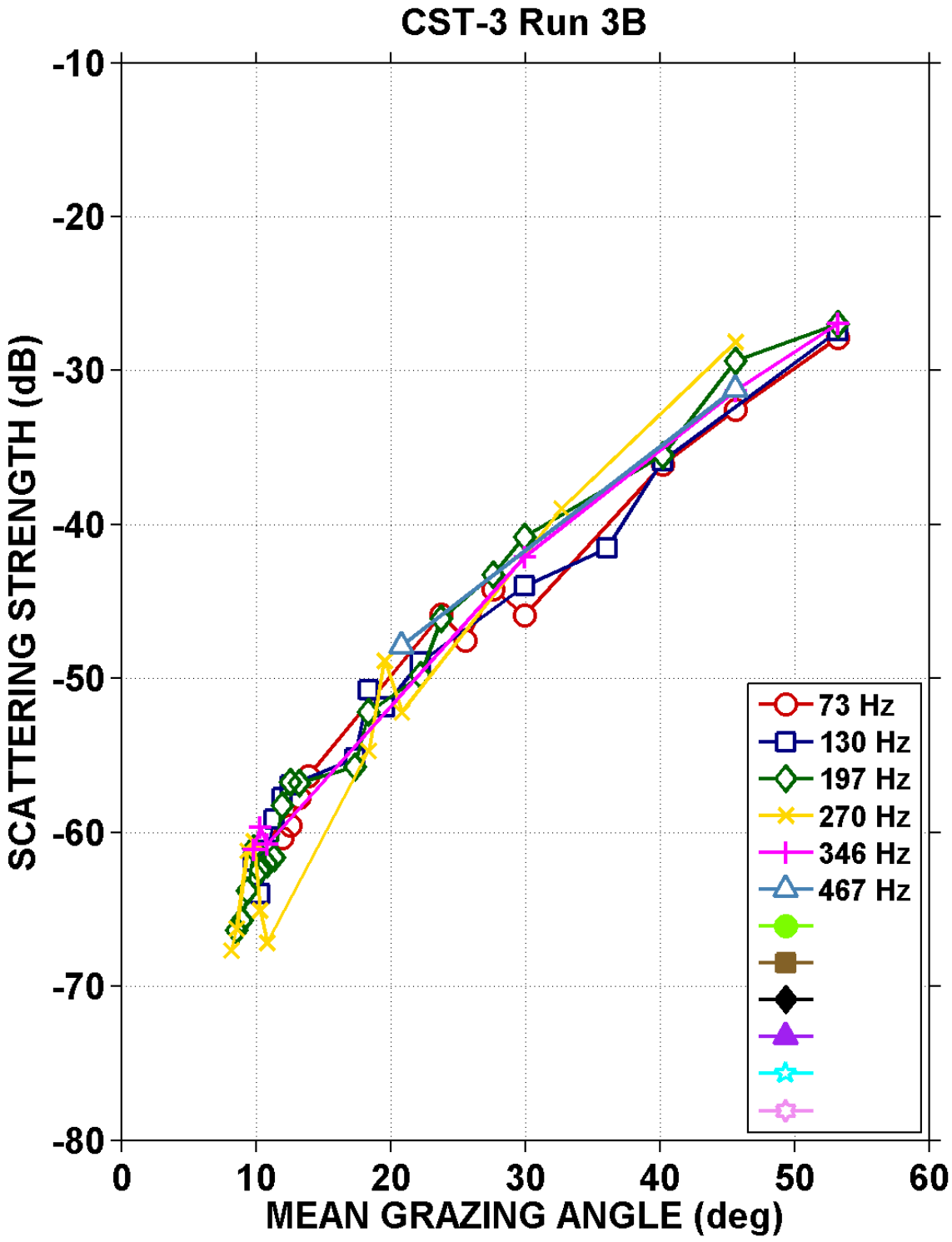

Fig. 4-5 – Surface backscattering strengths vs. mean grazing angle for CST-3 Run 3B.

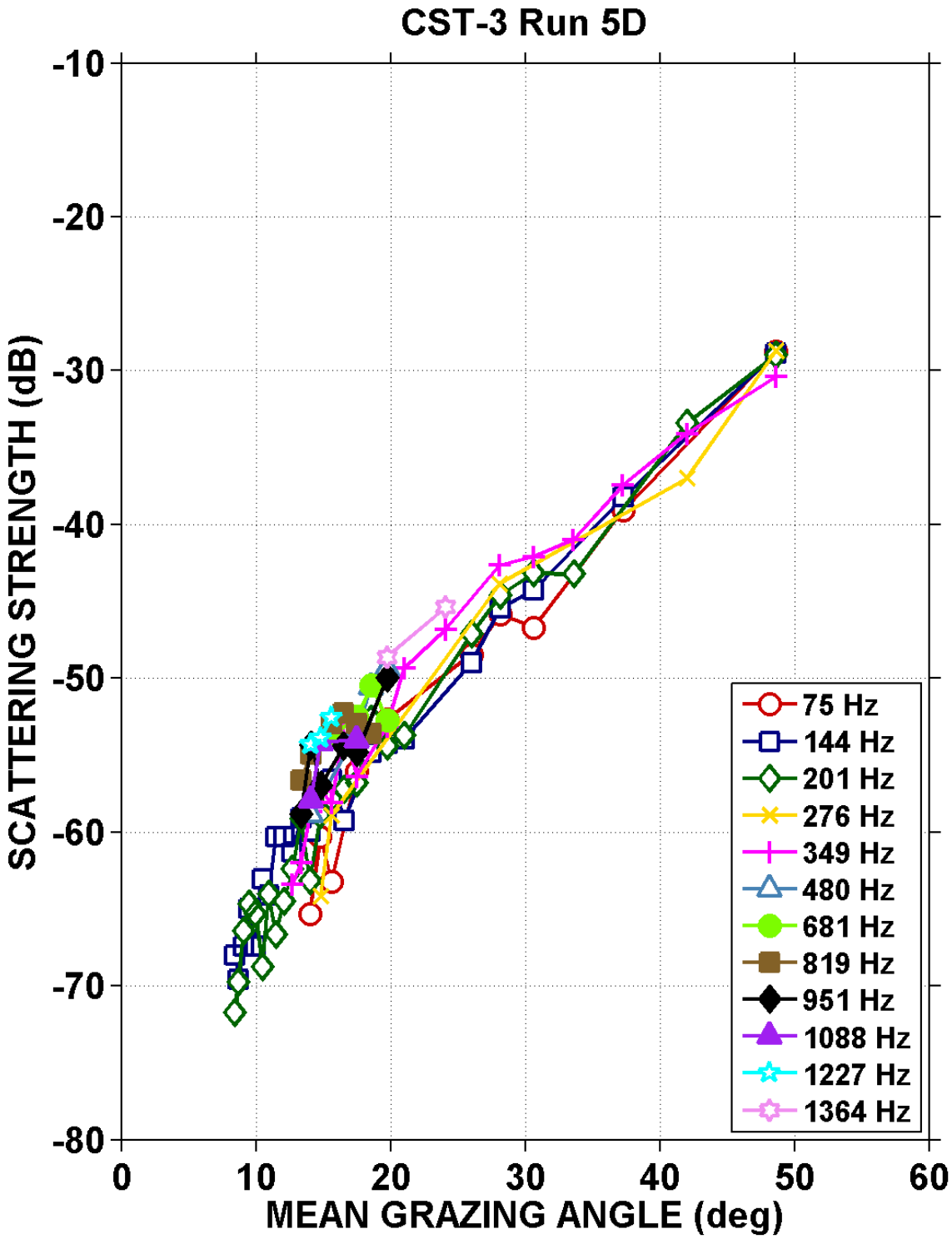

Fig. 4-6 – Surface backscattering strengths vs. mean grazing angle for CST-3 Run 5D.

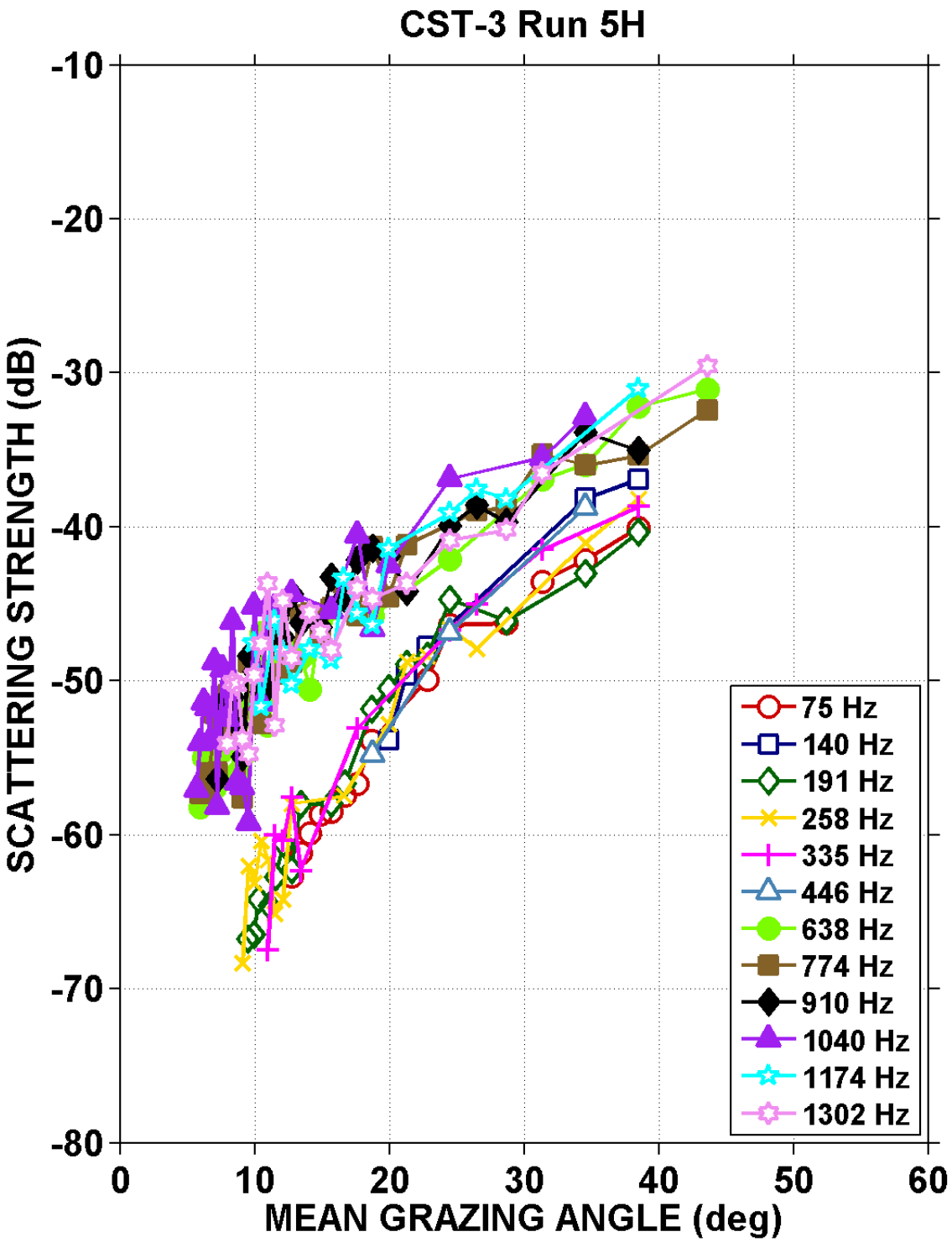

Fig. 4-7 – Surface backscattering strengths vs. mean grazing angle for CST-3 Run 5H.

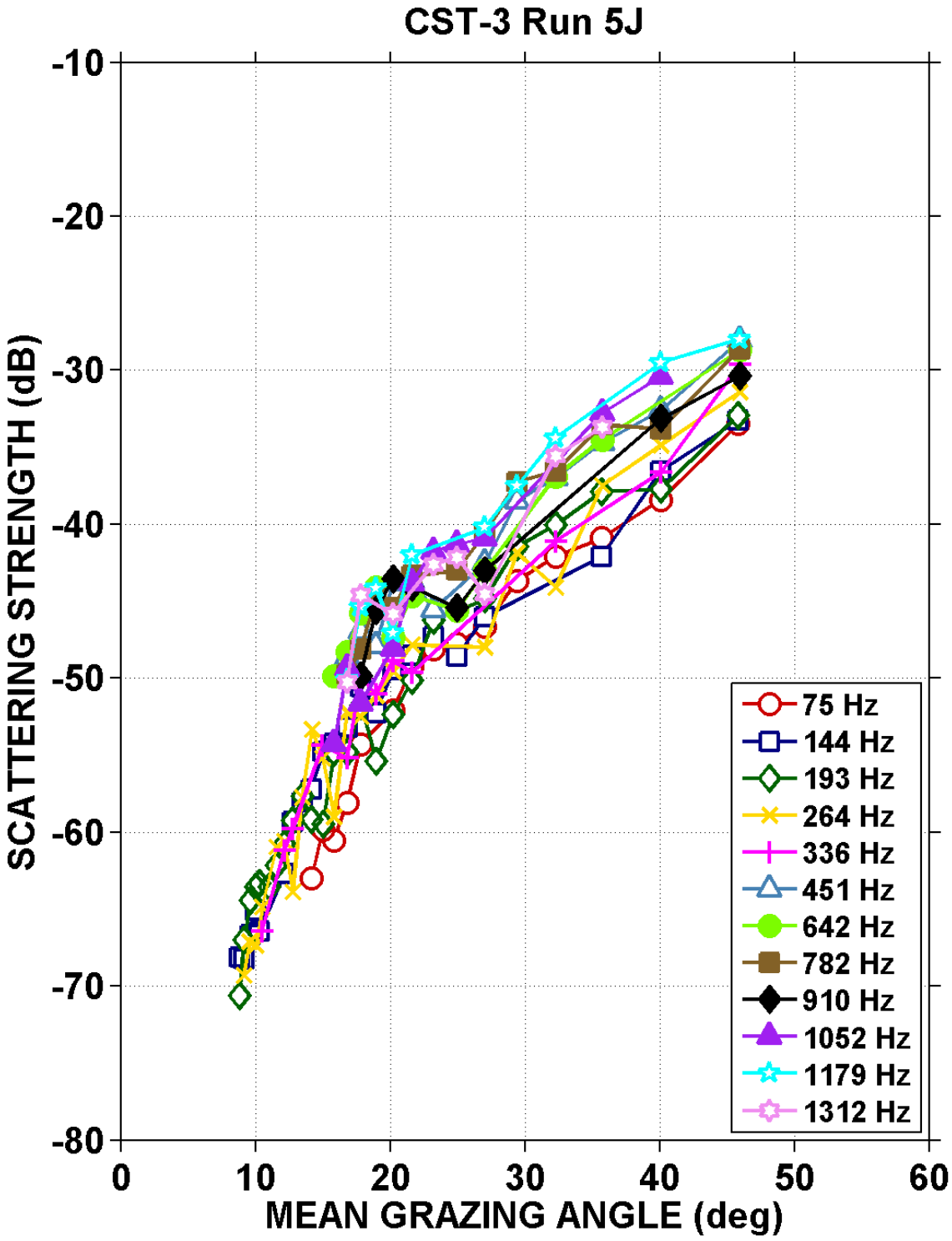

Fig. 4-8 – Surface backscattering strengths vs. mean grazing angle for CST-3 Run 5J.

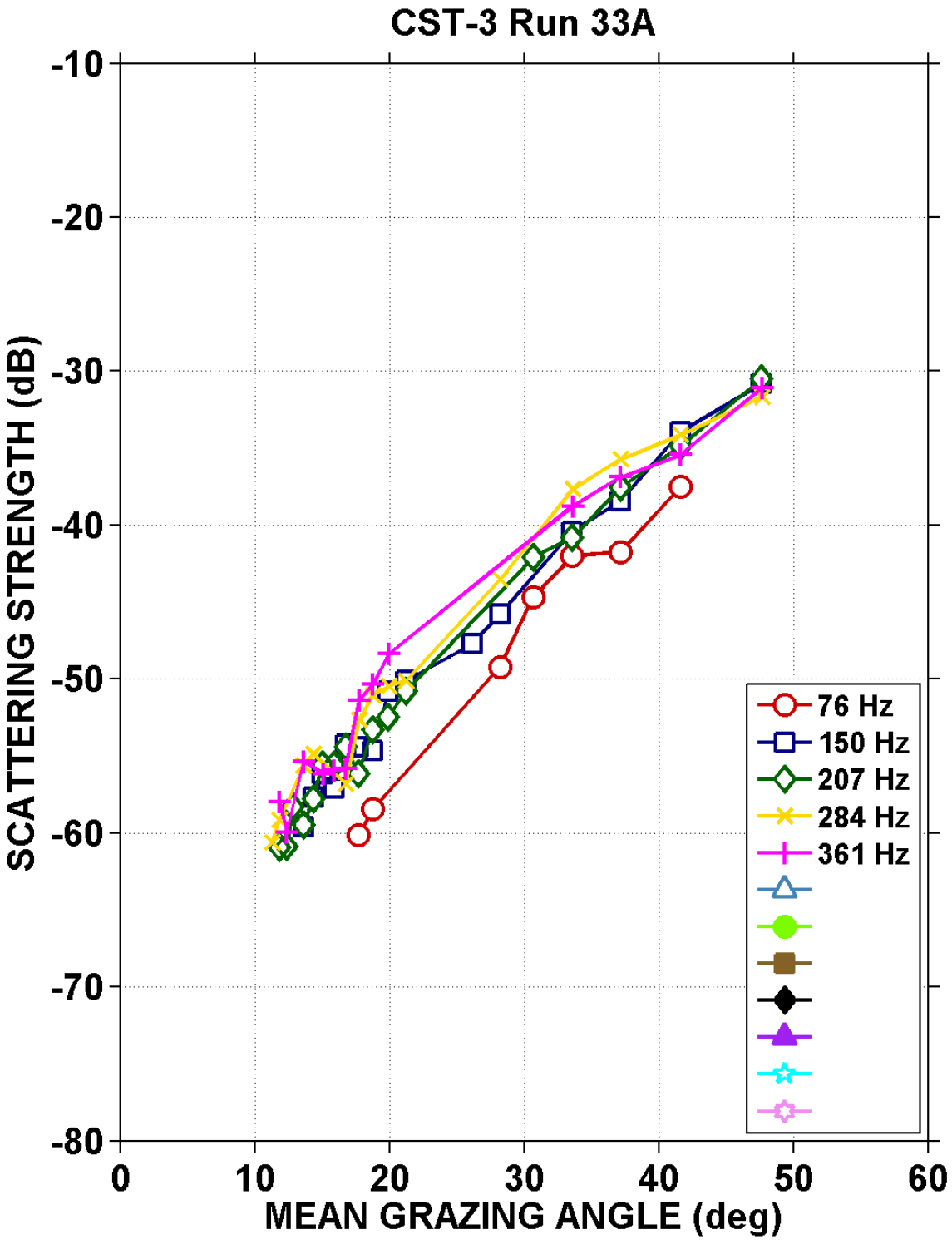

Fig. 4-9 – Surface backscattering strengths vs. mean grazing angle for CST-3 Run 33A.

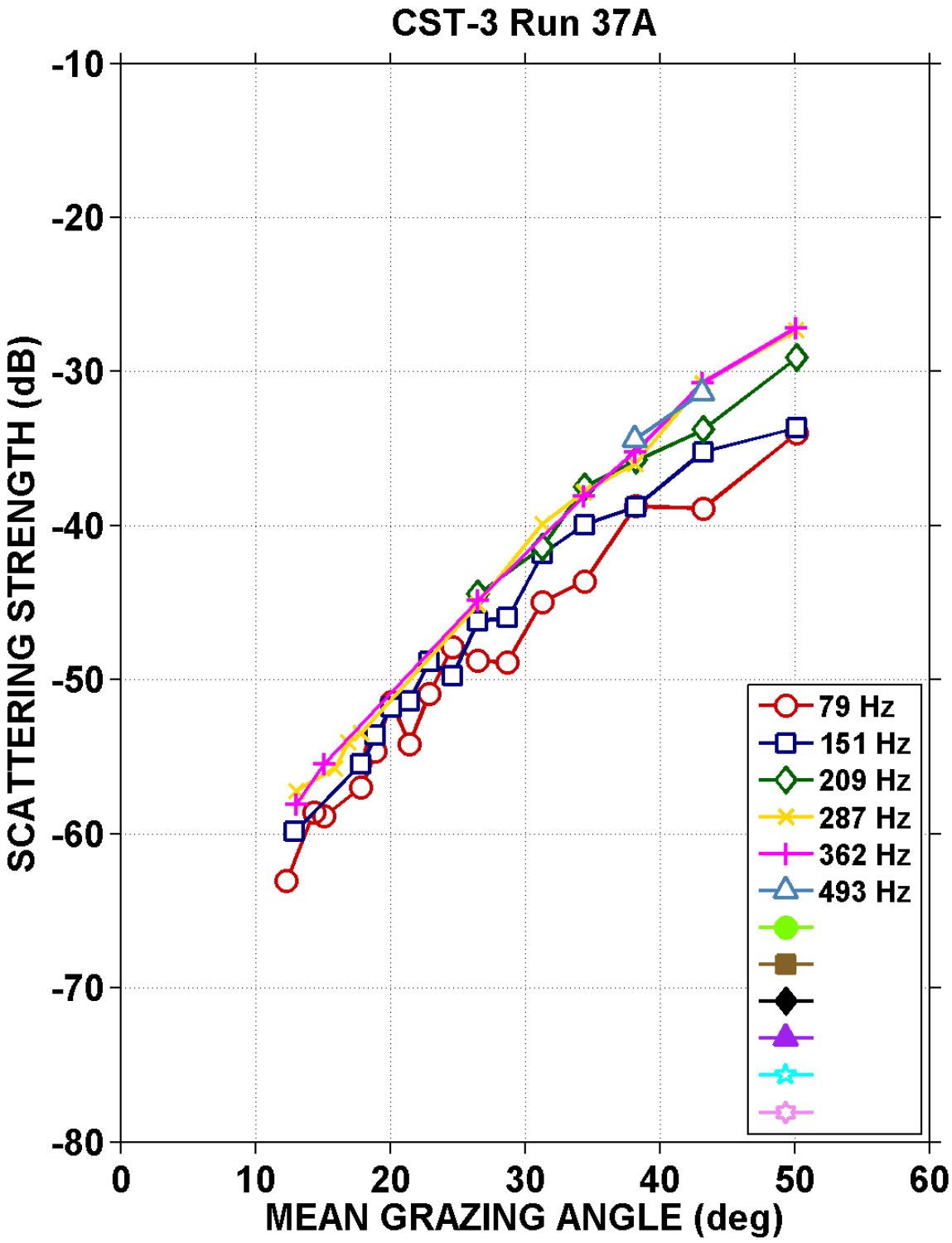

Fig. 4-10 – Surface backscattering strengths vs. mean grazing angle for CST-3 Run 37A.

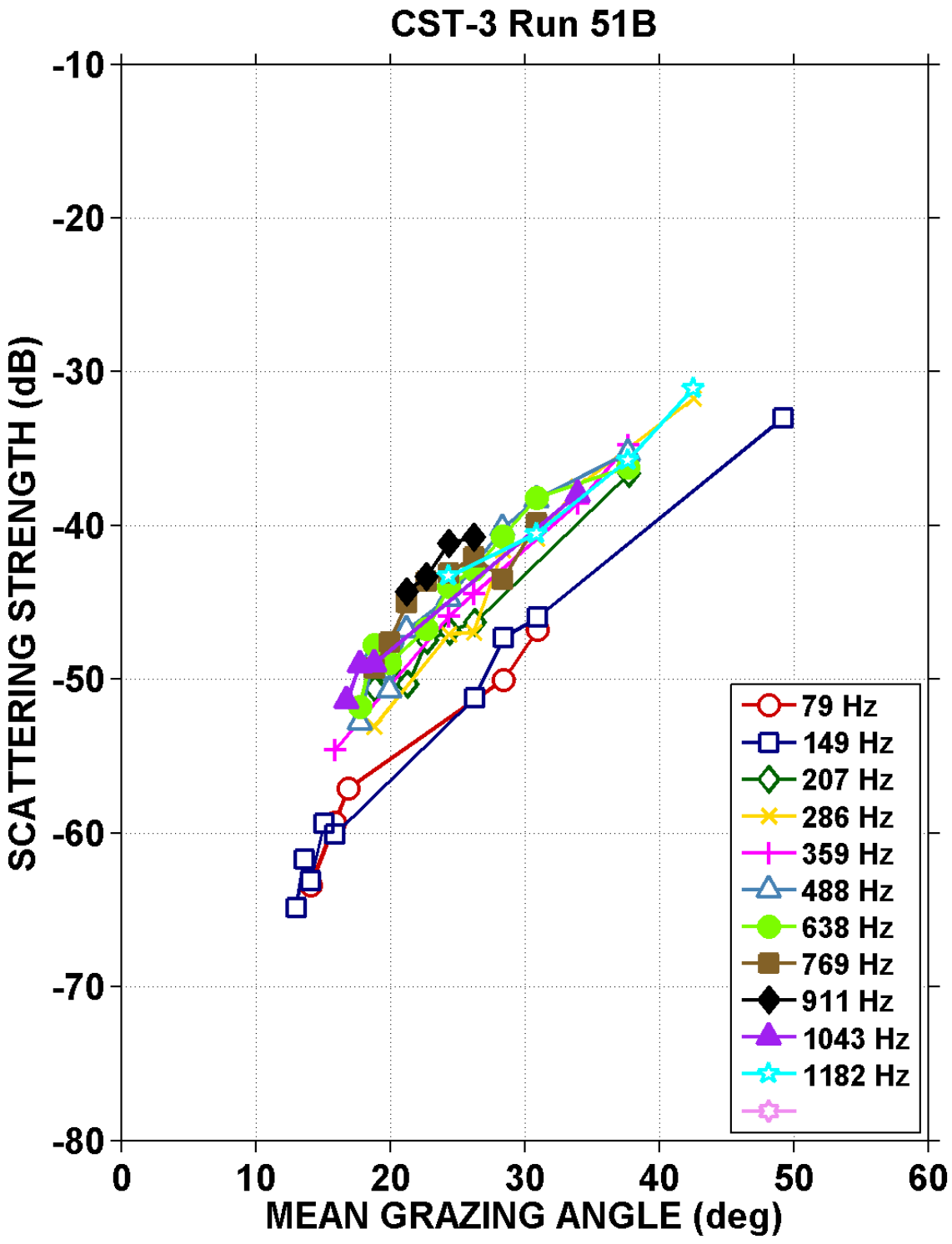

Fig. 4-11 – Surface backscattering strengths vs. mean grazing angle for CST-3 Run 51B.

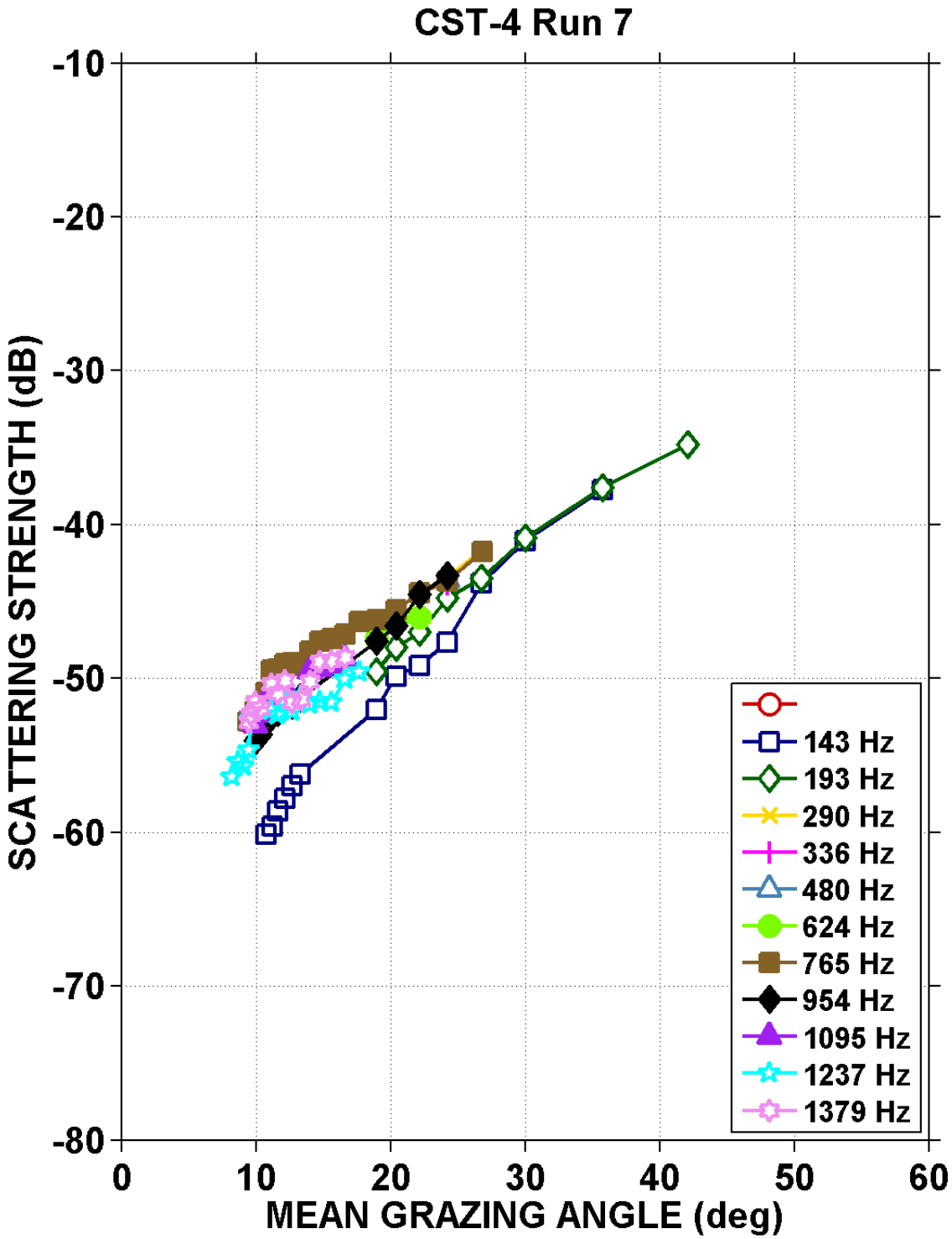

Fig. 4-12 – Surface backscattering strengths vs. mean grazing angle for CST-4 Run 7.

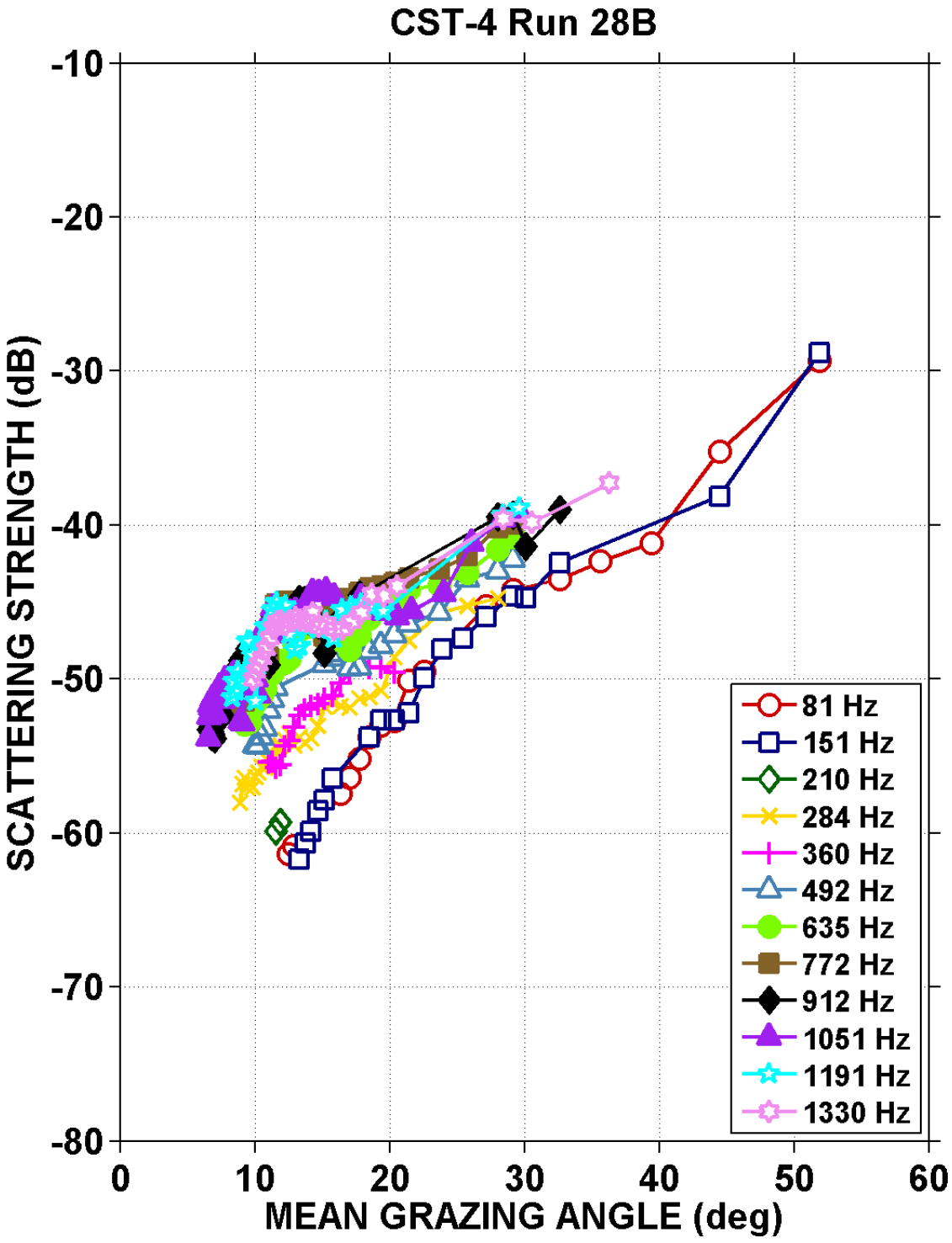

Fig. 4-13 – Surface backscattering strengths vs. mean grazing angle for CST-4 Run 28B.

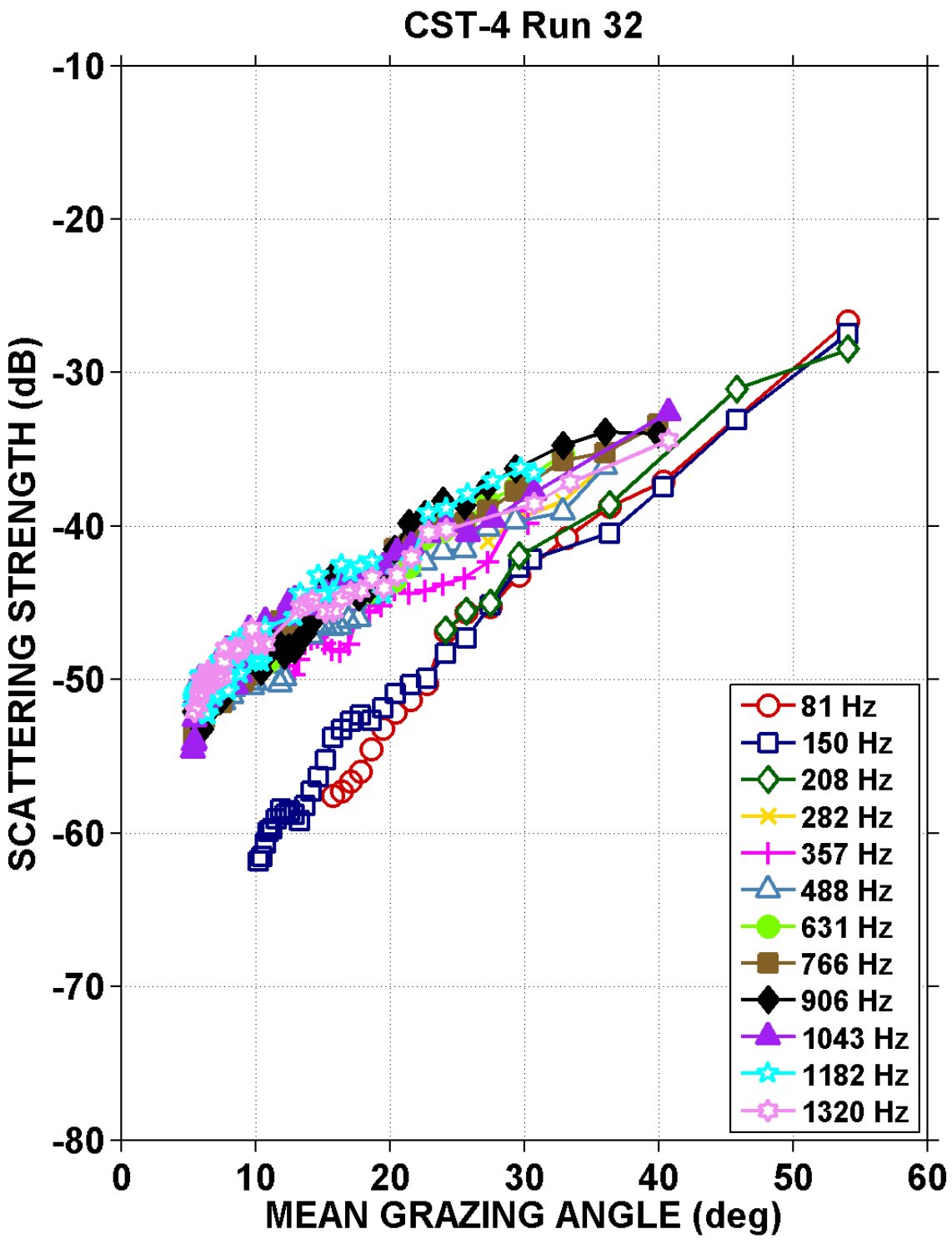

Fig. 4-14 – Surface backscattering strengths vs. mean grazing angle for CST-4 Run 32.

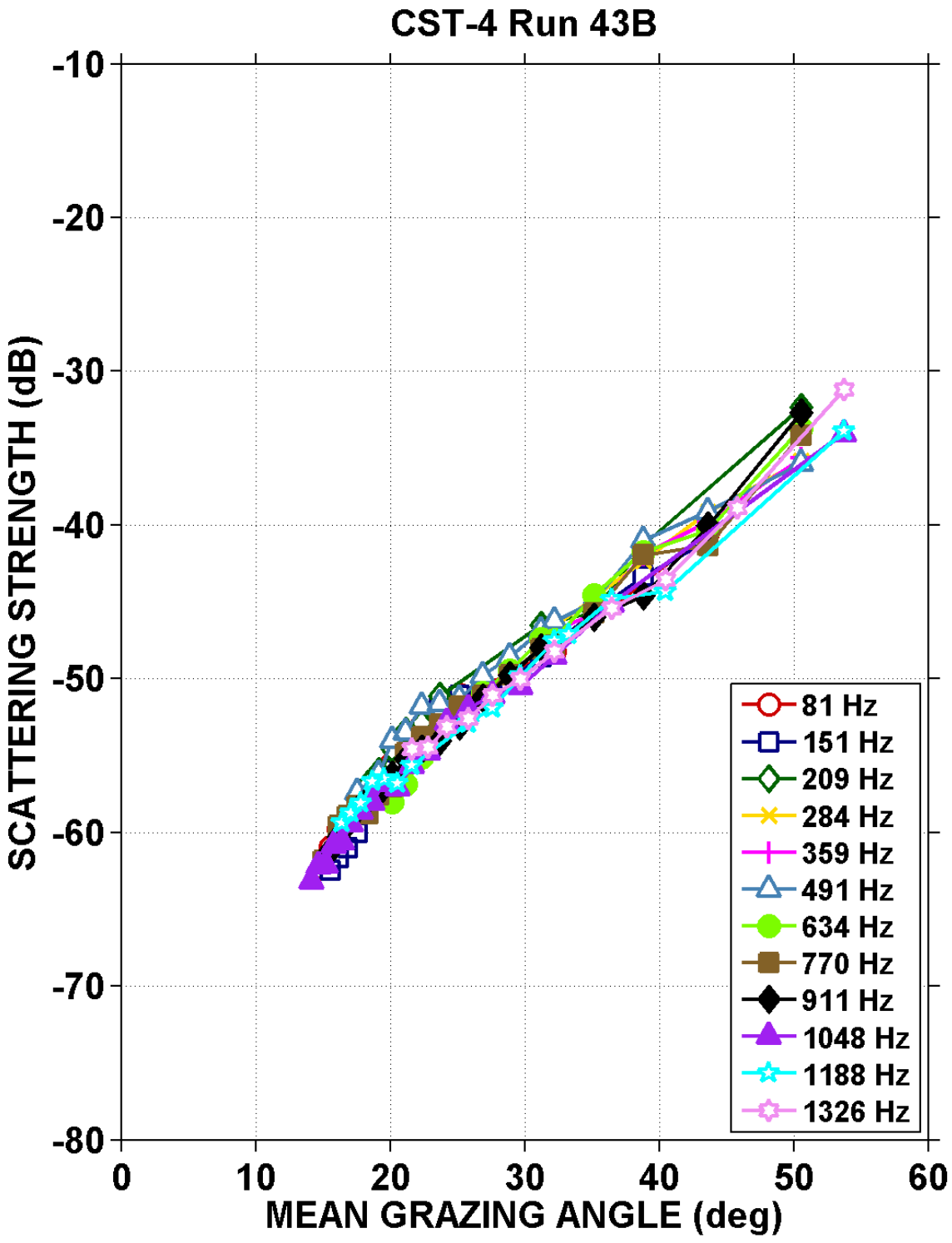

Fig. 4-15 – Surface backscattering strengths vs. mean grazing angle for CST-4 Run 43B.

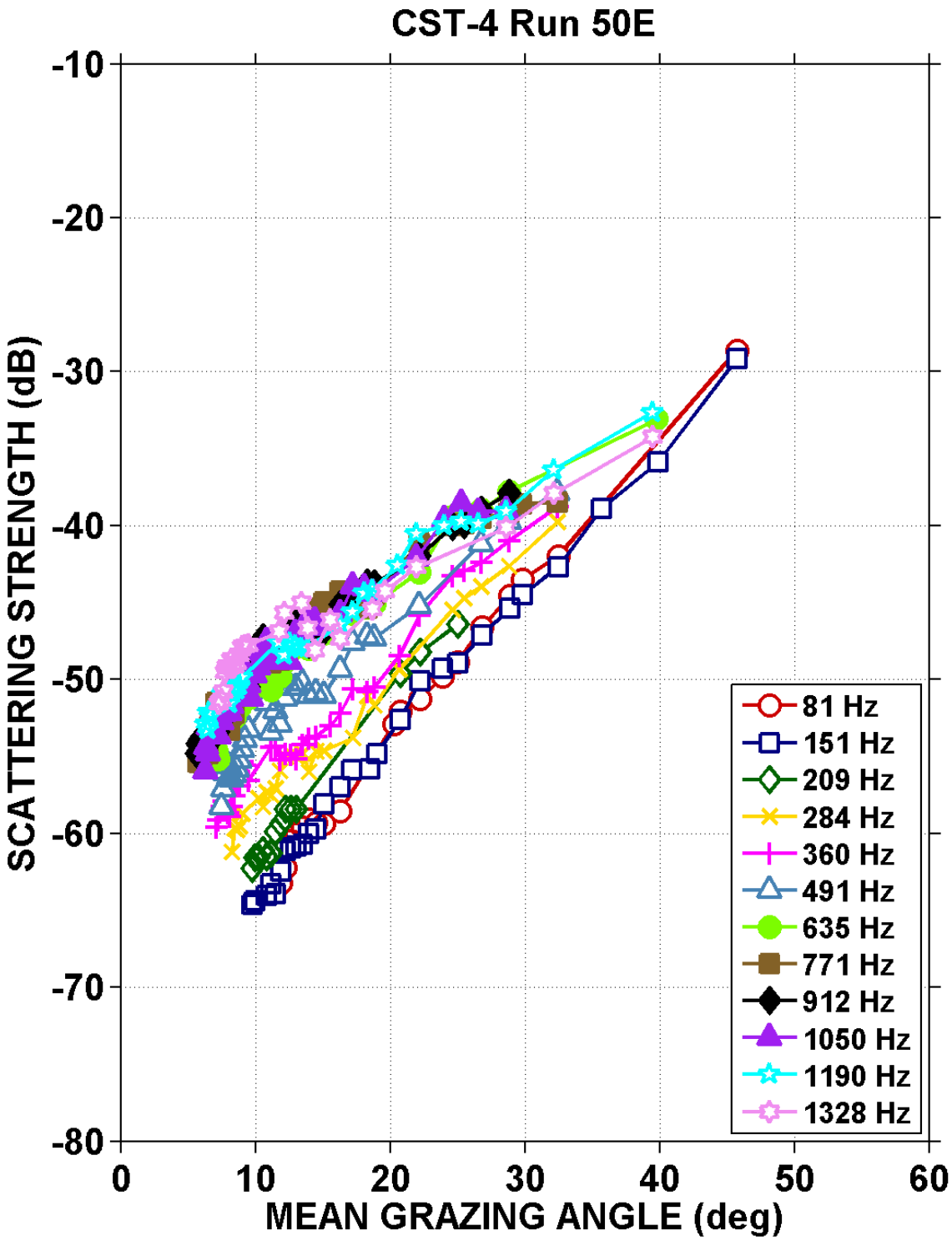

Fig. 4-16 – Surface backscattering strengths vs. mean grazing angle for CST-4 Run 50E.

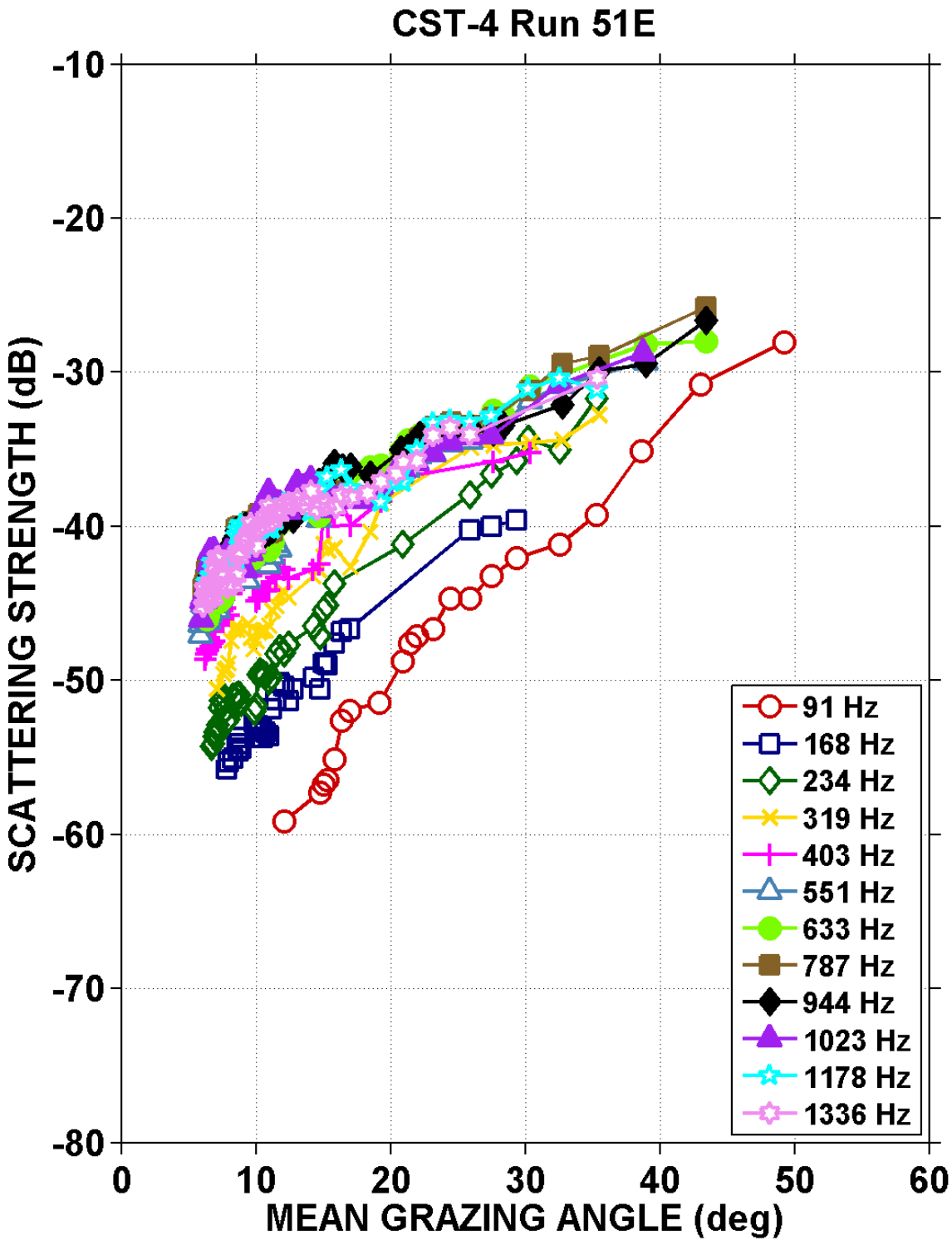

Fig. 4-17 – Surface backscattering strengths vs. mean grazing angle for CST-4 Run 51E.

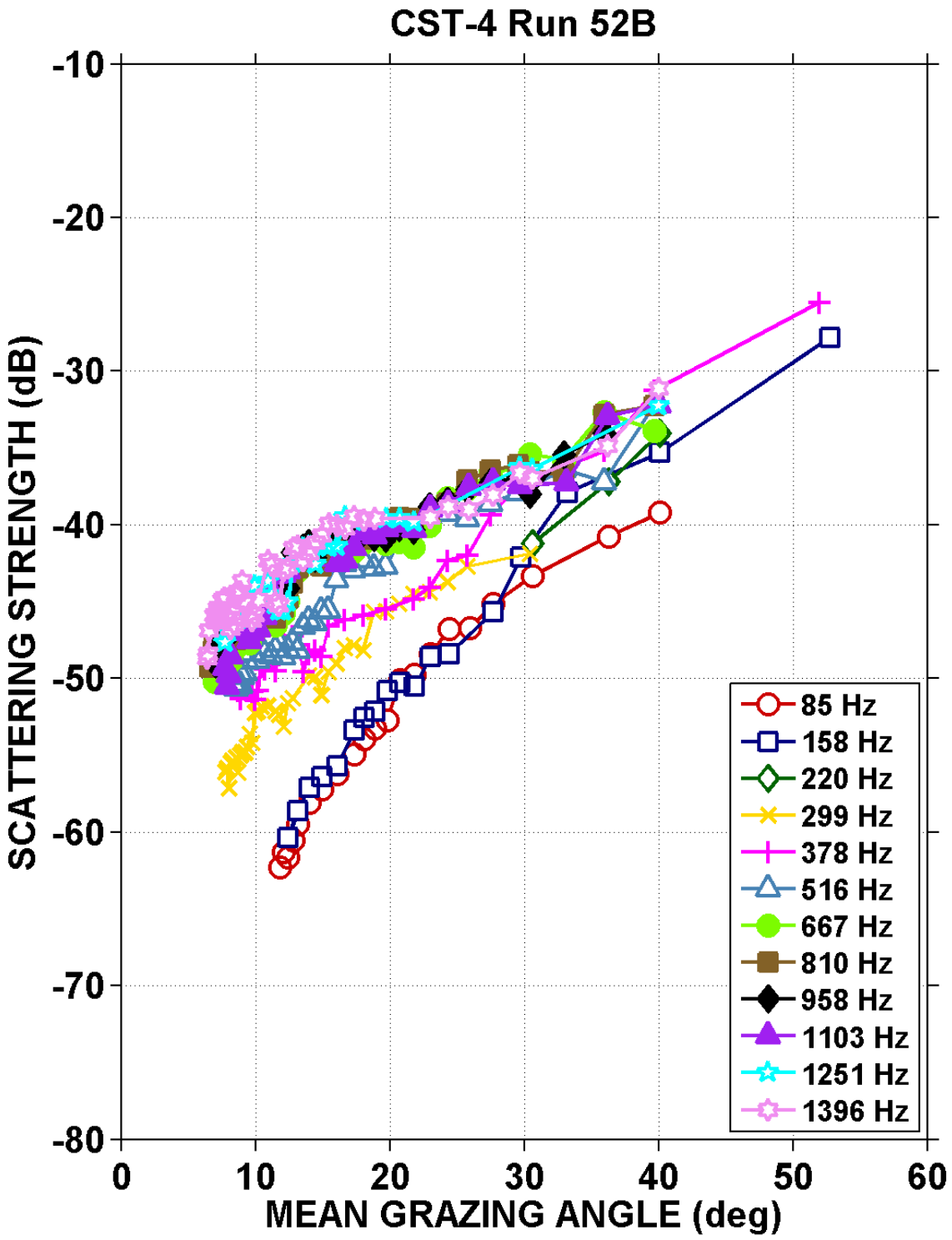

Fig. 4-18 – Surface backscattering strengths vs. mean grazing angle for CST-4 Run 52B.

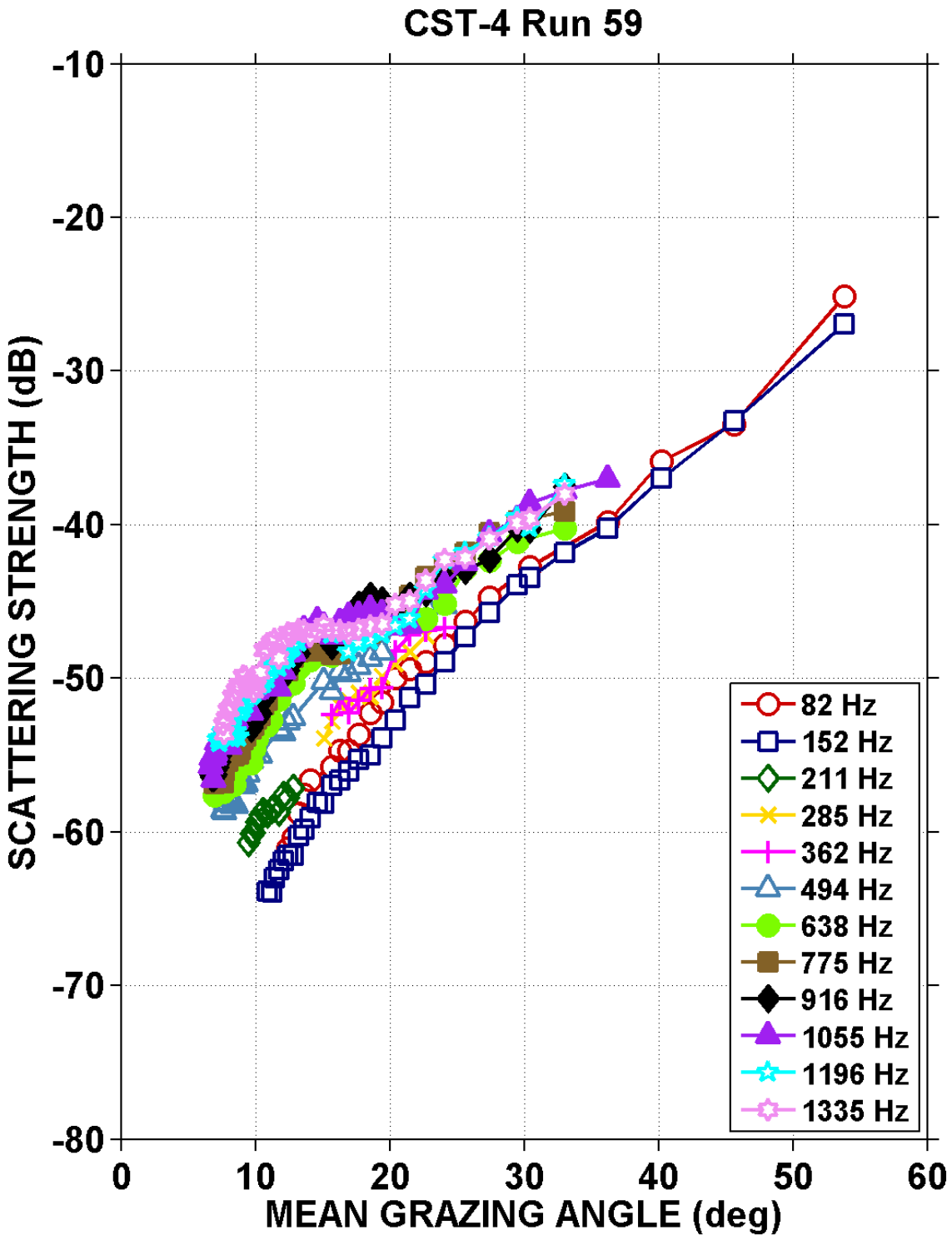

Fig. 4-19 – Surface backscattering strengths vs. mean grazing angle for CST-4 Run 59.

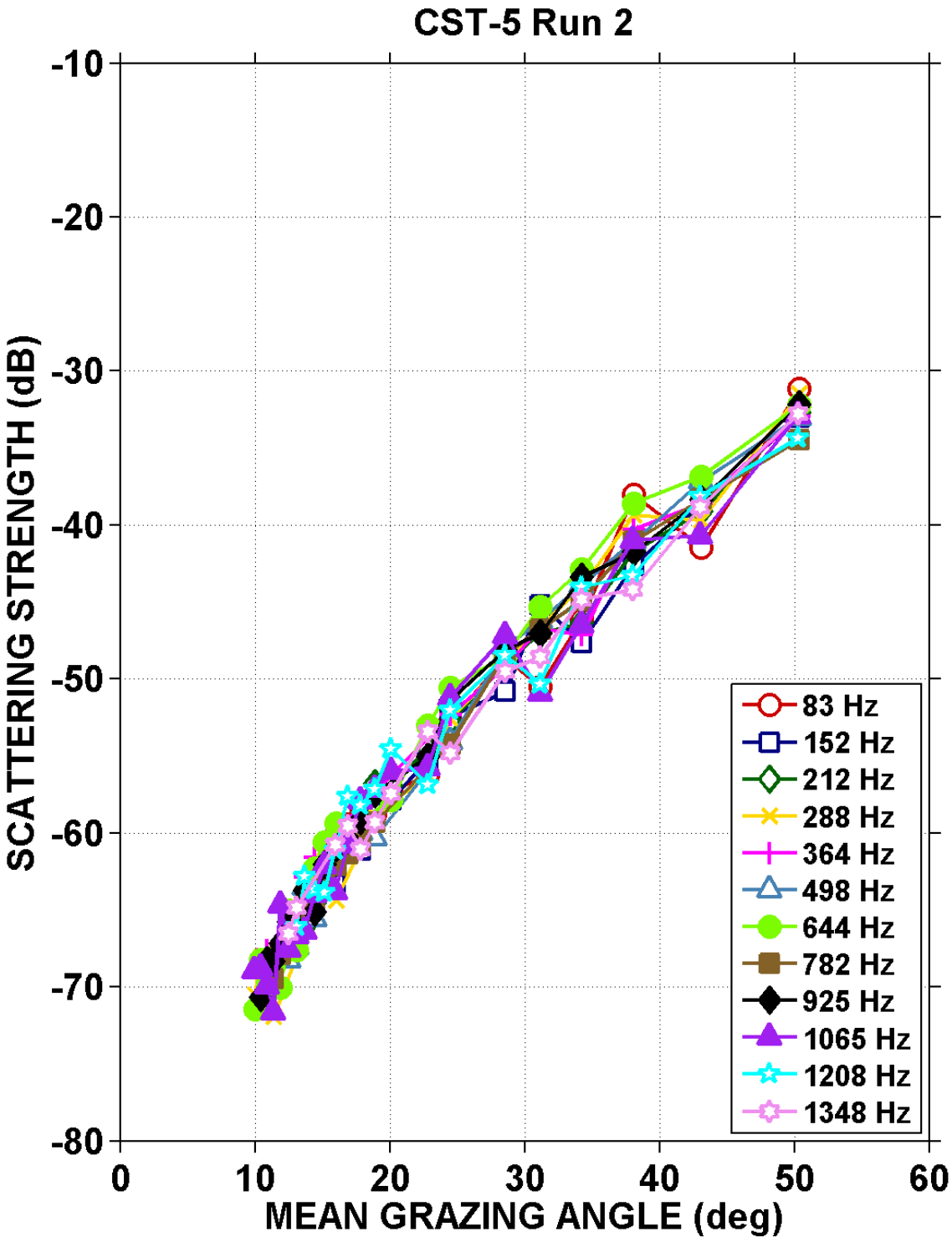

Fig. 4-20 – Surface backscattering strengths vs. mean grazing angle for CST-5 Run 2.

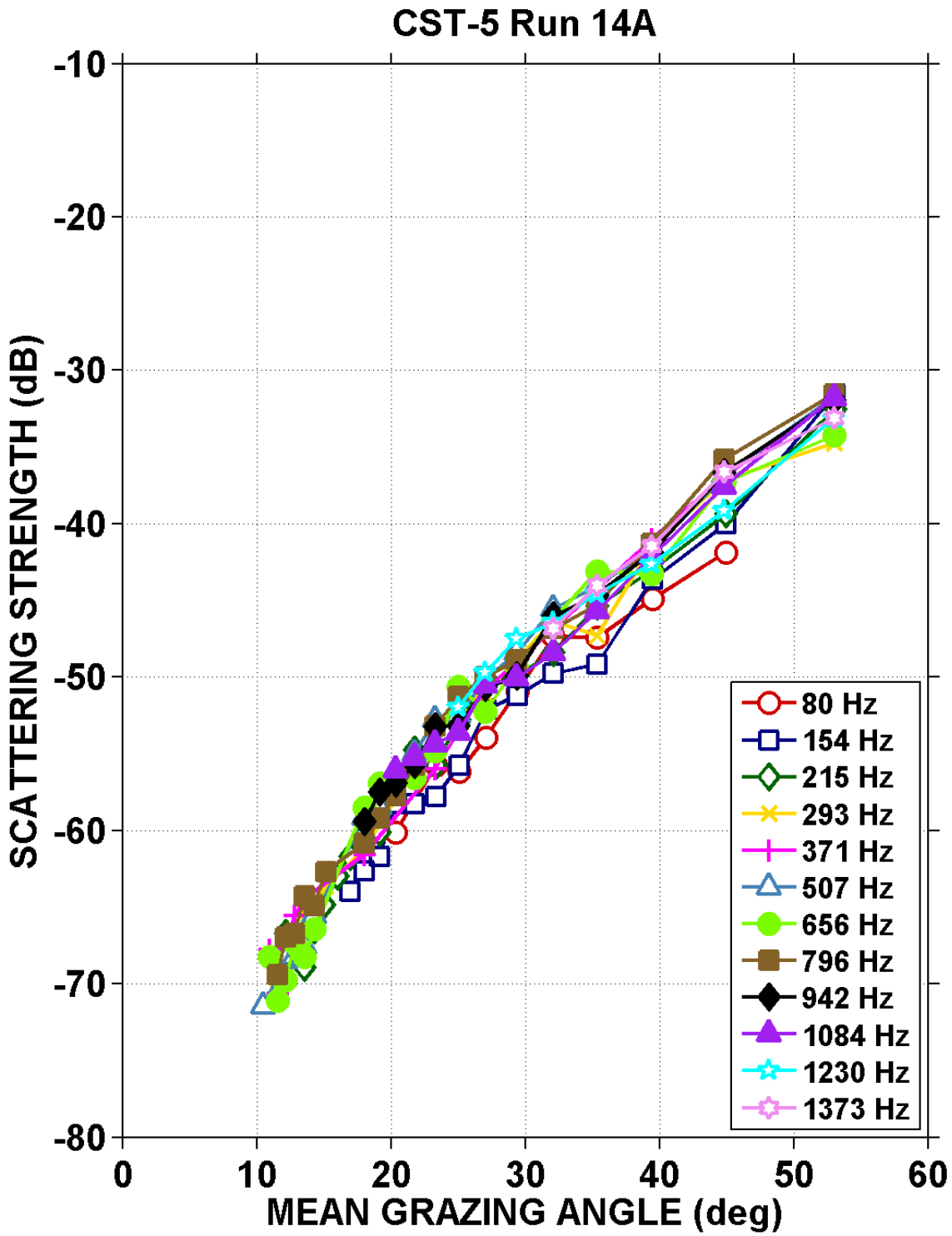

Fig. 4-21 – Surface backscattering strengths vs. mean grazing angle for CST-5 Run 14A.

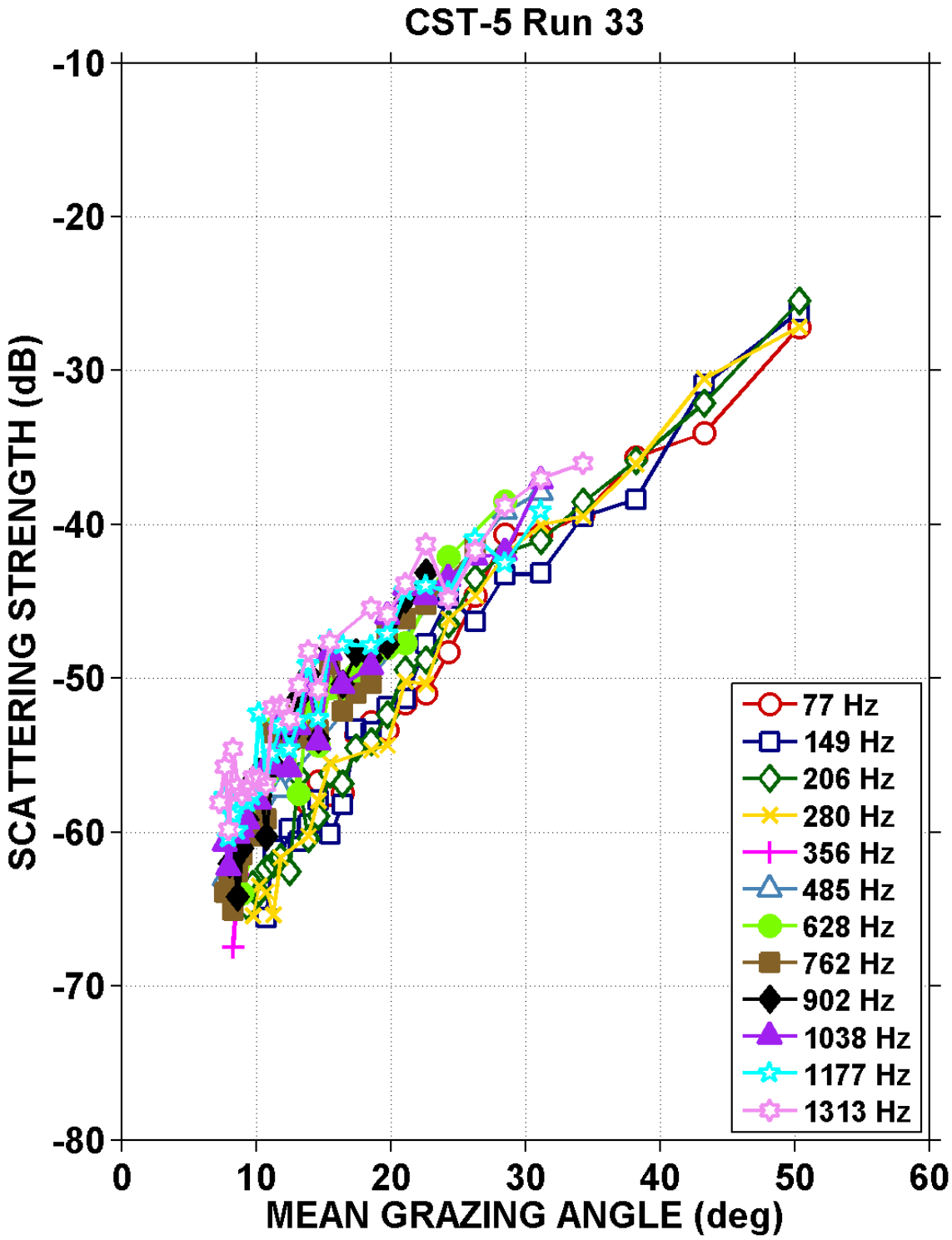

Fig. 4-22 – Surface backscattering strengths vs. mean grazing angle for CST-5 Run 33.

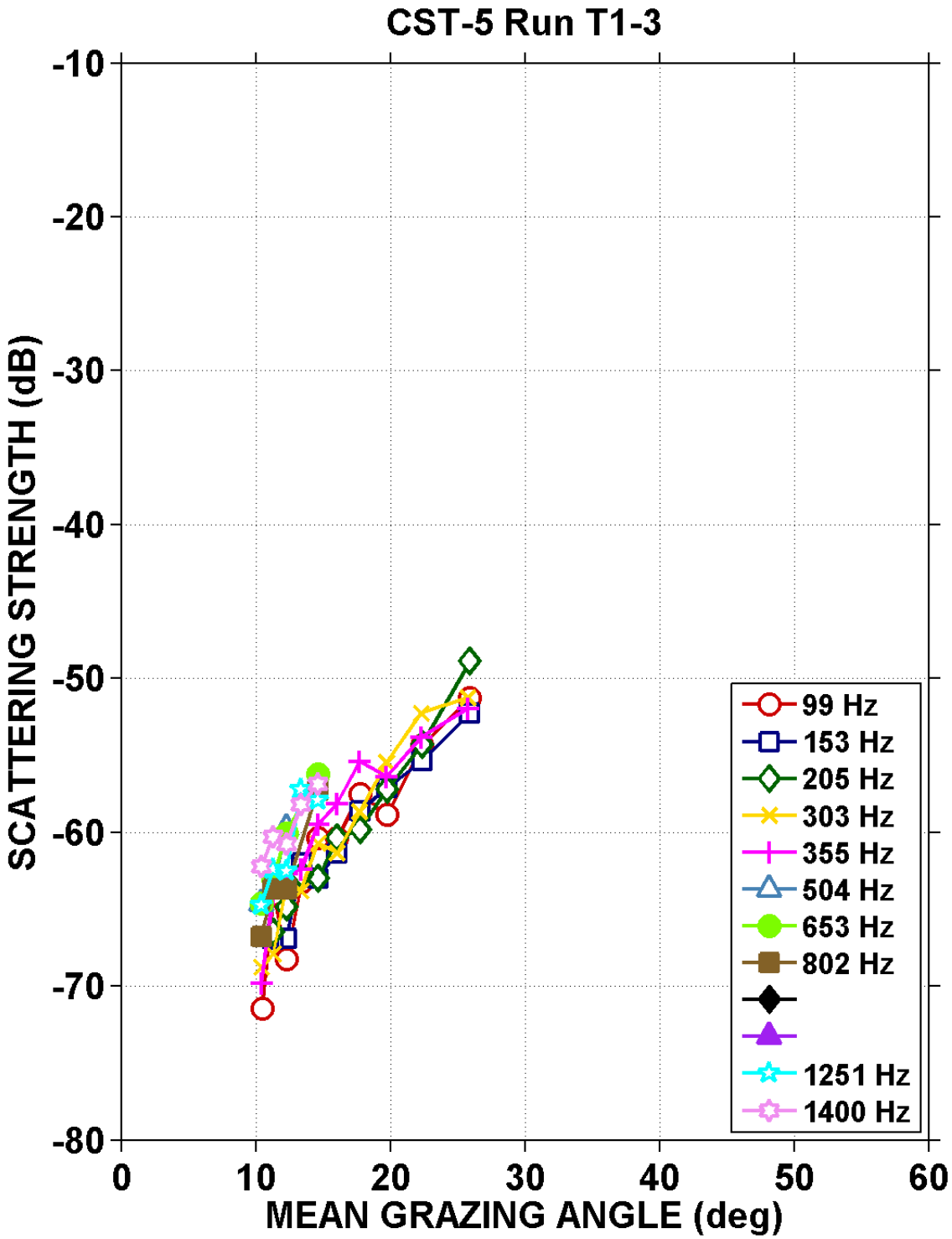

Fig. 4-23 – Surface backscattering strengths vs. mean grazing angle for CST-5 Run T1-3.

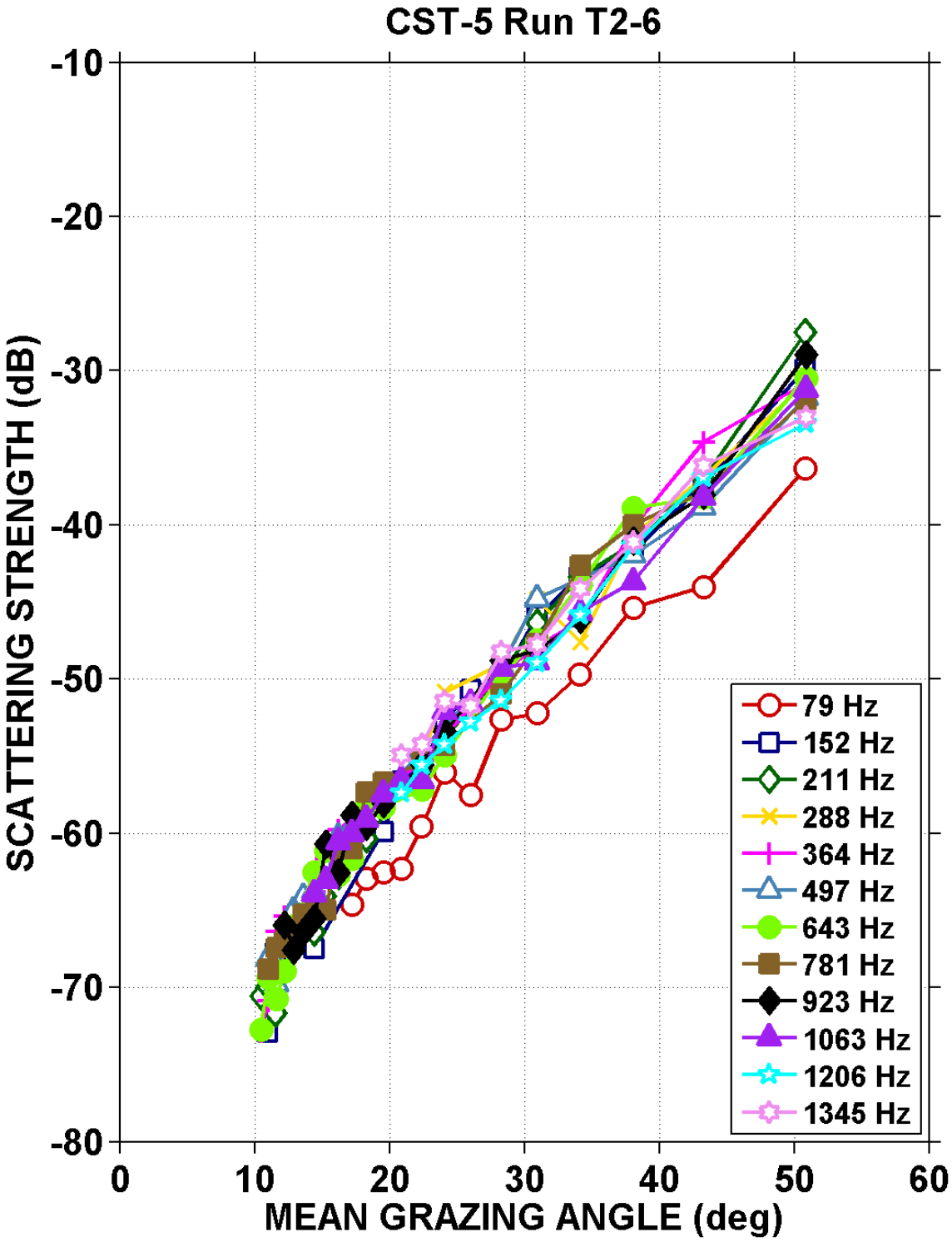

Fig. 4-24 – Surface backscattering strengths vs. mean grazing angle for CST-5 Run T2-6.

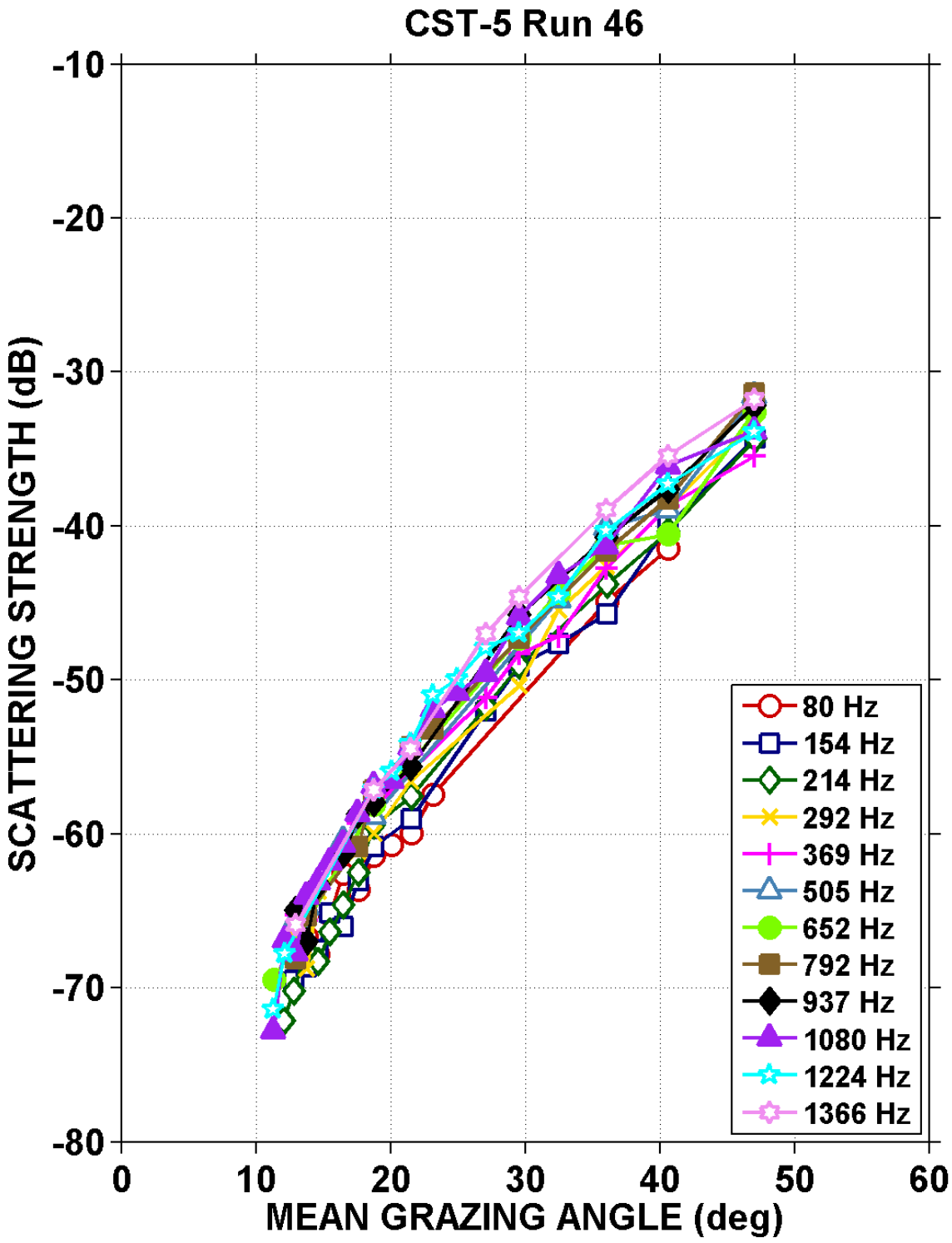

Fig. 4-25 – Surface backscattering strengths vs. mean grazing angle for CST-5 Run 46.

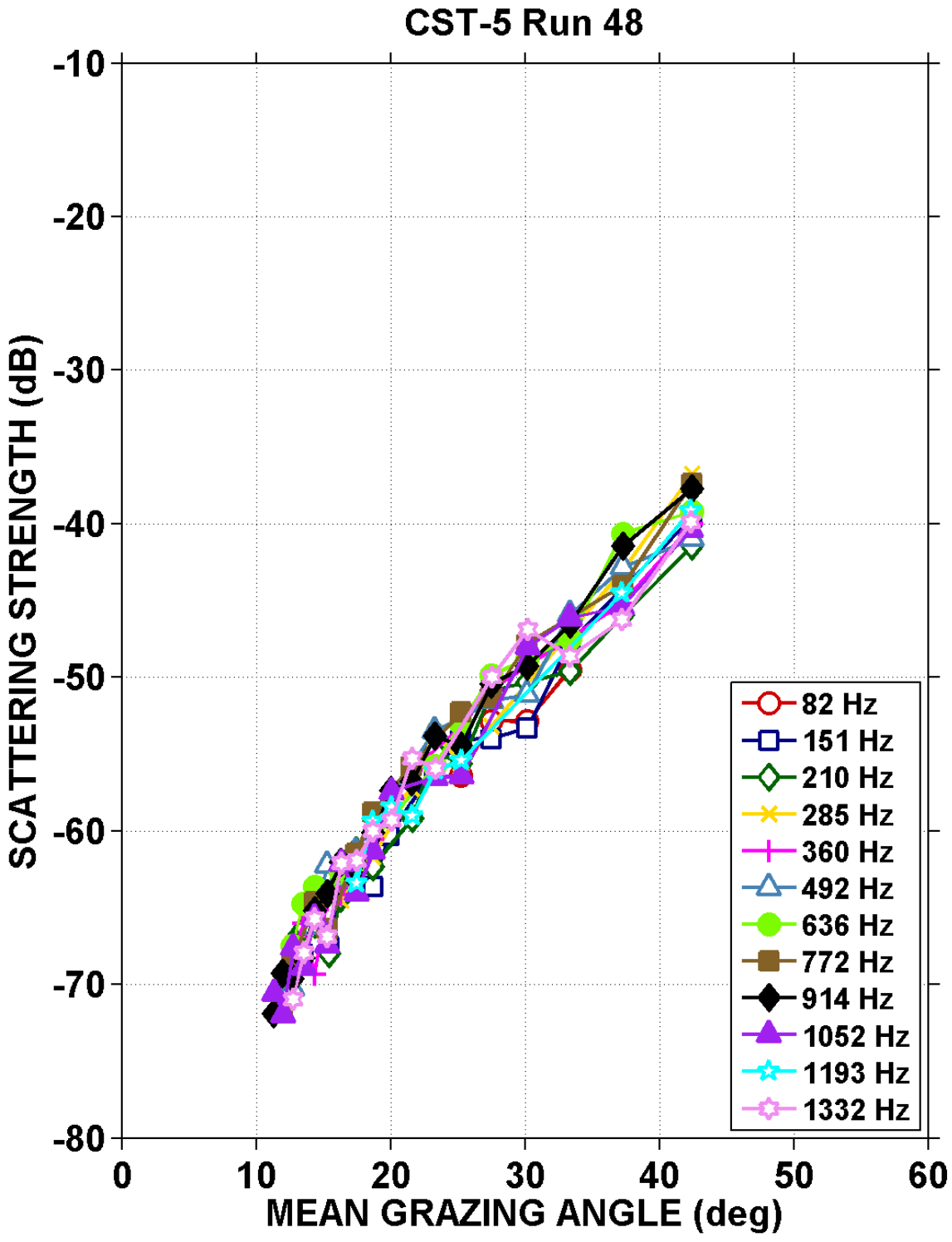

Fig. 4-26 – Surface backscattering strengths vs. mean grazing angle for CST-5 Run 48.

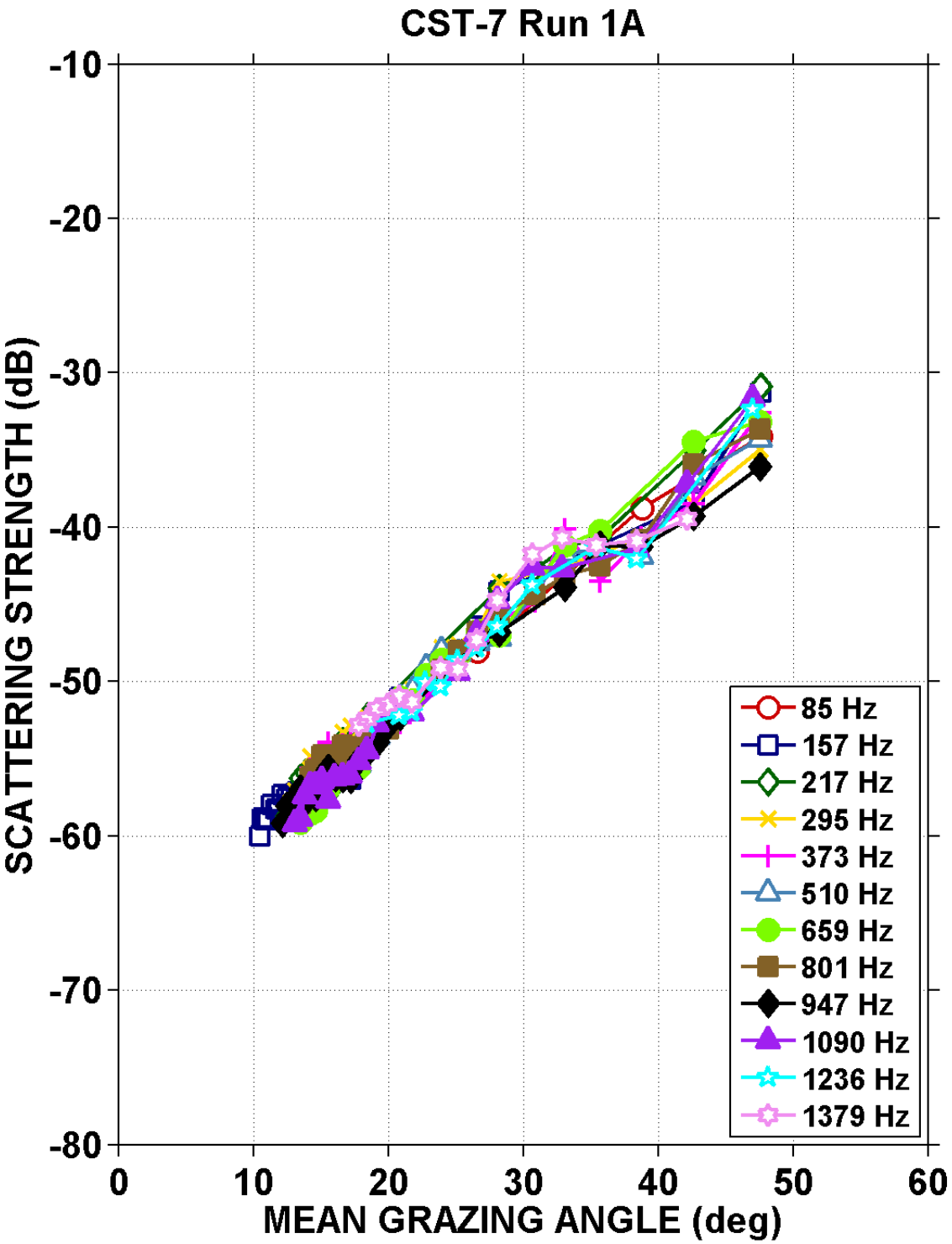

Fig. 4-27 – Surface backscattering strengths vs. mean grazing angle for CST-7 Run 1A.

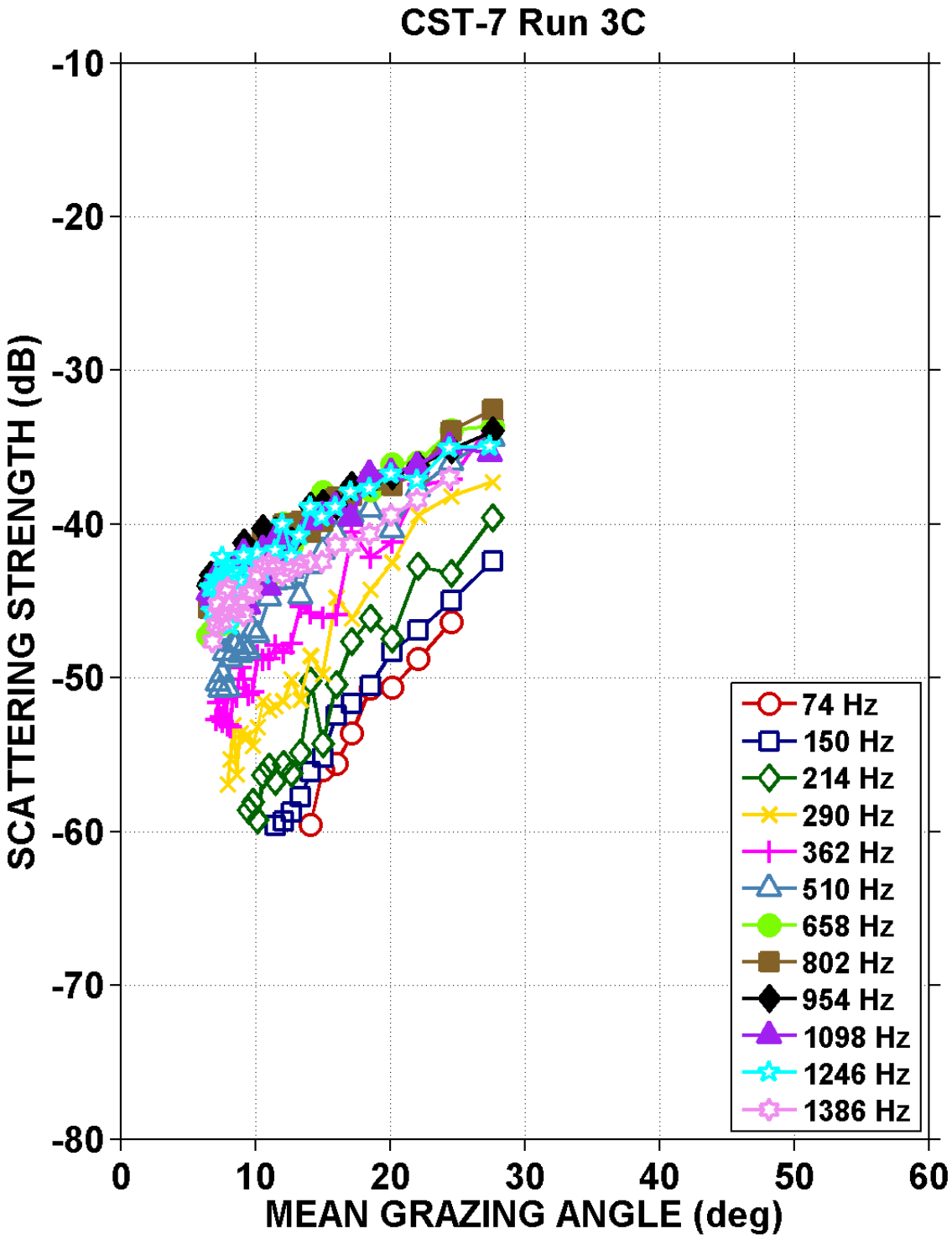

Fig. 4-28 – Surface backscattering strengths vs. mean grazing angle for CST-7 Run 3C.

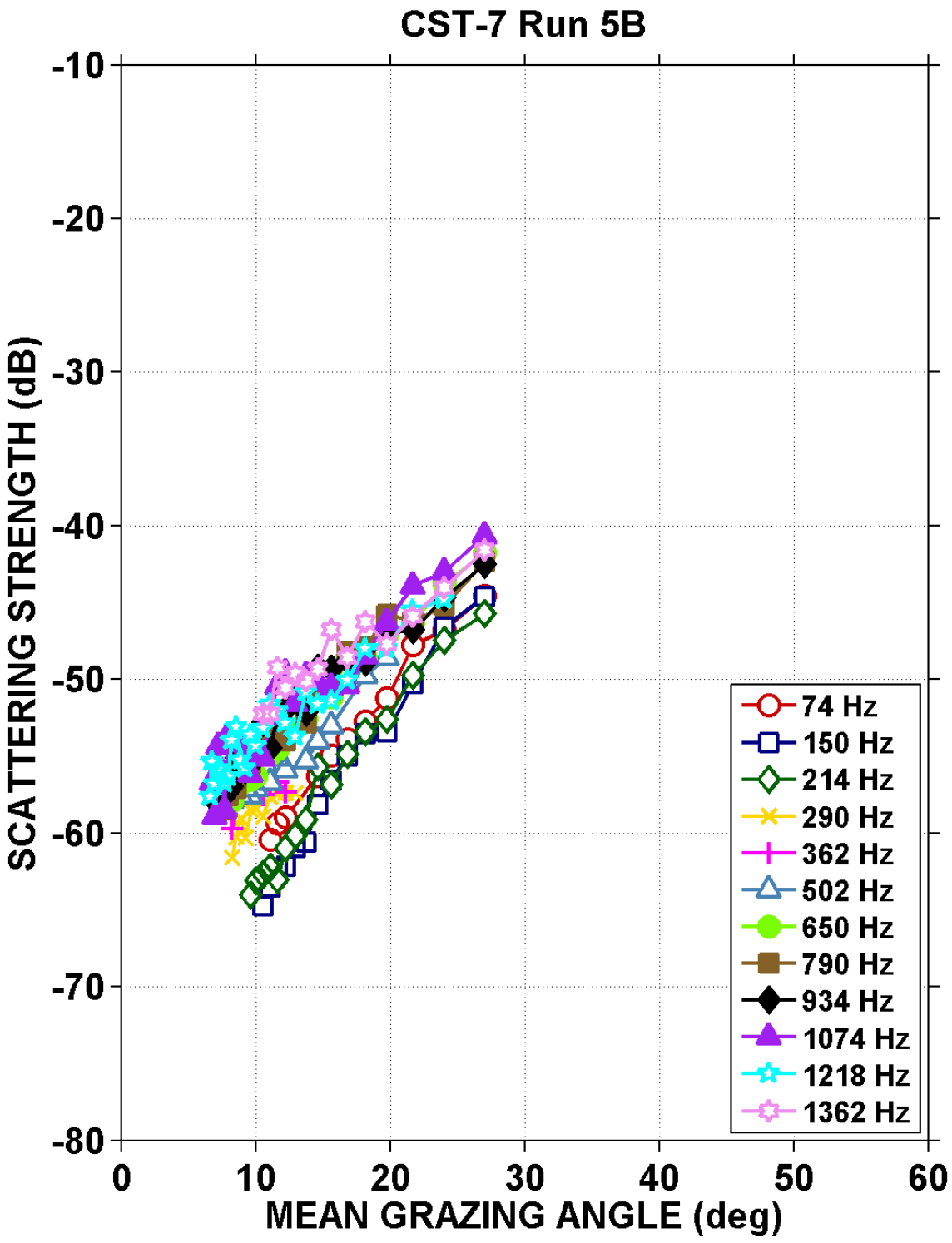

Fig. 4-29 – Surface backscattering strengths vs. mean grazing angle for CST-7 Run 5B.

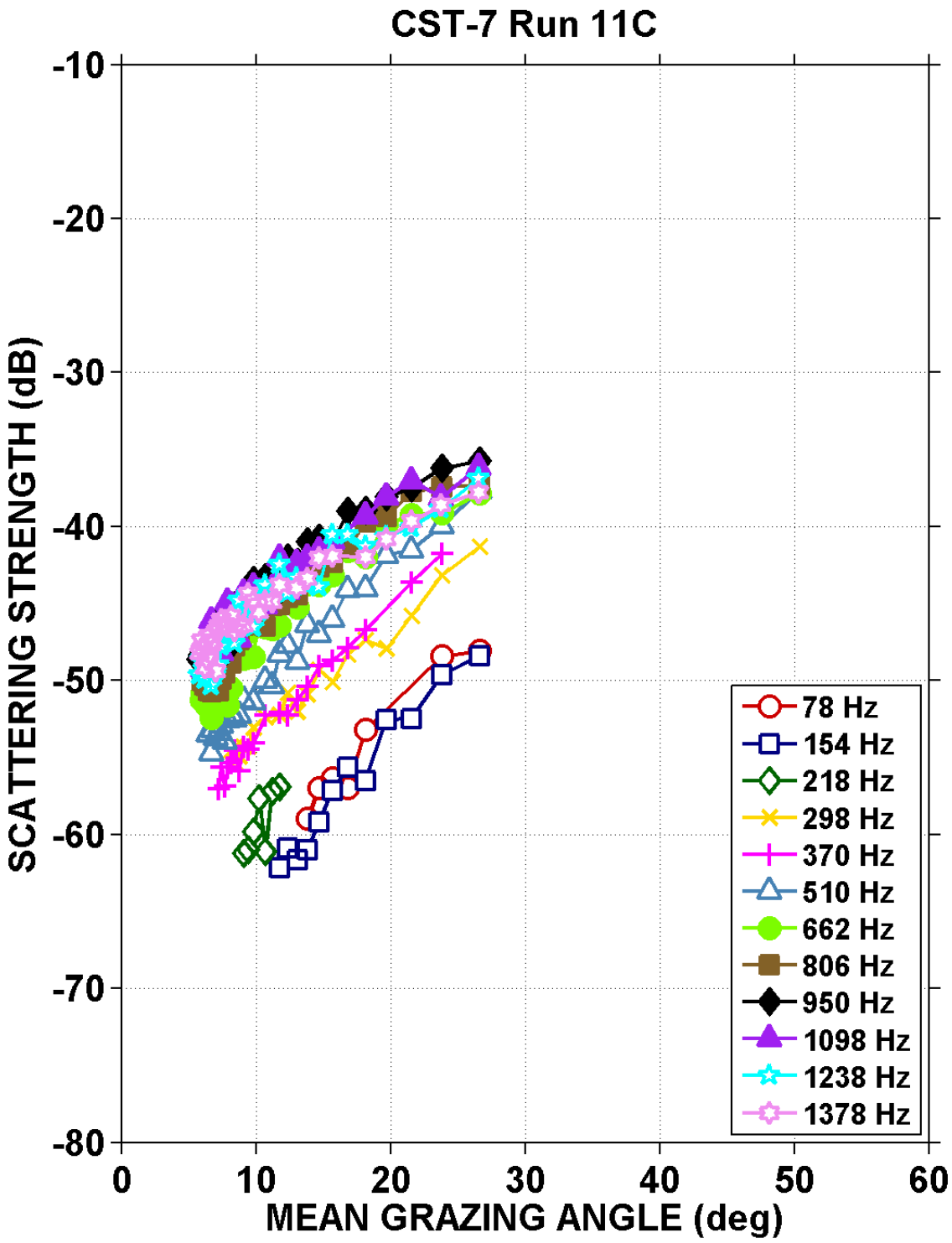

Fig. 4-30 – Surface backscattering strengths vs. mean grazing angle for CST-7 Run 11C.

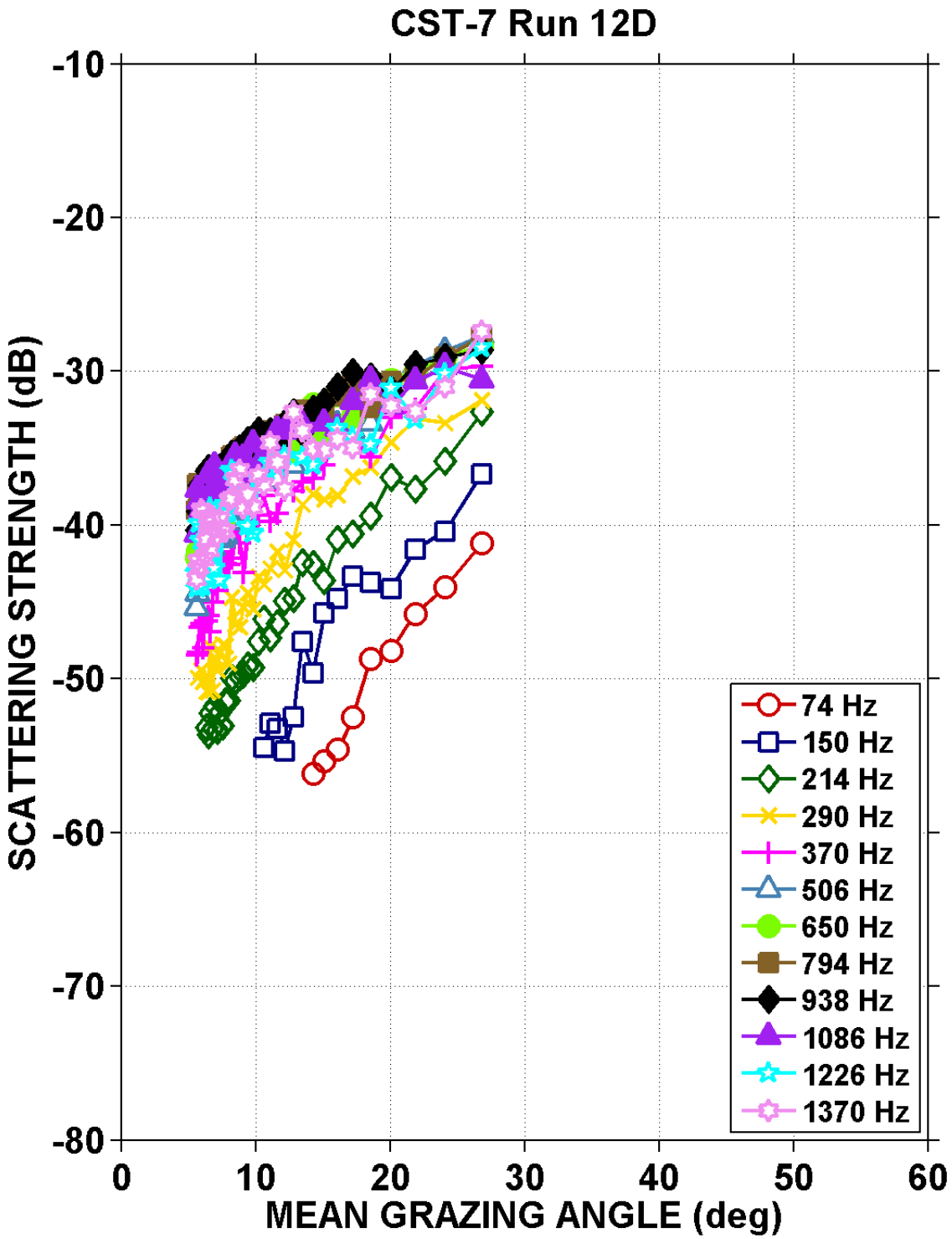

Fig. 4-31 – Surface backscattering strengths vs. mean grazing angle for CST-7 Run 12D.

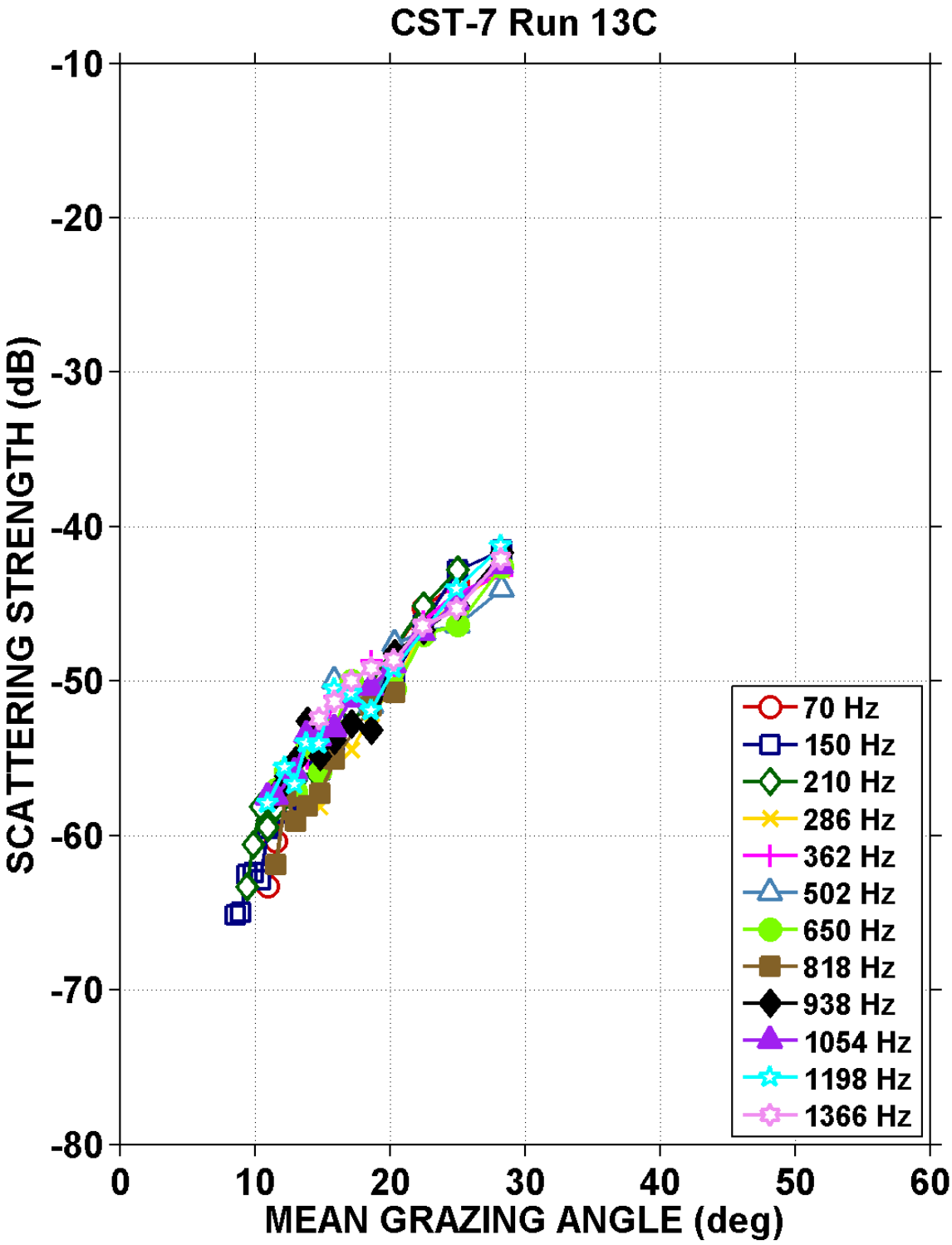

Fig. 4-32 – Surface backscattering strengths vs. mean grazing angle for CST-7 Run 13C.

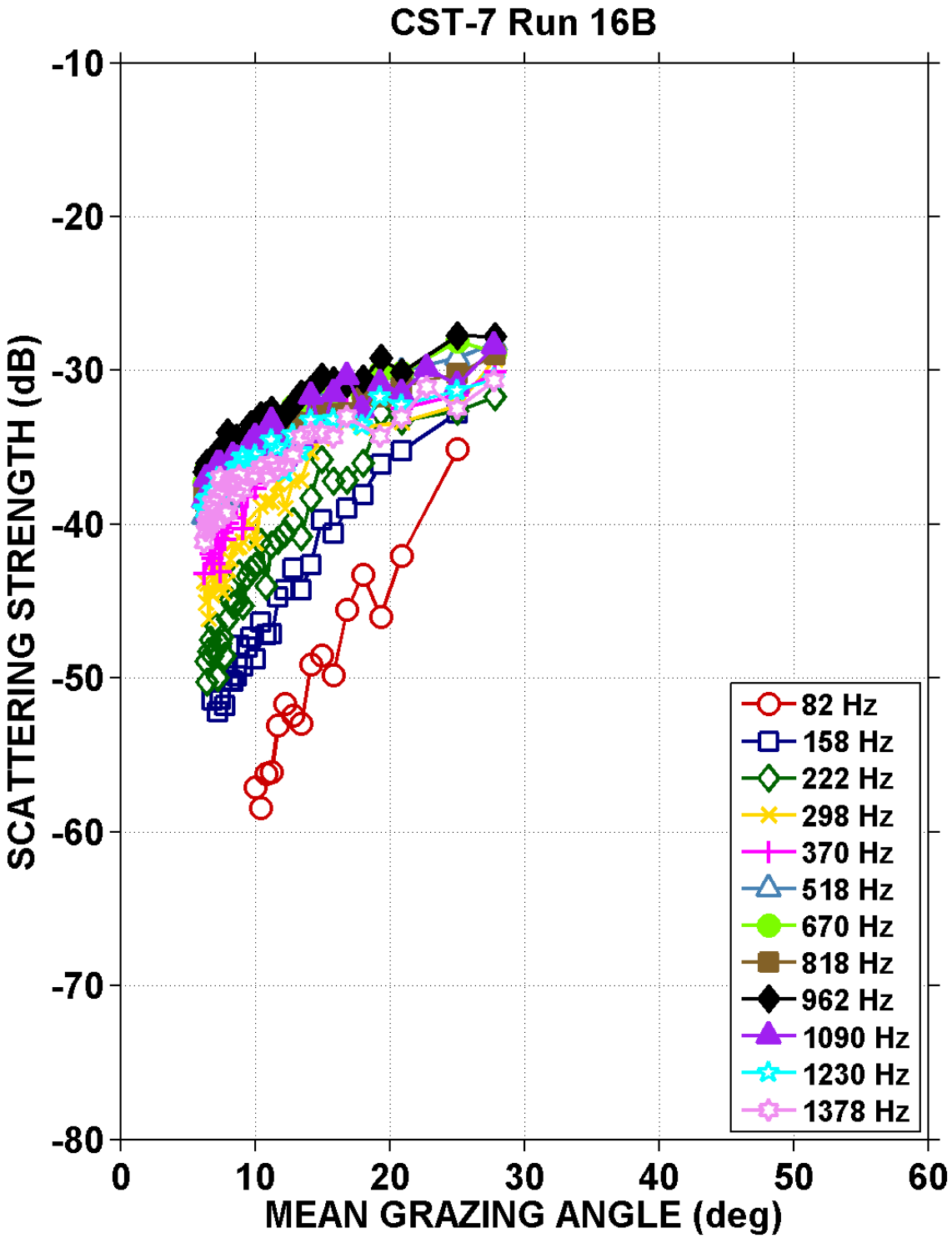

Fig. 4-33 – Surface backscattering strengths vs. mean grazing angle for CST-7 Run 16B.

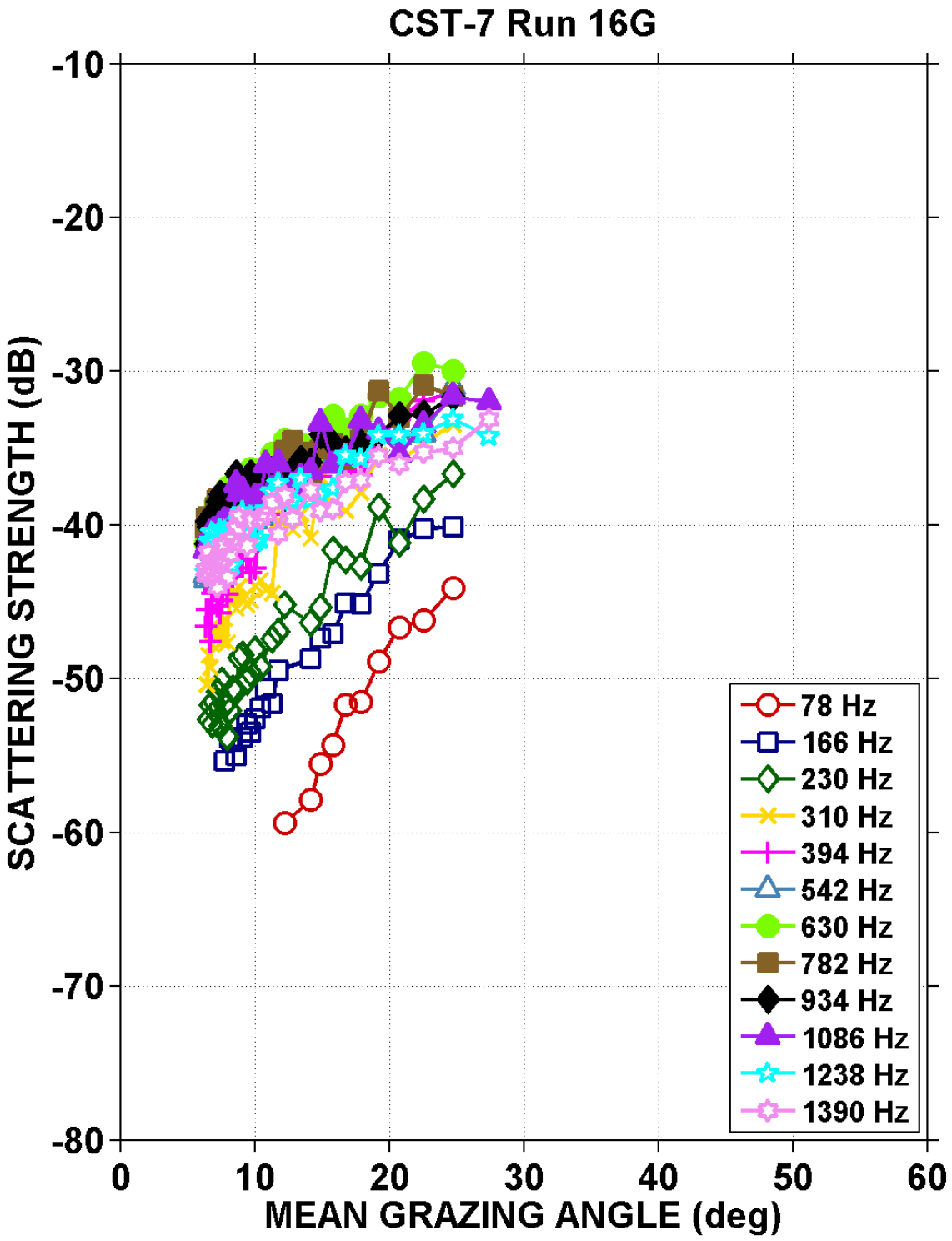

Fig. 4-34– Surface backscattering strengths vs. mean grazing angle for CST-7 Run 16G.

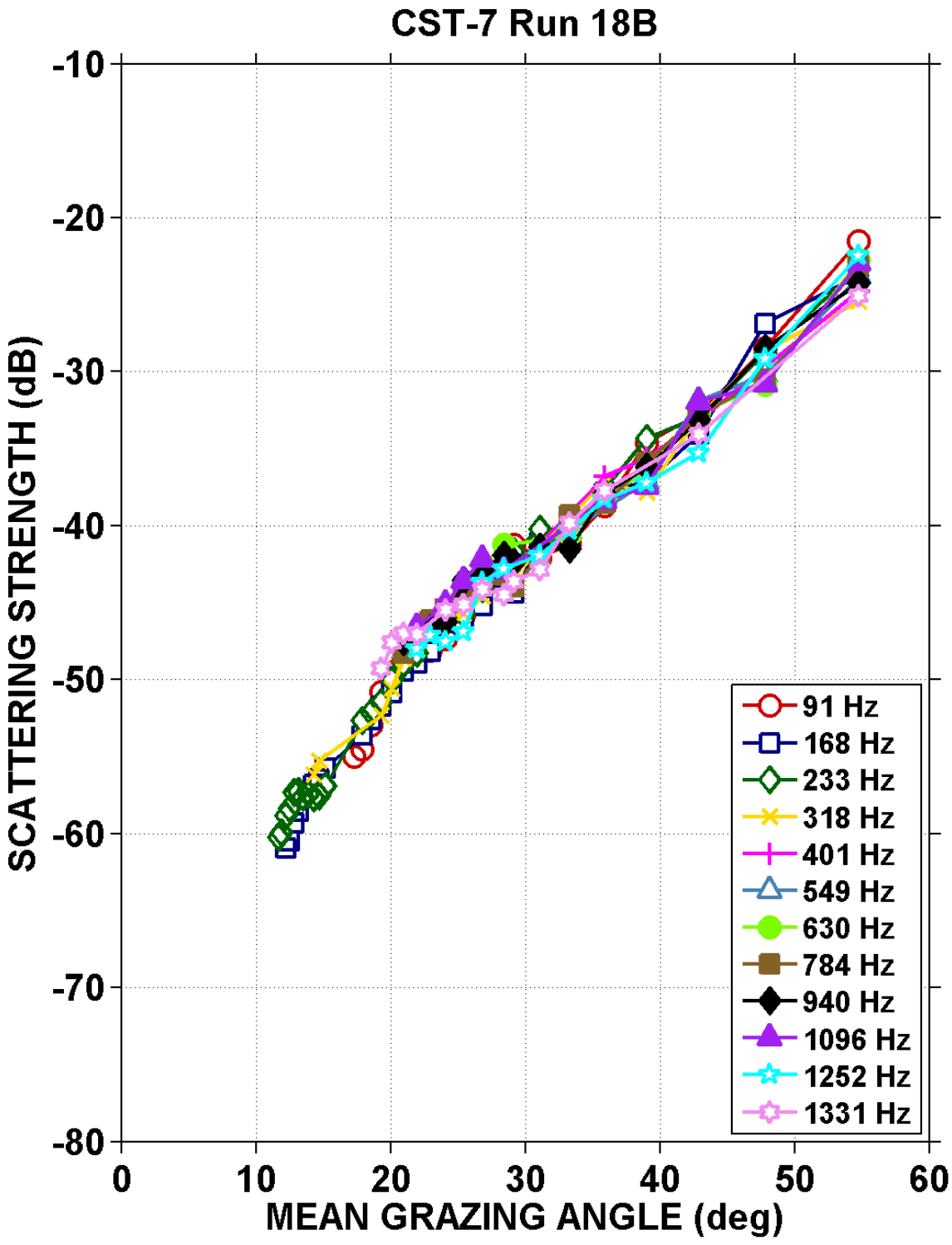

Fig. 4-35 – Surface backscattering strengths vs. mean grazing angle for CST-7 Run 18B.

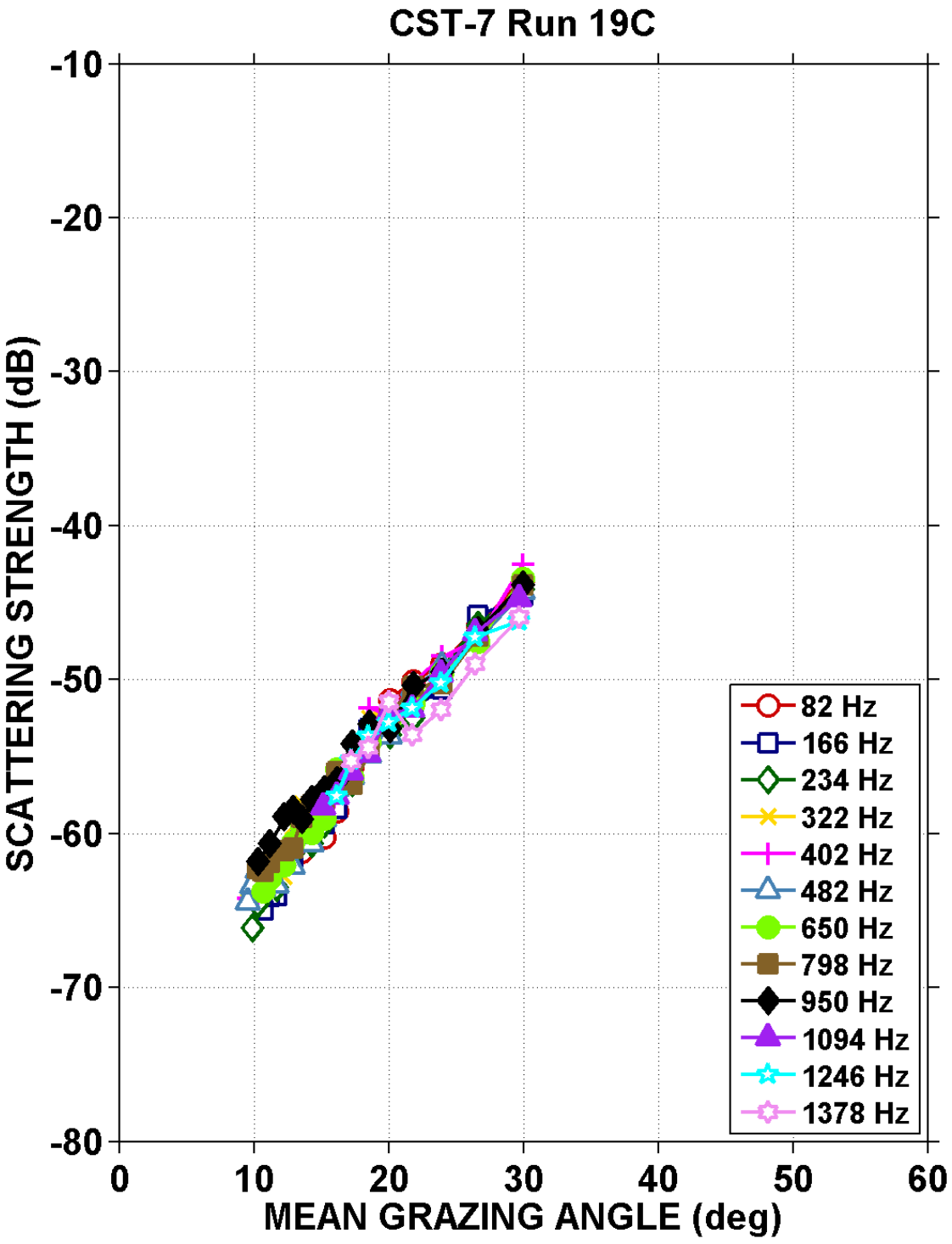

Fig. 4-36 – Surface backscattering strengths vs. mean grazing angle for CST-7 Run 19C.

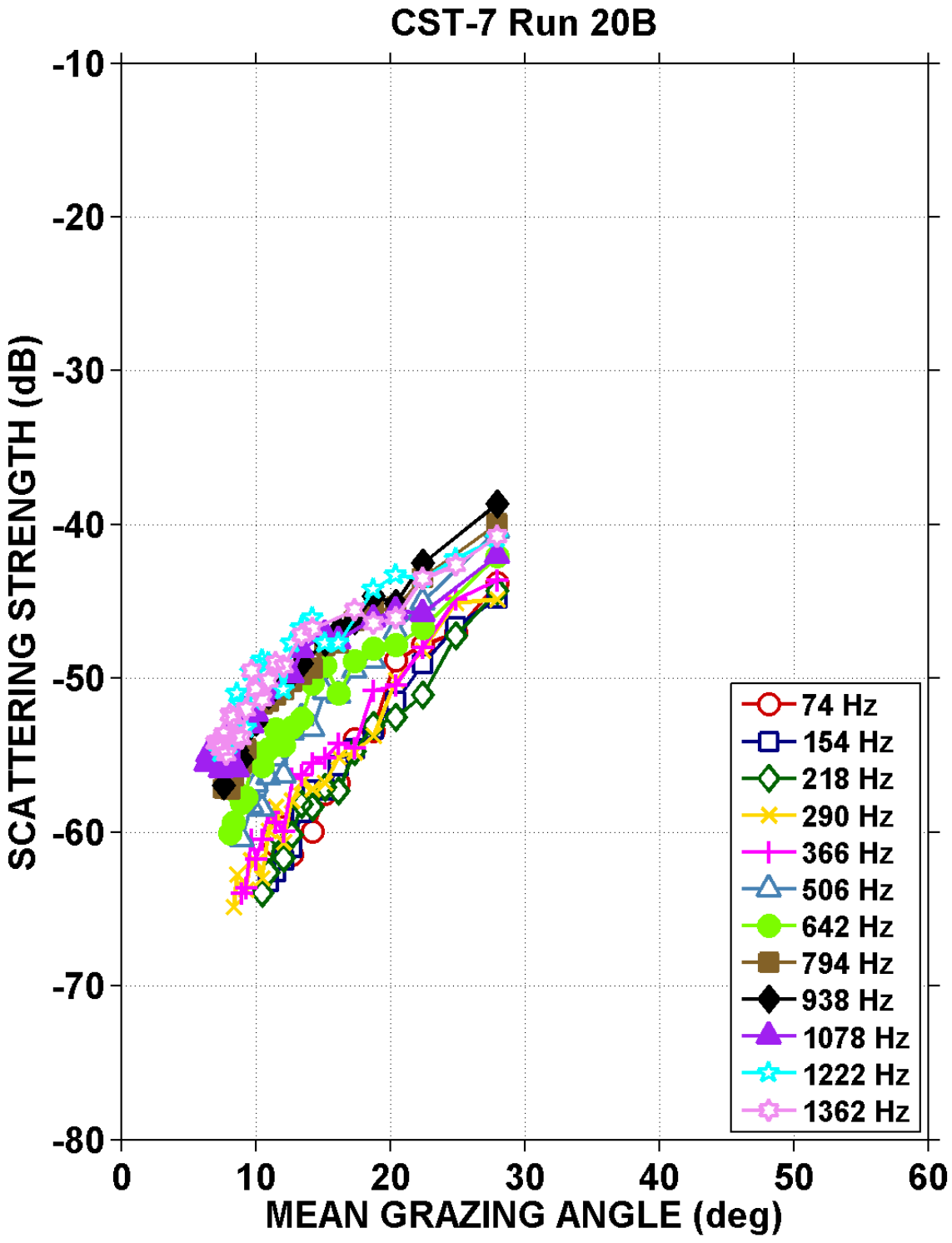

Fig. 4-37 – Surface backscattering strengths vs. mean grazing angle for CST-7 Run 20B.

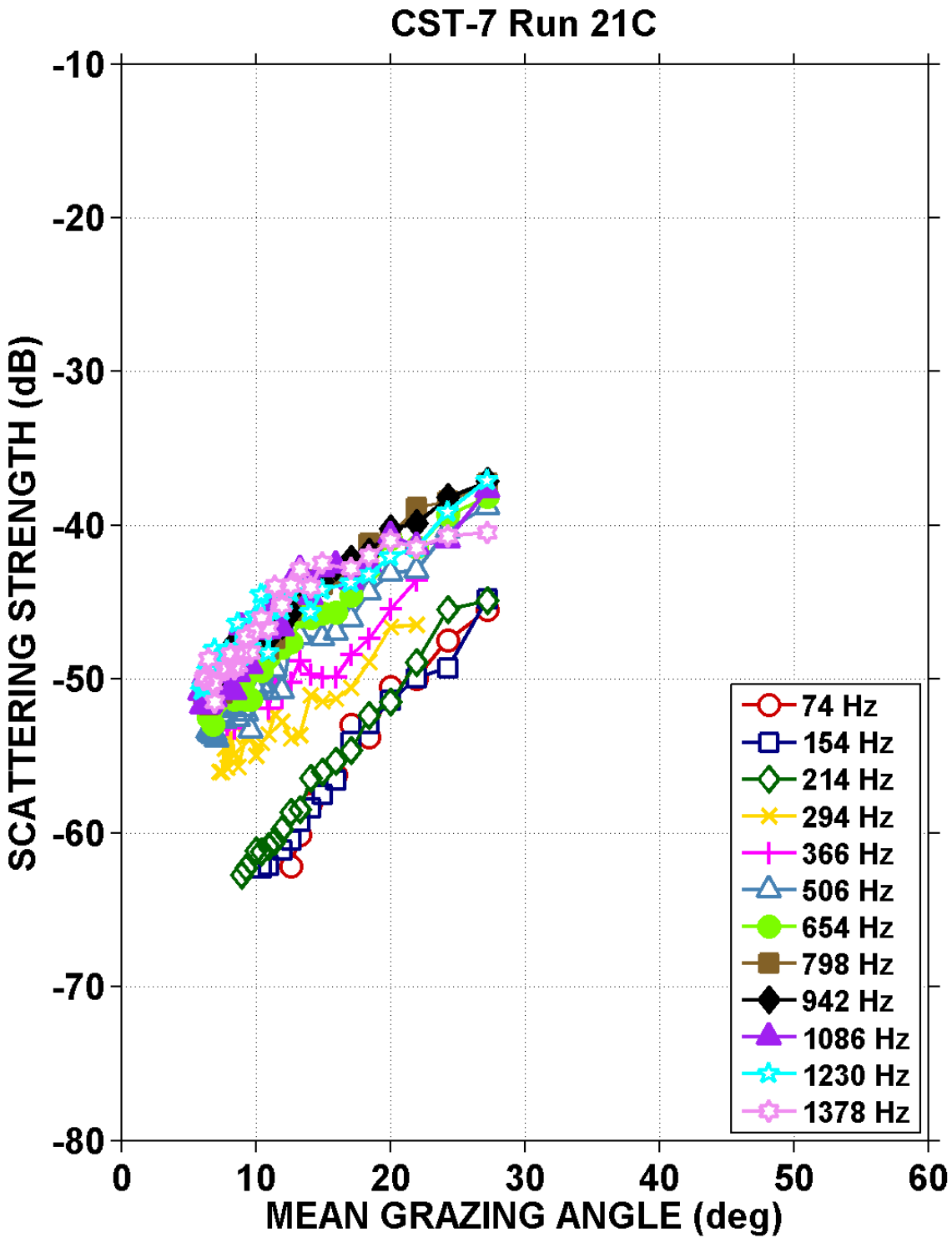

Fig. 4-38 – Surface backscattering strengths vs. mean grazing angle for CST-7 Run 21C.

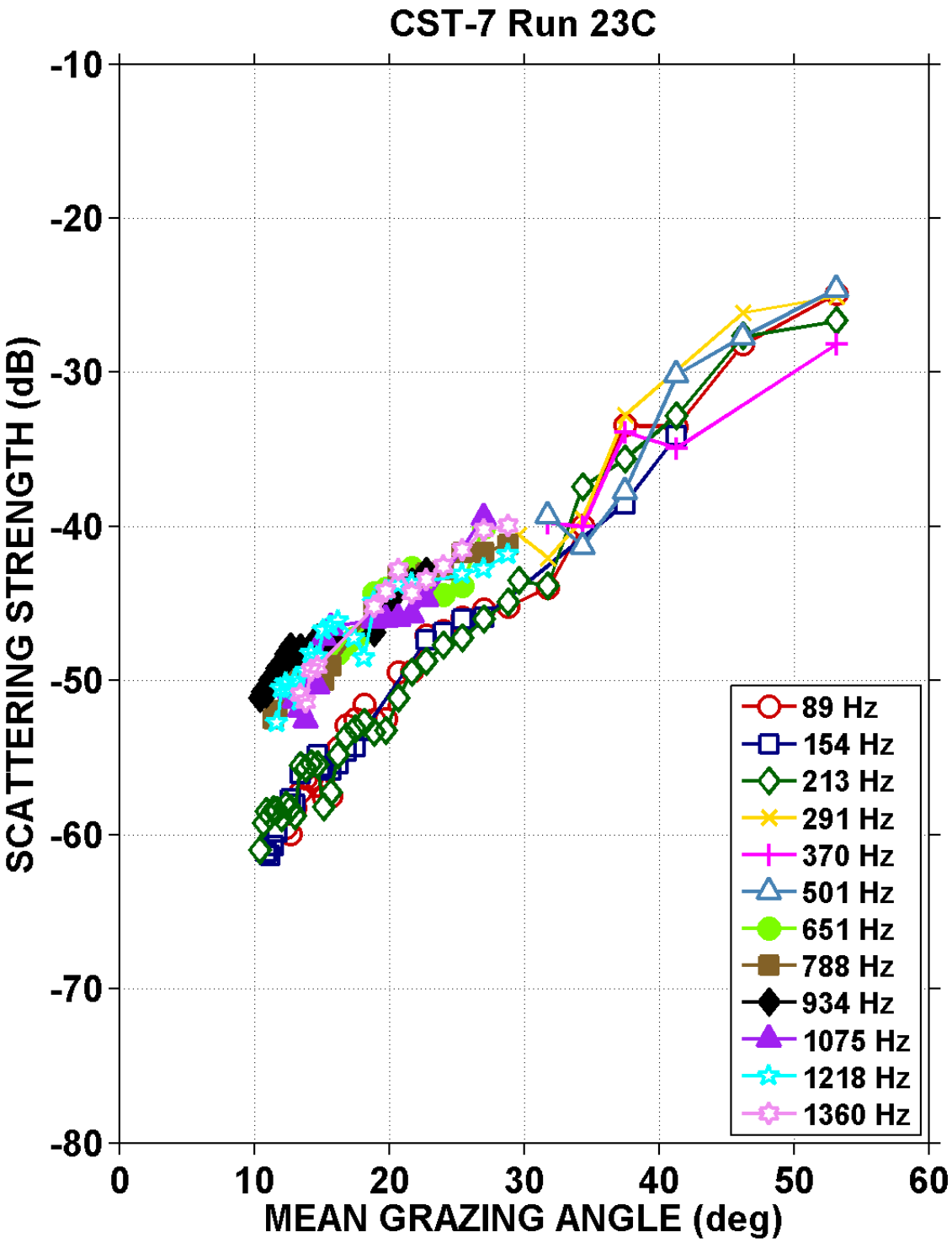

Fig. 4-39 – Surface backscattering strengths vs. mean grazing angle for CST-7 Run 23C.

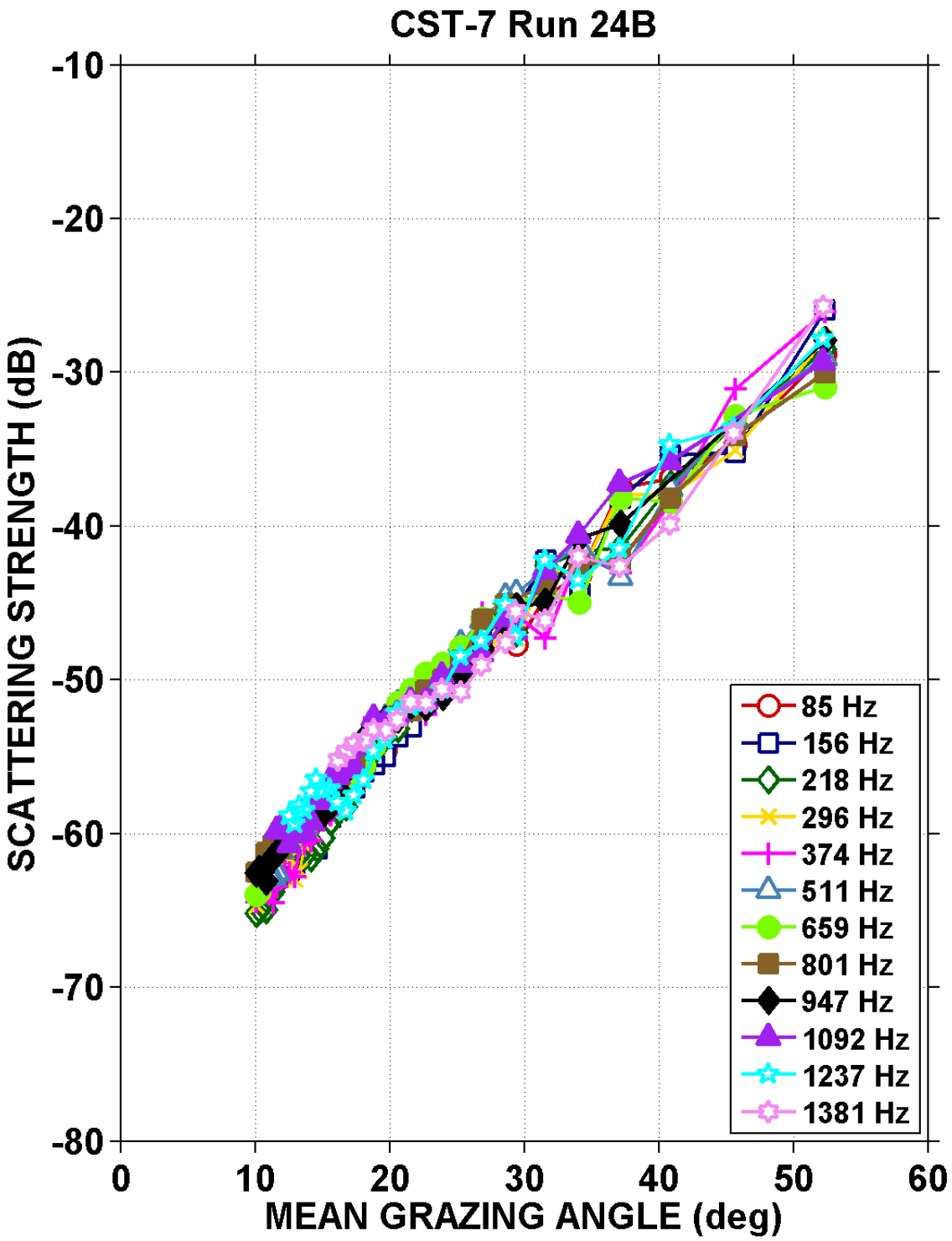

Fig. 4-40 – Surface backscattering strengths vs. mean grazing angle for CST-7 Run 24B.

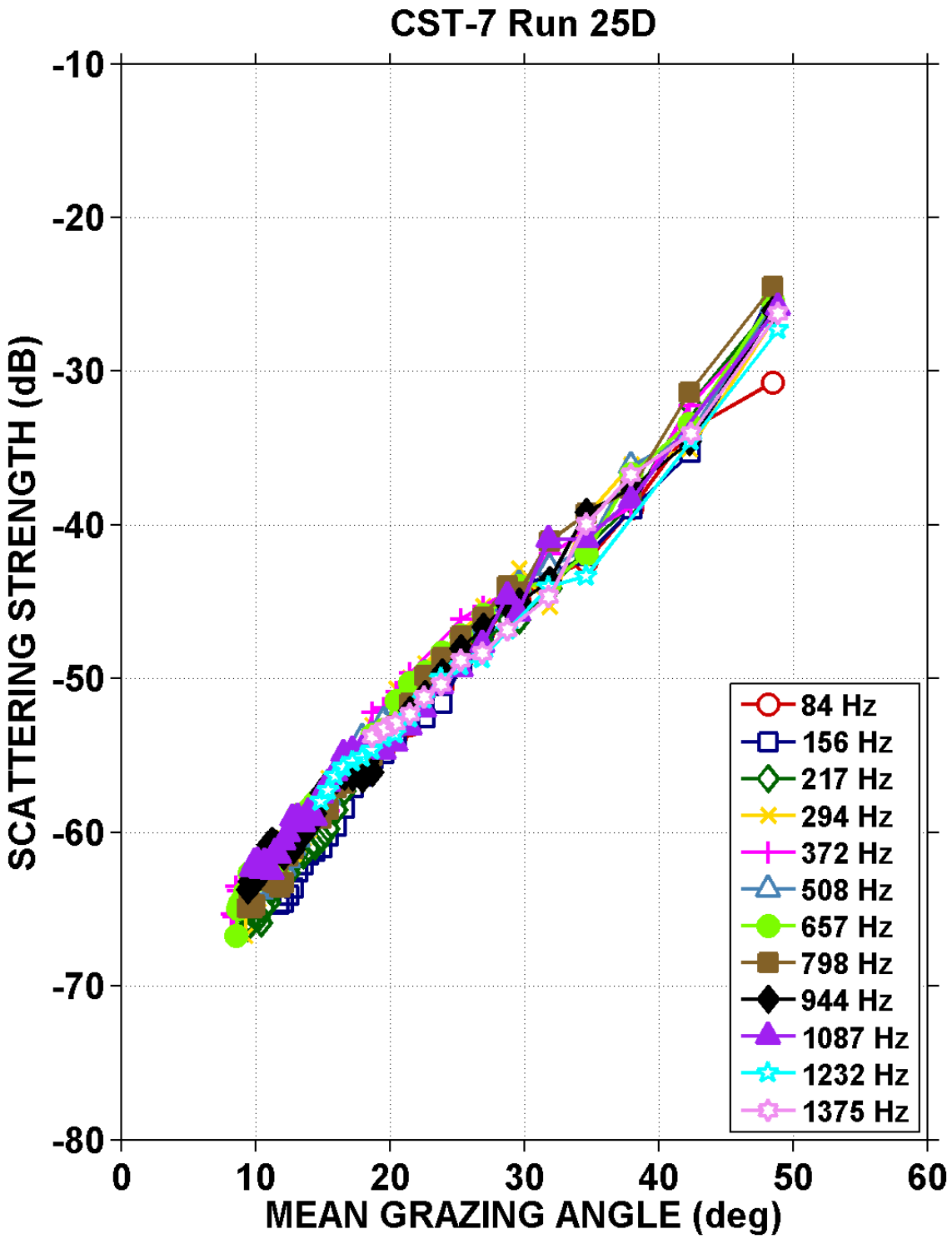

Fig. 4-41 – Surface backscattering strengths vs. mean grazing angle for CST-7 Run 25D.

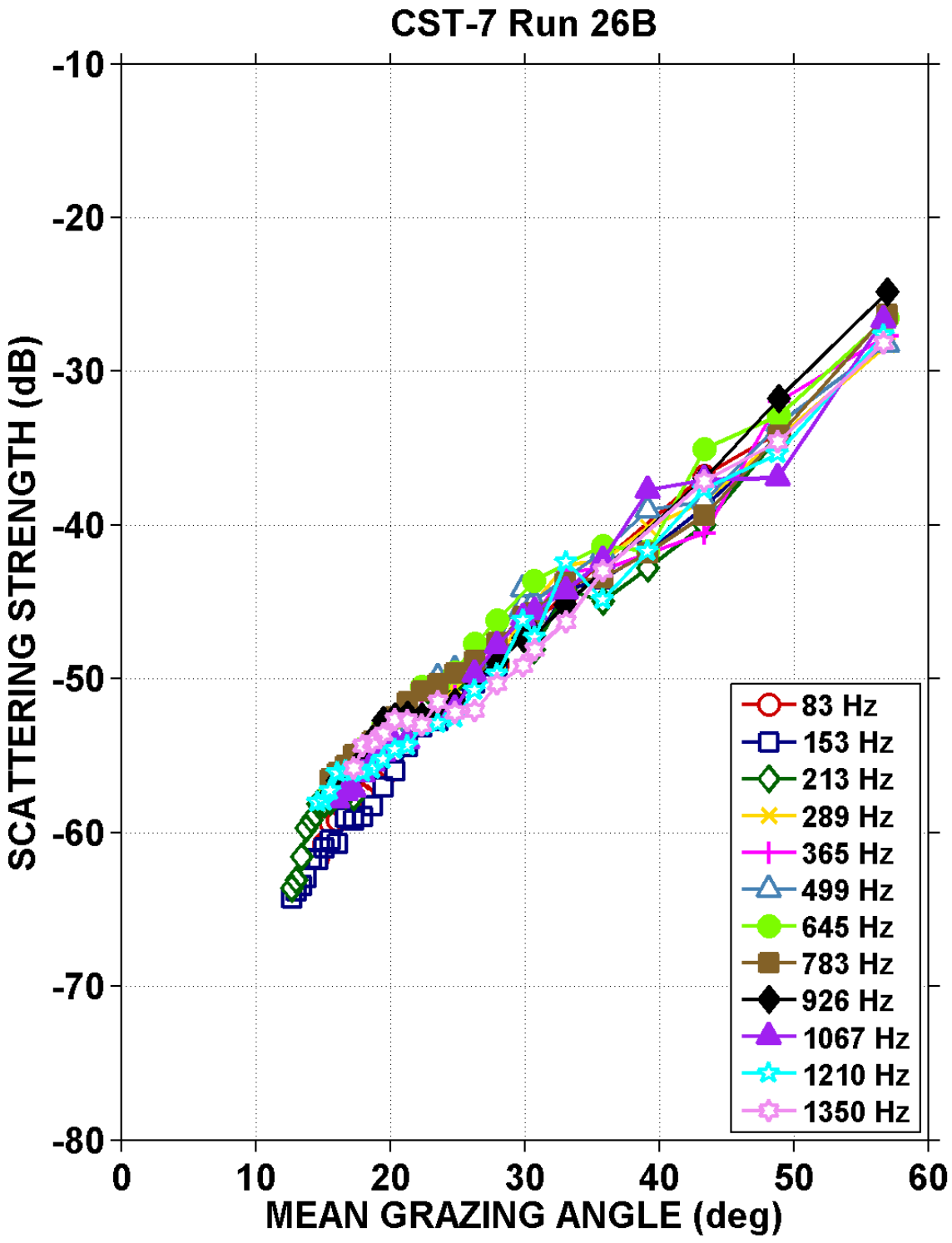

Fig. 4-42 – Surface backscattering strengths vs. mean grazing angle for CST-7 Run 26B.

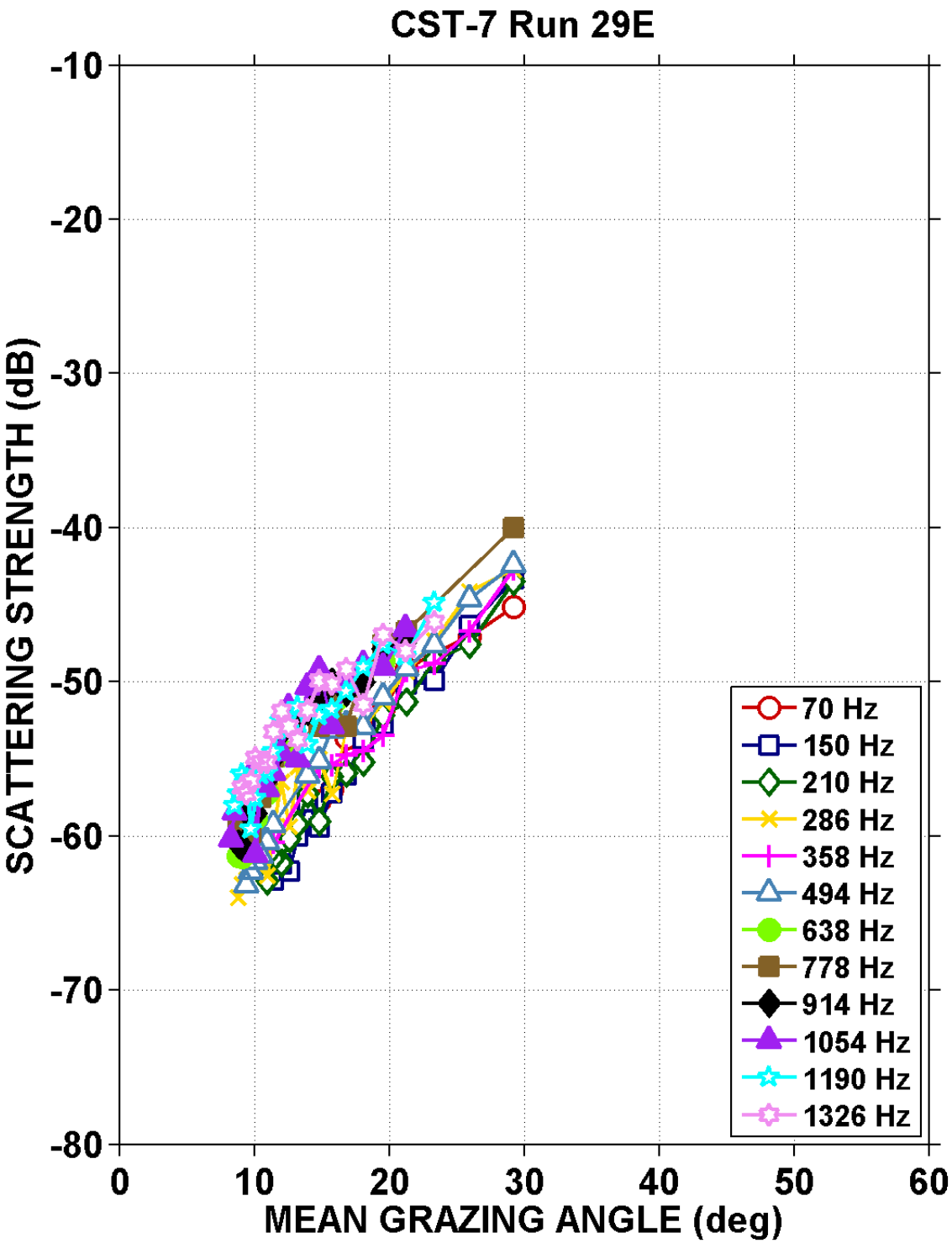

Fig. 4-43 – Surface backscattering strengths vs. mean grazing angle for CST-7 Run 29E.

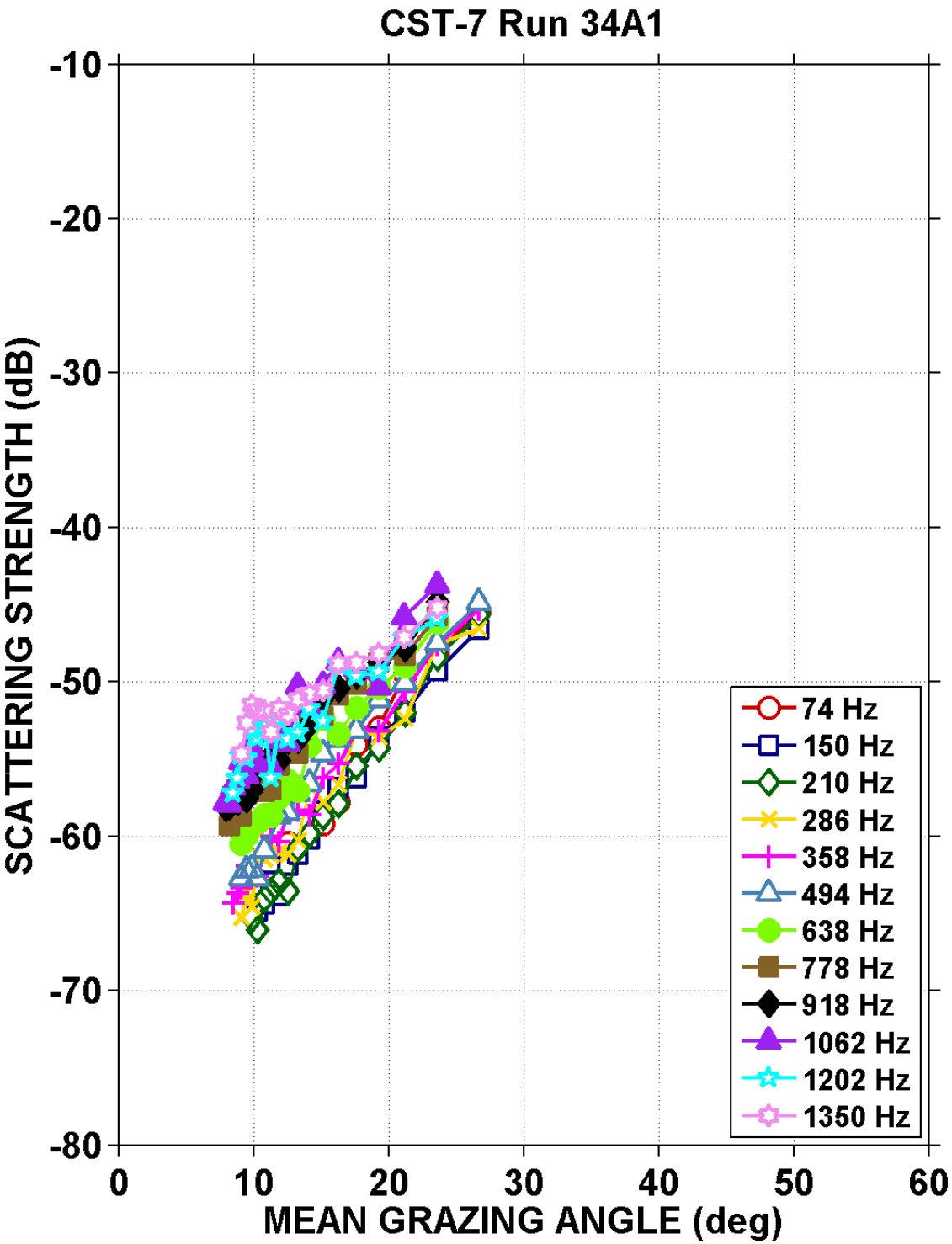

Fig. 4-44 – Surface backscattering strengths vs. mean grazing angle for CST-7 Run 34A1.

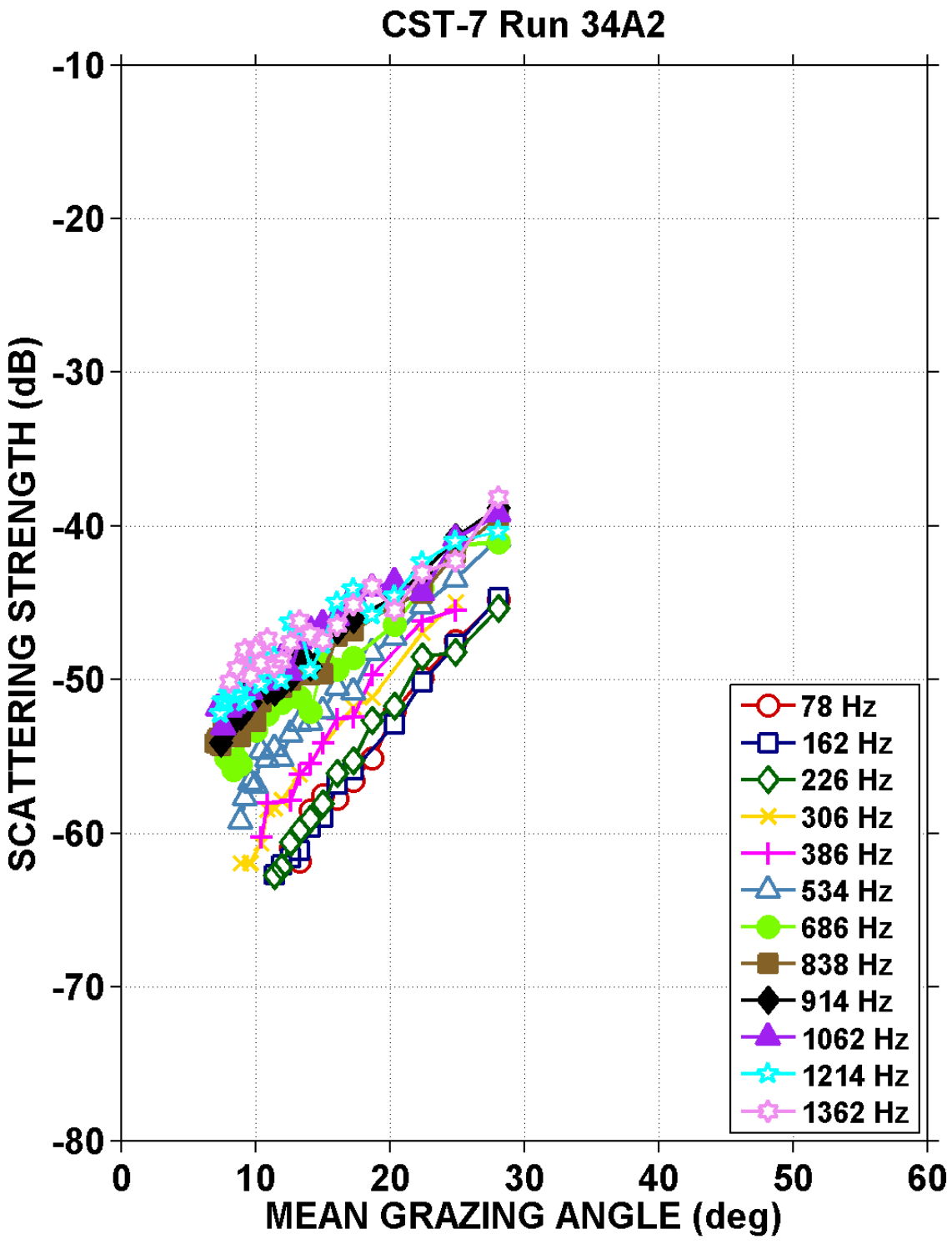

Fig. 4-45 – Surface backscattering strengths vs. mean grazing angle for CST-7 Run 34A2.

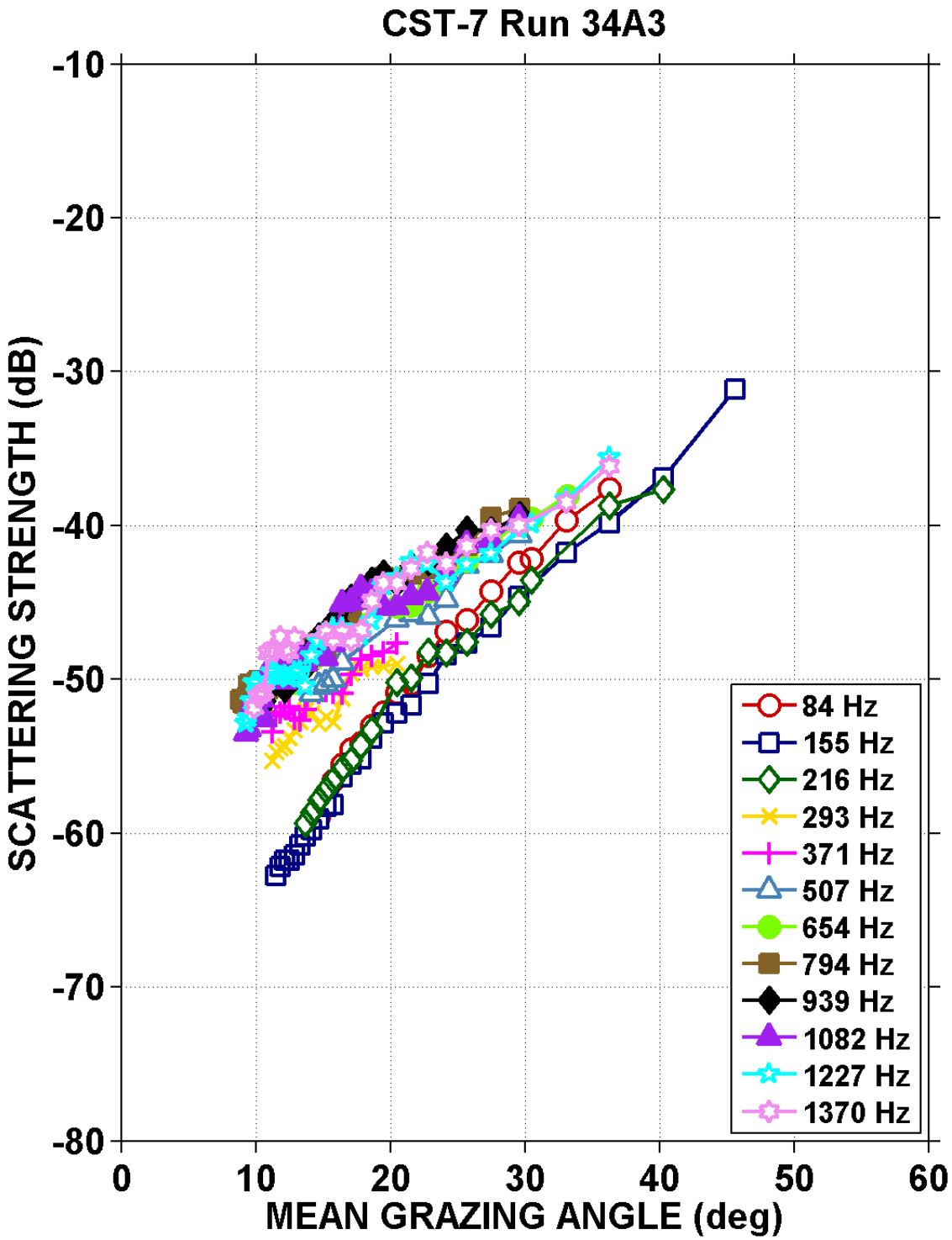

Fig. 4-46 – Surface backscattering strengths vs. mean grazing angle for CST-7 Run 34A3.

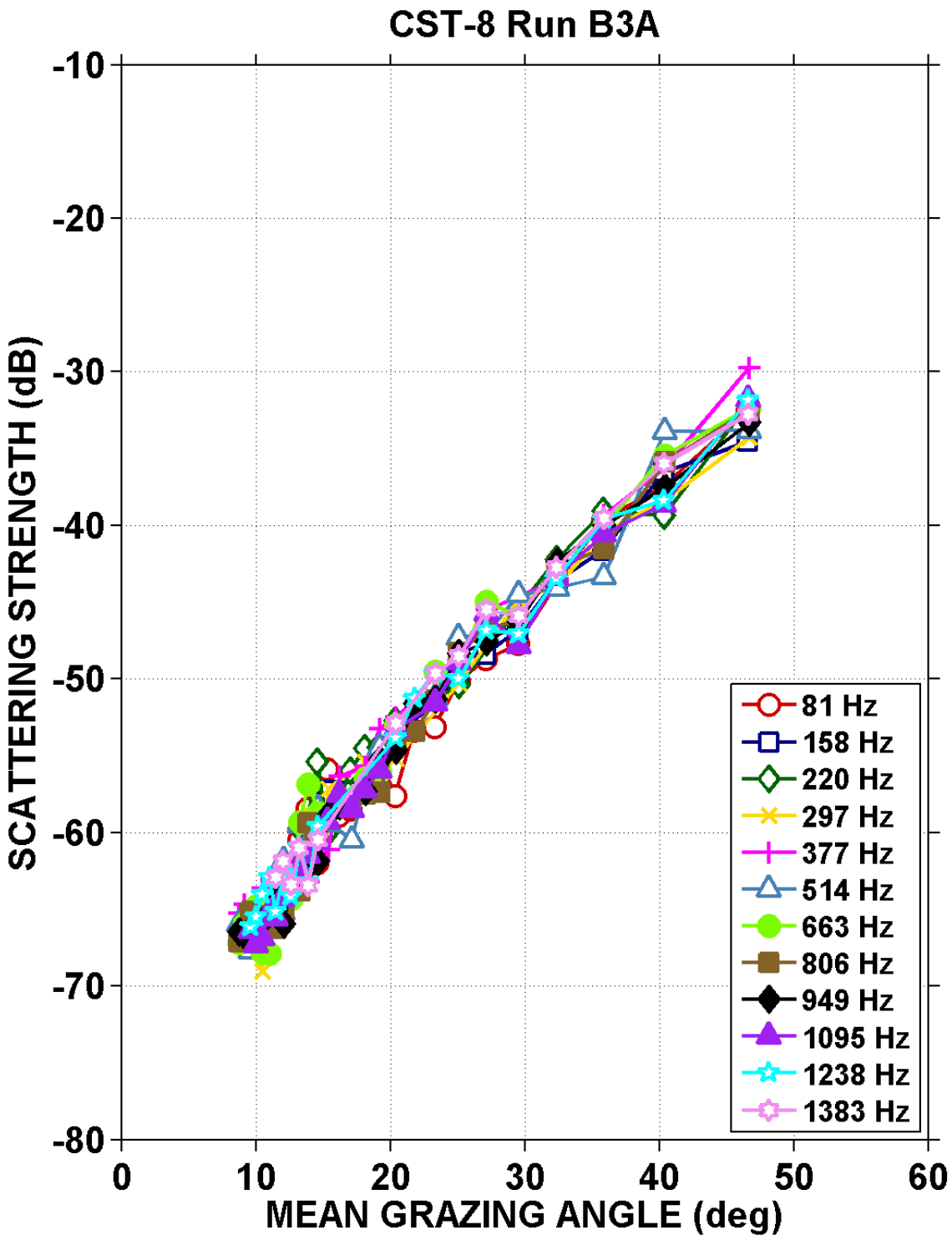

Fig. 4-47 – Surface backscattering strengths vs. mean grazing angle for CST-8 Run B3A.

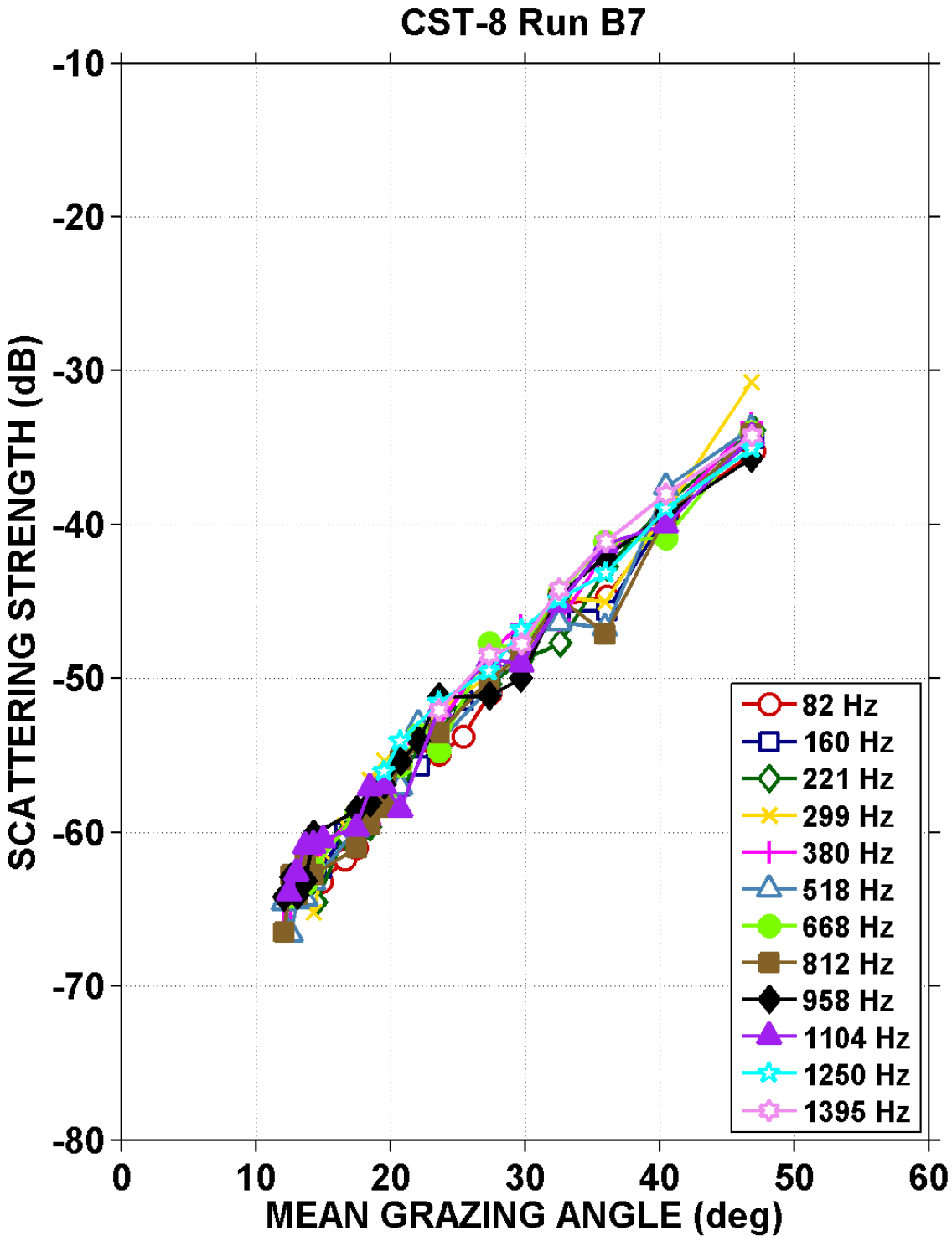

Fig. 4-48 – Surface backscattering strengths vs. mean grazing angle for CST-8 Run B7.

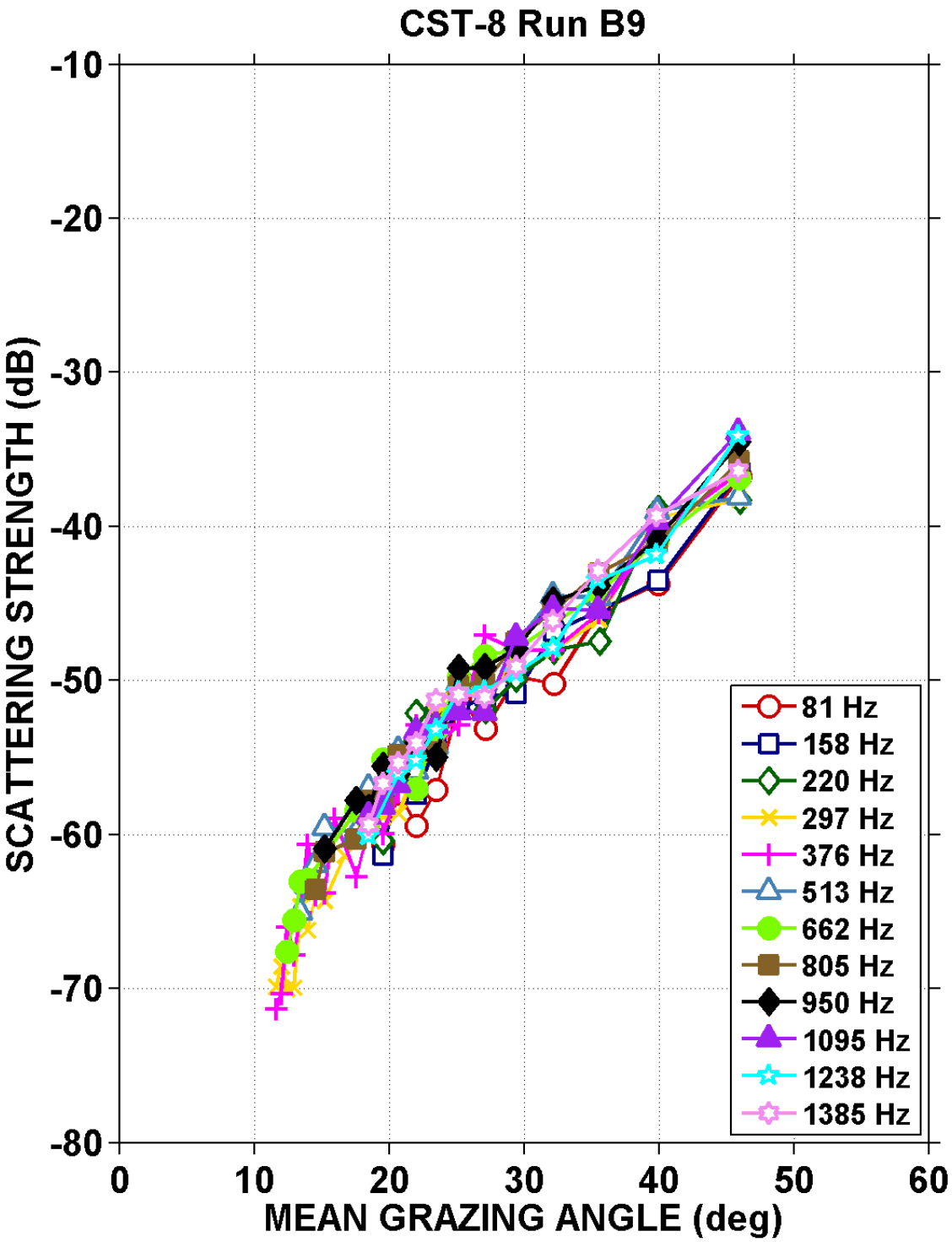

Fig. 4-49 – Surface backscattering strengths vs. mean grazing angle for CST-8 Run B9.

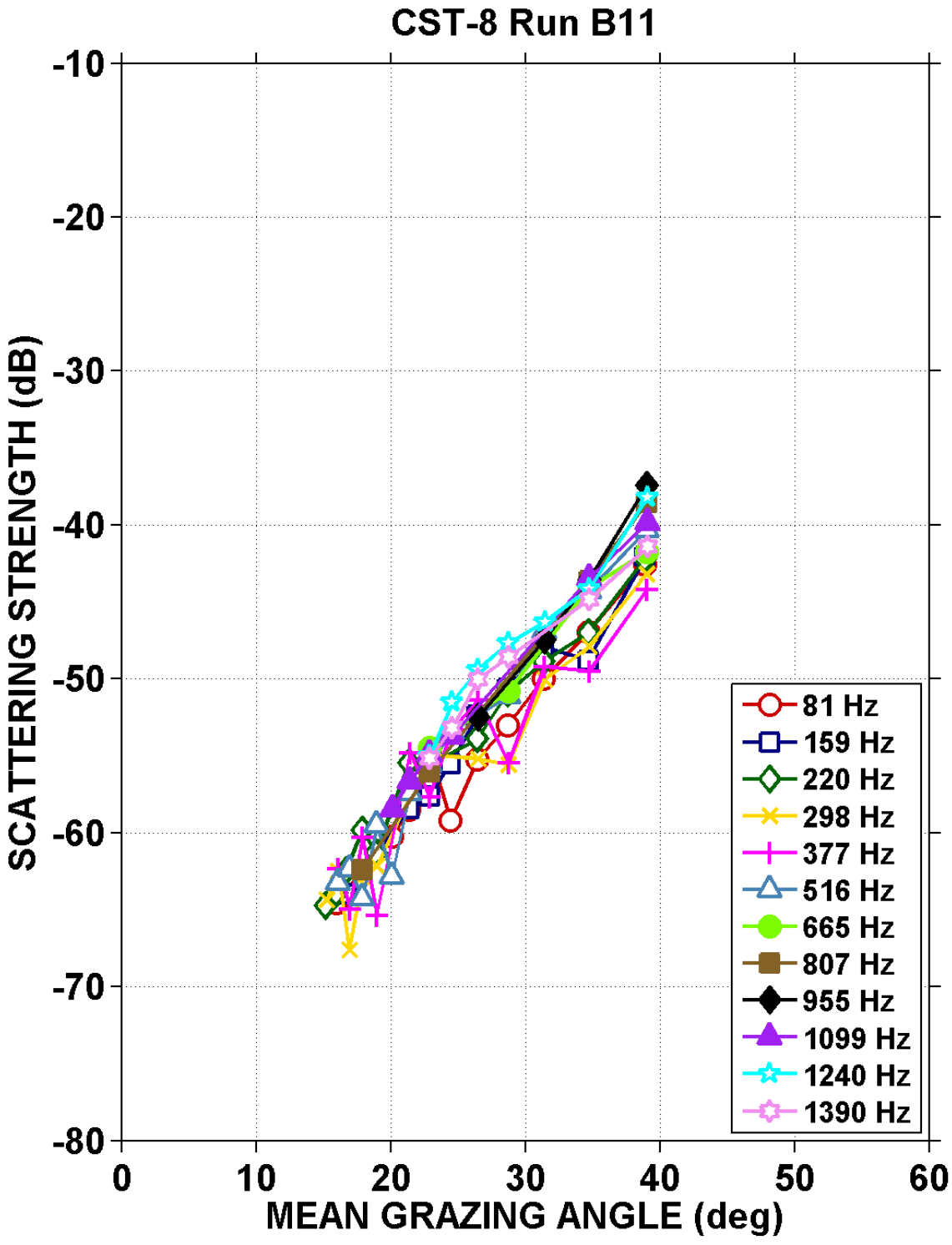

Fig. 4-50 – Surface backscattering strengths vs. mean grazing angle for CST-8 Run B11.

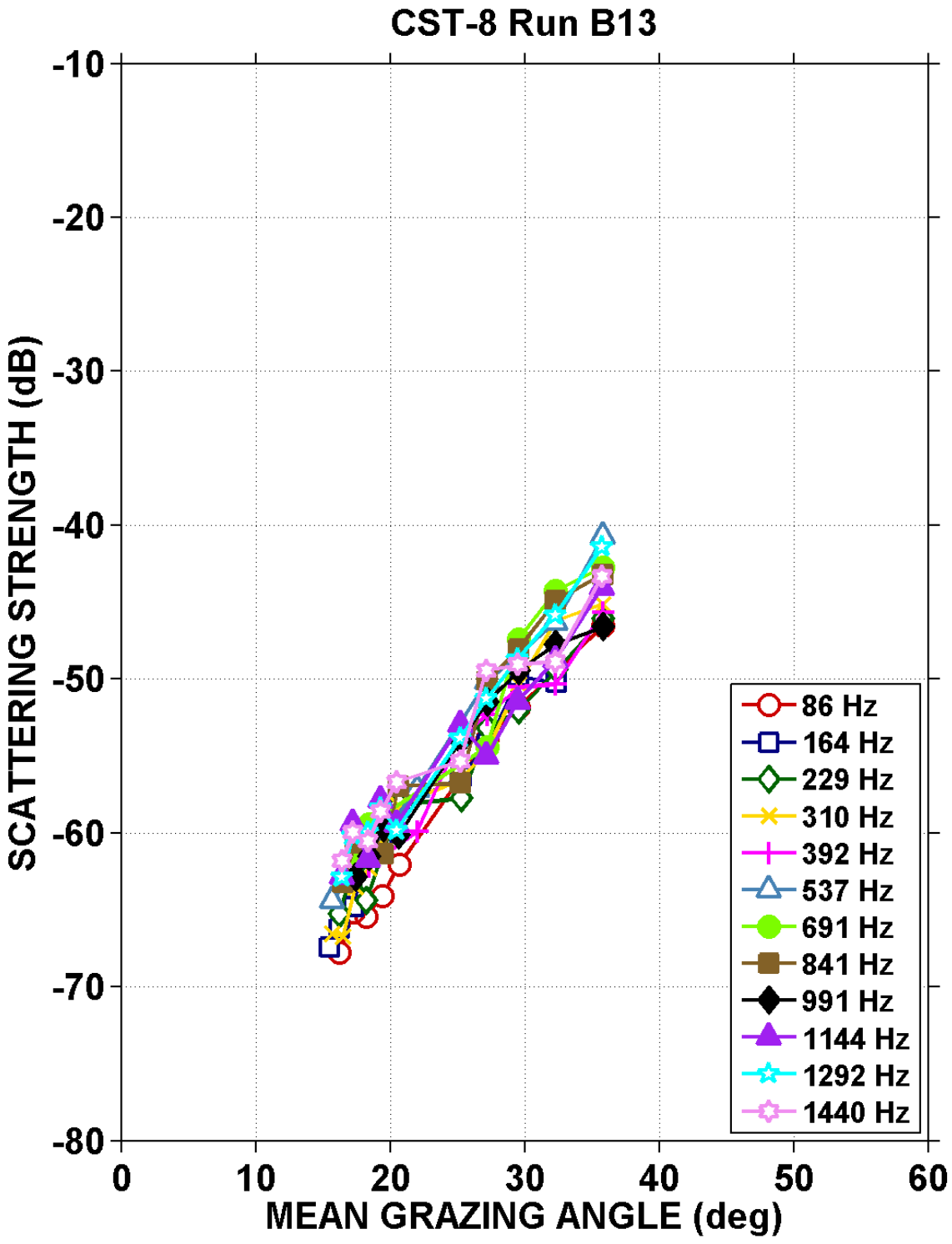

Fig. 4-51 – Surface backscattering strengths vs. mean grazing angle for CST-8 Run B13.

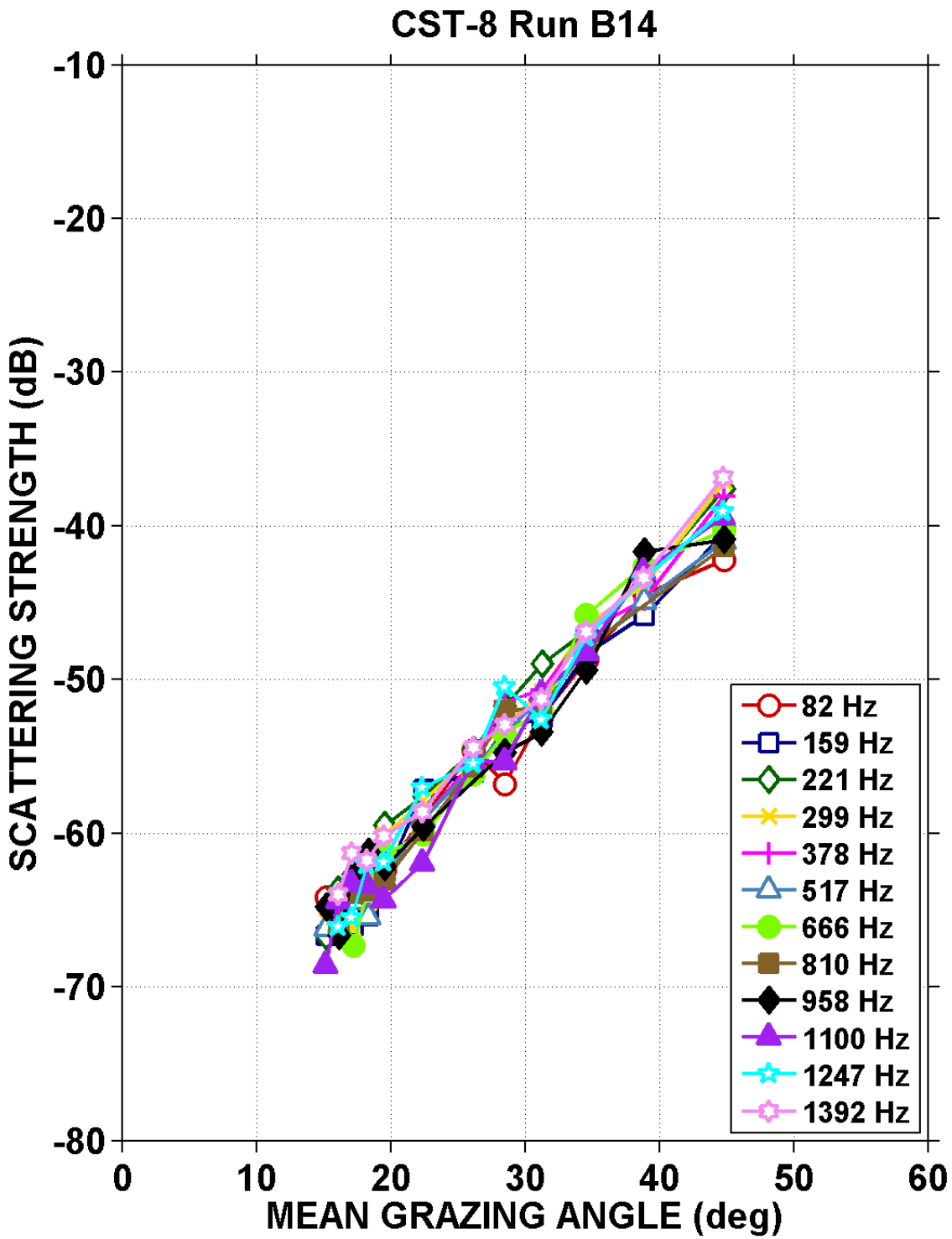

Fig. 4-52 – Surface backscattering strengths vs. mean grazing angle for CST-8 Run 14.

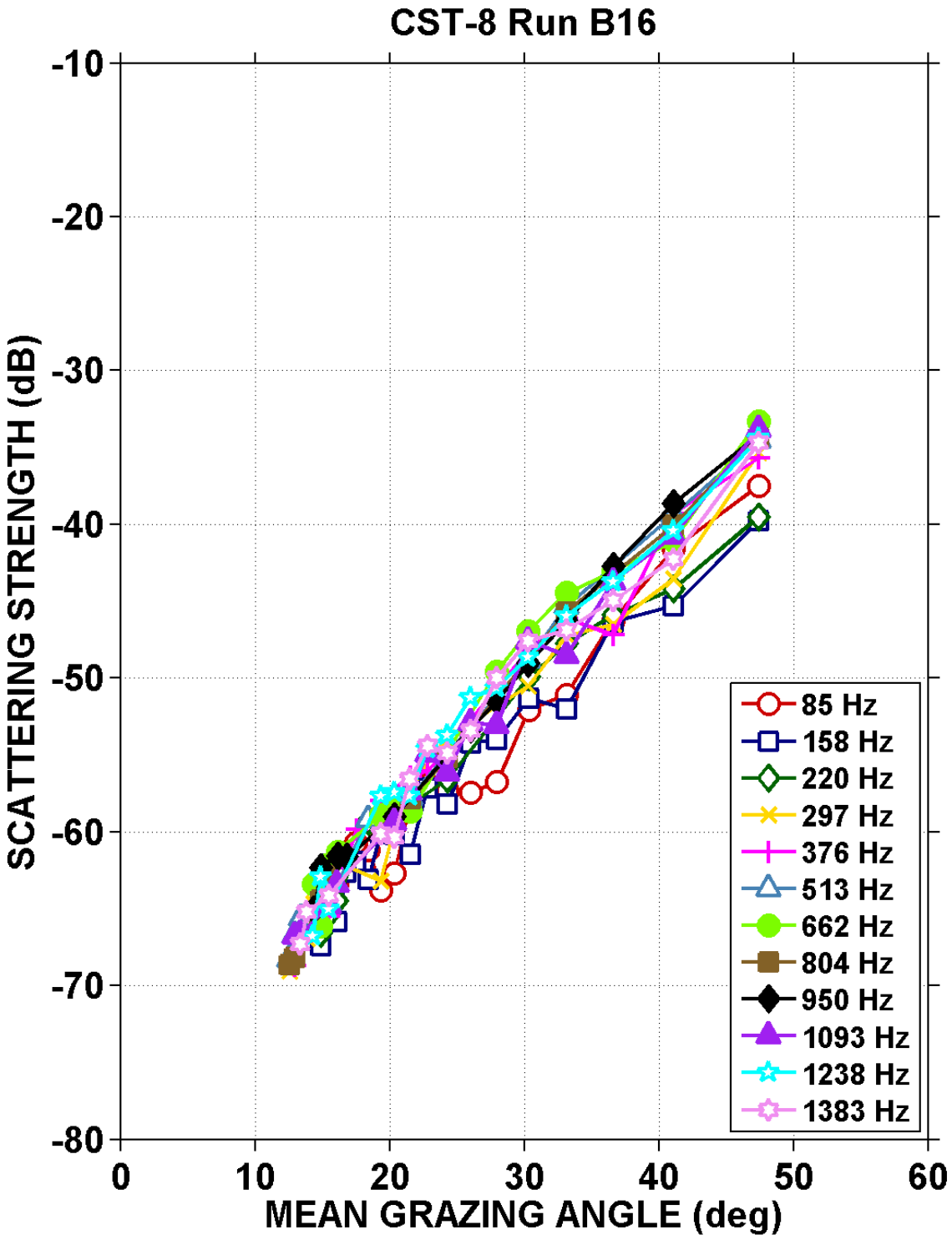

Fig. 4-53 – Surface backscattering strengths vs. mean grazing angle for CST-8 Run B16.

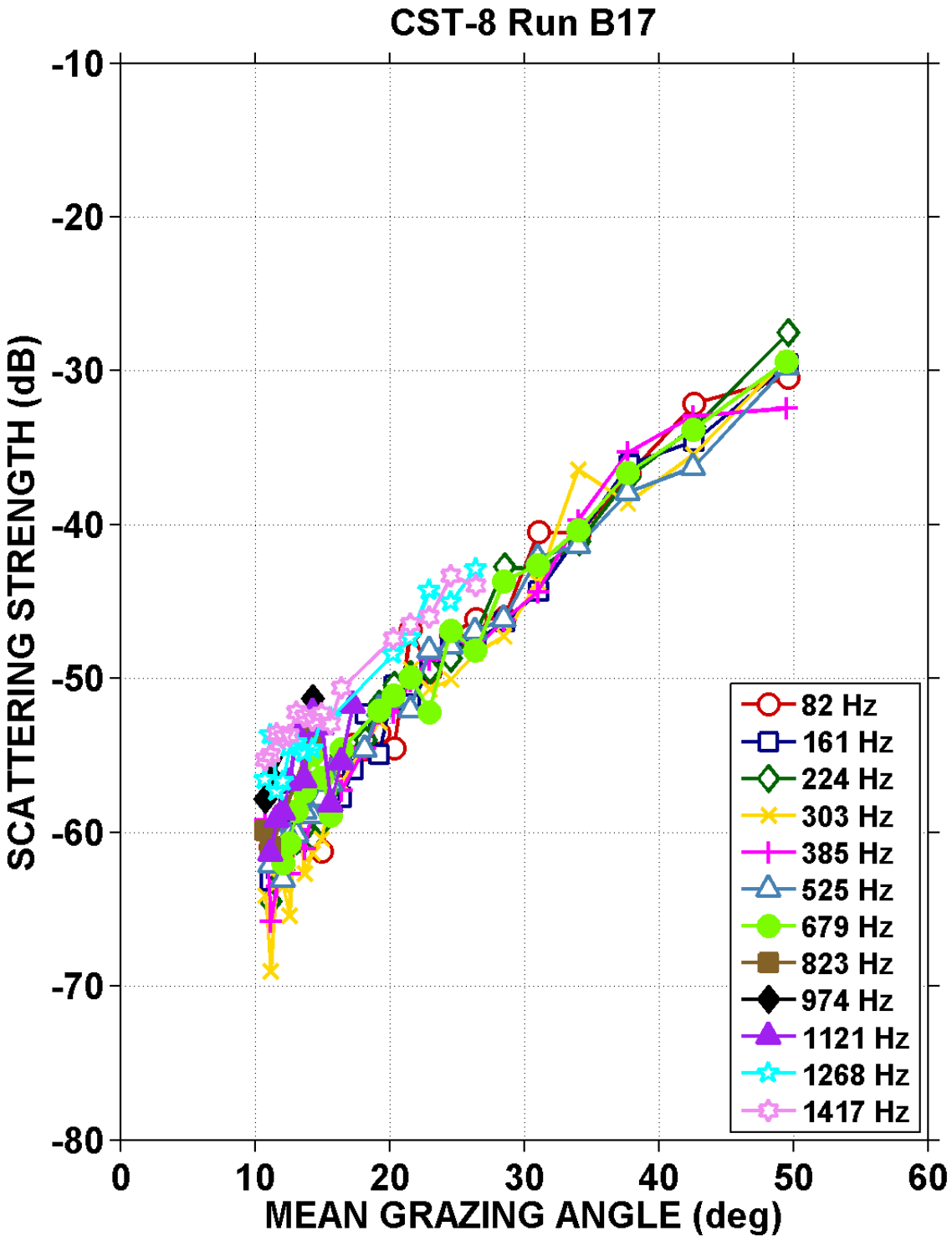

Fig. 4-54 – Surface backscattering strengths vs. mean grazing angle for CST-8 Run B17.

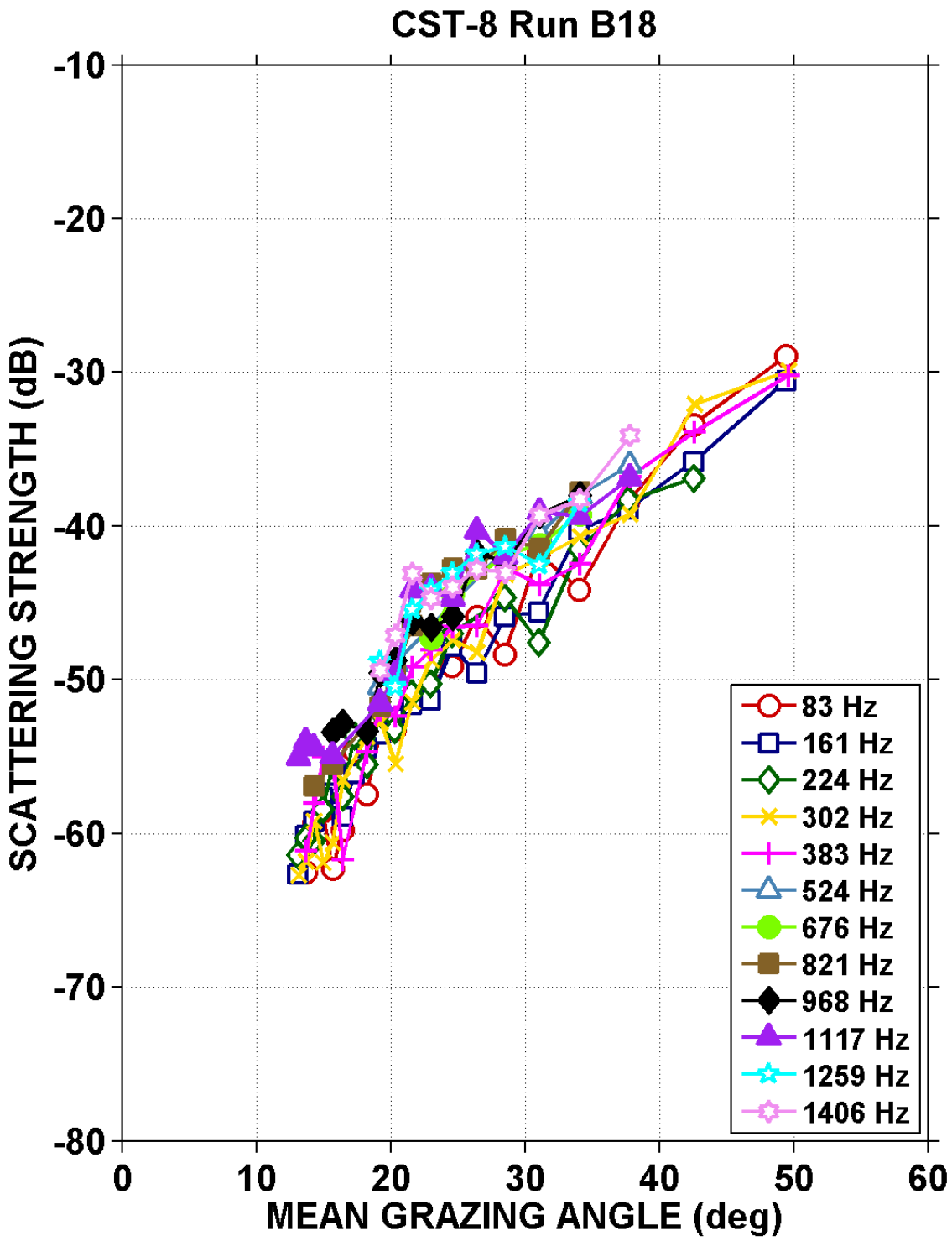

Fig. 4-55 – Surface backscattering strengths vs. mean grazing angle for CST-8 Run B18.

5. CROSS-RUN CST SSS EXAMPLES

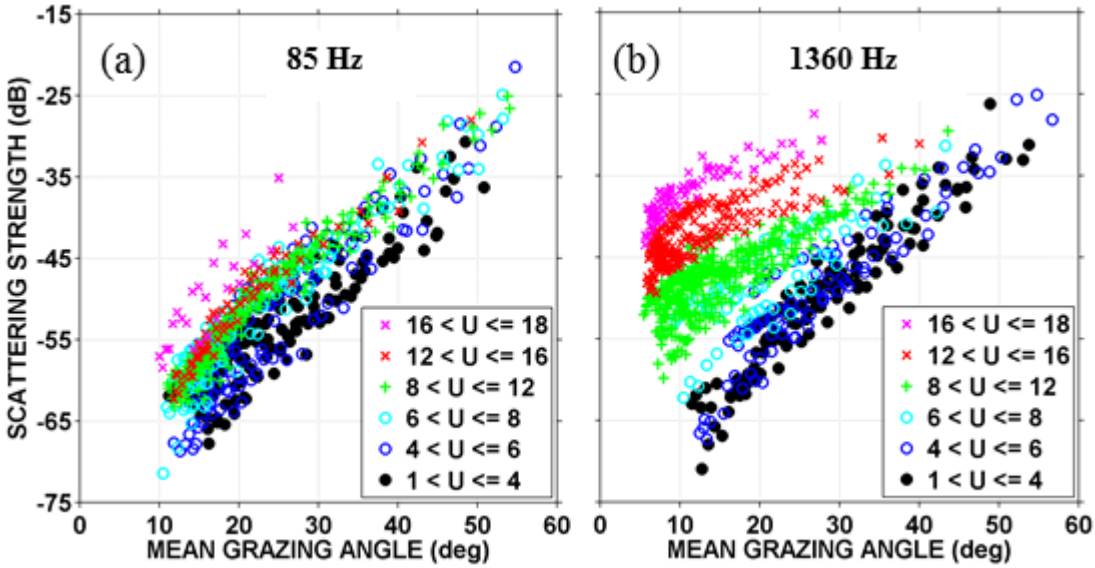

Fig. 5-1 – Cross-CST SUS SSS results at (a) 85 Hz and (b) 1360 Hz, color-coded by wind speed (U) groupings.

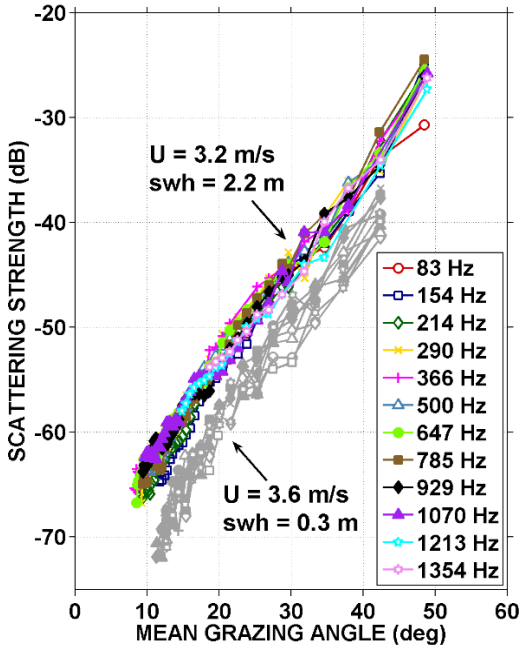

Fig. 5-2 – A low-wind-speed example from 2 CST runs illustrating the influence of SWH on SSS.

For an overview of direct-path CST surface-scattering results using coherent sources, see the matched-filter wideband-LFM CST-7 results of Fig. 5a,b in Fialkowski *et al.* (2004).

ACKNOWLEGDMENTS

This work was supported by the Office of Naval Research.

REFERENCES

1. Capps, S.B., and Zender, C.S., "Surface wind speed distributions: Implications for climate and wind power," presentation at JPL, Pasadena, CA, January 2009

2. Capps, S.B., and Zender, C.S., "Estimated global ocean wind power potential from QuikSCAT observations, accounting for turbine characteristics and siting," *J. Geophys. Res*. **115**, D09101, doi:10.1029/2009JD012679 (2010)

3. J.M. Fialkowski, R.C. Gauss, and D.M. Drumheller, "Measurements and Modeling of Low-Frequency Near-Surface Scattering Statistics," IEEE J. Ocean. Engr. **29**, 197-214 (2004)

4. Gauss, R.C., Fialkowski, J.M., and Wurmser, D., "Assessing the Variability of Near-Boundary Surface and Volume Reverberation Using Physics-Based Scattering Models," in *Impact of Littoral Environmental Variability on Acoustic Predictions and Sonar Performance*, ed. N.G. Pace and F.B. Jensen, 16-20 Sept. 2002, Lerici, Italy (Kluwer Academic, Dordrecht), pp. 345-352 (2002)

5. Gauss, R.C., Fialkowski, J.M., and Wurmser, D., "A Low- and Mid-Frequency Bistatic Scattering Model for the Ocean Surface," in *OCEANS '05 MTS/IEEE*, 19-23 Sept. 2005, Washington, DC (IEEE/MTS, 2005) (CD-ROM)

6. Gauss, R.C., Fialkowski, J.M., and Wurmser, D., "Measurements and modeling of low-frequency air-sea–interface scattering," J. Acoust. Soc. Am. **119**, 3309 (A) (2006a)

7. Gauss, R.C., Fialkowski, J.M., and Wurmser, D., "Low-to-High Frequency Bistatic Sea-Surface Scattering Models," in *Proceedings of the 8th European Conference on Underwater Acoustics – ECUA 2006*, ed. S.M. Jesus and O.C. Rodríguez, 12-15 June 2006, Carvoeiro, Portugal (Tipografia União, Portugal), Vol. 1, pp. 223-228 (2006b)

8. Gilbert, K.E., "A stochastic model for scattering from the near-surface oceanic bubble layer," *J. Acoust. Soc. Am.* **94**, 3325-3334 (1993)

9. Hanson, J. L., "Wind sea growth and swell evolution in the Gulf of Alaska," Ph.D. Dissertation, The Johns Hopkins University, Laurel, MD, 1996, 151 pp

10. Hanson, J.L., "Winds, waves and bubbles at the air-sea boundary," *Johns Hopkins APL Tech. Dig.* **14**, 200-208 (1993)

11. Love, R.H., "A Comparison of volume scattering strength data with model calculations based on quasisynoptically collected fishery data," *J. Acoust. Soc. Am.* **94**, 2255-2268 (1993)

12. McDaniel, S.T., "Sea surface reverberation: A review," *J. Acoust. Soc. Am.* **94**, 1551-1559 (1993)

13. Nero, R.W., and Huster, M.E., "Low-frequency acoustic imaging of Pacific salmon on the high seas," *Can. J. Fish. Aquat. Sci.* **53**, 2513-2523 (1996)

14. Nero, R.W., Thompson, C.H., and Love, R.H., "Abyssopelagic Grenadiers: The Probable Cause of Low-Frequency Scattering at Great Depths off the Oregon and California Coasts," Deep-Sea Res. **44**, 627-645 (1997).

15. Nicholas, M., Ogden, P.M., and Erskine, F.T., "Improved empirical descriptions for acoustic surface backscatter in the ocean," *IEEE J. of Ocean Engr*. **23**, 81-95 (1998)

16. Ogden, P.M., and Erskine, F.T., "Surface scattering measurements using broadband explosive charges in the Critical Sea Test experiments," *J. Acoust. Soc. Am.* **95**, 746-761 (1994a)

17. Ogden, P.M., and Erskine, F.T., "Surface and volume scattering measurements using broadband explosive charges in the Critical Sea Test 7 experiment," *J. Acoust. Soc. Am.* **96**, 2908-2920 (1994b)

18. Ogden, P.M., and Erskine, F.T., *Bottom scattering strengths measured using explosive sources in the Critical Sea Test Program*. Naval Research Laboratory, Washington, DC, NRL/FR/7140--97-9822, Feb. 5, 1997

19. Urick, R.J., *Principles of Underwater Sound*, 2nd ed., Mc-Graw Hill, New York, NY, 1983, ch. 4

20. Zittel, J.D., Erskine, F.T., Holland, C.W., Eller, A.I., Soukup, R.J., Raff, B.E., and Ellison, W.T., *Critical Sea Test Final Report*, SPAWAR CST/LLFA-WP-USWAC-9, Johns Hopkins University, Applied Physics Laboratory, Laurel, MD, 1996.